Study of Ballistic Graphene Nanoribbon FET and Carbon Nanotube FET for Device Applications

By

Md. Reaz Haider Pavel (11221050)

Md. Zishan Ibne Hussain (11121055)

A.B.M. Rakibul Ahsan (11221033)

A Thesis

Submitted as the partial Fulfillment for the Degree of Bachelor of Science in Electrical and Electronic Engineering

Department of Electrical and Electronic Engineering

BRAC University

Dhaka-1212, Bangladesh

CERTIFICATE OF APPROVAL

The thesis entitled **"Study of Ballistic Graphene Nanoribbon FET and Carbon Nanotube FET for Device Applications"** submitted by **Md. Reaz Haider Pavel, Md. Zishan Ibne Hussain** and **A.B.M. Rakibul Ahsan** has been accepted satisfactorily in partial fulfillment of the requirement for the degree of Bachelor of Science in Electrical and Electronic Engineering.

Supervisor

(Dr. Sharif Mohammad Mominuzzaman)
Department of Electrical and Electronic Engineering
Bangladesh University of Engineering and Technology (BUET)

CANDIDATE DECLARATION

It is hereby declared that this thesis or any part of it has not been submitted elsewhere for the award of any degree or diploma.

Author

Md. Reaz Haider Pavel

Author

Md. Zishan Ibne Hussain

Author

A.B.M. Rakibul Ahsan

ACKNOWLEDGEMENT

First and foremost, we are very much grateful to Almighty ALLAH for giving us eternal blessings on choosing the correct path towards the target of this work.

This work has been performed through inspiration and constant guidance of several kind people. Most importantly, we would like to thankfully acknowledge the help of **Dr. Sharif Mohammad Mominuzzaman,** Professor, Department of Electrical and Electronic Engineering (EEE), Bangladesh University of Engineering and Technology (BUET), Dhaka. His experience and in depth knowledge in the field of nanotechnology, constantly guided us towards completion of the work. His guidance and insightful discussions enlightened us throughout the thesis work. Thanks for his encouragement and trust on our ability to work on this topic. It would not be possible to complete this work without his informative assistance and motivation.

We would also like to thank **Dr. A.K.M. Azad** who referred our group to Professor Mominuzzaman and always believed in our abilities.

A special thanks to **Atanu Kumar Saha,** faculty of EEE department of BRAC University, for his persuasive consultations throughout our thesis.

We are indebted to **Sheikh Ziauddin Ahmed**, faculty of EEE department of BRAC University, for his generosity and **Syed Mahmud Hasan** for taking the time out of his busy schedule to help us out with our work.

Finally, we would like to thank our parents and well-wishers for their constant support, motivation and their patience.

ABSTRACT

The need for technological progression in the field of electronics has been persistently escalating. So far silicon has been the most important fabrication material of preference for meeting the current demands. However, silicon itself has few of its own limitations; Silicon based integrated circuits and the scaling of silicon MOSFET design faces complications like tunneling effect, gate oxide thickness effect etc. which has given the extensive perimeter for new materials with improved characteristics to emerge.

In up to date periods, graphene and carbon nanotube have shown huge promise as materials that can swap silicon-based materials in the future due to their outstanding electrical properties and other characteristics. Simulation studies of graphene nanoribbon field-effect transistors (GNRFETs) and carbon nanotube field-effect transistors (CNTFETs) at different contact temperatures are presented in this thesis paper using models that have been methodically developed and are of increasing thoroughness and versatility. This thesis covers the studies and modeling of graphene nanoribbon and carbon nanotube, which includes band structures and current-voltage graphical plots. Also, an analysis has been presented which shows the effect by varying contact temperatures for relative dielectric constant and chirality on the device performance, in particular on the drain current.

The purpose of this paper is to the study behaviour of graphene nanoribbon transistors and carbon nanotube transistors. The simulation is carried out using NanoTCAD ViDES program and the main focus is on the changes in the I-V characteristic curves for transfer and output characteristics for relative dielectric constant and chirality for different contact temperatures. The obtained results were used to make a comparative analysis of the device performance of GNRFET and CNTFET. We confirmed our work by contrasting of our results with other recognized academic papers published under the same category.

Table of Contents

List of Tables

List of Figures

Chapter 1

INTRODUCTION

The objective of this paper is to present a comprehensive discussion about the contact temperature effect on the ballistic graphene nanoribbon and carbon nanotube transistor. This research also establishes a relative analysis of the transfer and output characteristics of ballistic barrier graphene nanoribbon and carbon nanotube transistor. The scrutiny is carried out by shifting contact temperatures for different parameters on input and comparing the consequence with the result of other research groups. Being the first chapter, this chapter presents the background of the research, objective, and the extent of this research work. The chapter itself also comes up with the outline of the thesis. Finally, this chapter summing up the content of each chapter.

1.1 Overview and Research Incentive

Silicon has been the structural block for the electronics sector till today. This emerging technology paced at a rate which over turn the historic pace of Moore's law [1]. Even so, the scaling limits of silicon are approaching the closing stages since many problems come up as devices become smaller in size. Problems like tunneling effect, short-channel effect etc. come into the picture and these effects hinder the device performance. It is therefore essential that silicon be substituted by other materials which will take device advancement to a whole new level. On basis of that, it is of intense concern to identify reliable, suitable and most importantly effective new materials which can be a super substitute of silicon platform with sustainable properties that can out run the existing silicon technology. New materials with superior electronic, optical and mechanical properties emerge as a result to allow devices scaling to continue to the atomic scale. Nanosize devices open many pathways to exploit the physical and chemical properties at the nanoscale. Chemical synthesis, self-assembly, and template self-assembly promise the precise fabrication of device structures or even the entire functional entity. Thus, the reasonable new nanoelectronic devices can be originated based on completely new system architecture for instance: nanotubes, nanoribbons, nanowires, molecular devices and unique nanoelectronics devices [1].

Among diverse material systems and structures, grapheme and carbon nanotubes shown meticulous promises according to their nanoscale size and unique electronic properties. Due to their low dimensionality, nanostructures such as quantum dots, carbon nanotubes (CNTs) possess unique properties that make them promising candidates for future technology applications [2]. Though a through and relentless study have been performed but yet to understand how a graphene and carbon nanotube transistor operates and how to improve their performance [3] [4] [5]. In recent times both of them have been fabricated which showed an improved performance than a silicon transistor of identical size.

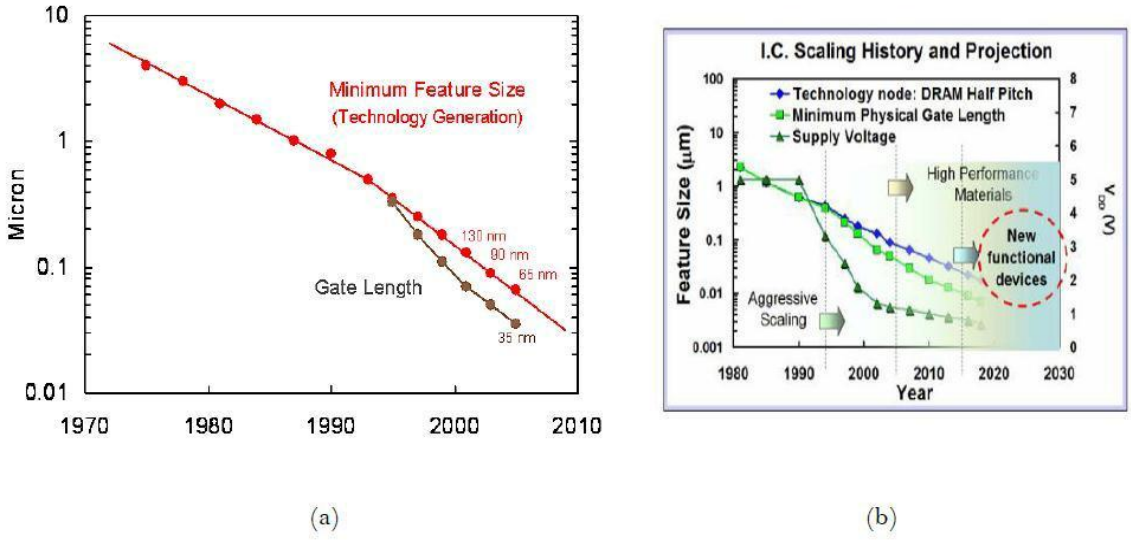

Figure 1.1: (a) Moore's law and (b) IC technology projection. [1]

In this thesis substantial simulation of GNRFETs and CNTFETs for the different temperatures is extended. In order to explore the infinite outcomes for GNRFETs and CNTFETs, it is compulsory to build up an elementary understanding of the basic physics. This research therefore deals with the I-V characteristics of ballistic GNRFETs and CNTFETs and thus enhances our depth of knowledge regarding the fundamental physics that governs their behavior in other devices.

1.2 Objectives of the Research

The scaling of silicon-based transistors has been the dynamic factor behind the large growth of the technology industry over the last few decades. However, this miniaturization imposes some limits on the silicon-based transistors. Thus, researchers have been aggravated to explore and ascertain other alternative technology like graphene and carbon nanotubes for better functioning of the current devices. Because of having low dimensionality and outstanding electronic properties; Graphene and

carbon nanotubes are the potential materials for future nanoelectronics, both as interconnects and as critical elements like channel materials for field-effect transistors. At present, ballistic graphene nanoribbon field-effect transistor(GNRFET) and carbon nanotube field-effect transistor (CNTFET) are indulged as two of the nanoelectronic devices that have vast prospective to be treated as a switching device for future. We are planning to make an extended comparative analysis between these two types of transistors for different temperatures. The nucleus parts of our research work to summarize are:

- Analyze the graphene nanoribbon and carbon nanotube device models and the limitation of Si MOSFET.
- Understand the basic of graphene nanoribbon and carbon nanotube physics and focus on their electrical properties.
- Comprehend the device characteristics, fundamental equation and mathematical model of GNRFET and CNTFET.
- Realize theoretical difference between graphene nanoribbon based FET and carbon nanotubes based FET.
- Using mathematical model simulation investigate the I-V characteristics of GNRFET and CNTFET by varying different parameters and make an unalloyed comparison with different research group result.
- By examining the objective stated above, we can deduce total GNRFET and CNTFET characterization and form a complete understanding of the effect of changing different parameters on transfer and output characteristics of these two transistors.

1.3 Extents of Work

The research paper has been constrained to the following scopes of work due to lack of resources, proficiency and restricted time frame.

- ✓ By using NanoTCAD ViDES [6] simulate Schottky barrier Graphene Nanoribbon field-effect transistor (GNRFET) and Carbon Nanotube field-effect transistor (CNTFET) and generate I-V curves.
- ✓ Simulate the transfer and output characteristics by changing temperature for different parameters like chirality, dielectric constant and channel length.
- ✓ Comparing the obtained results with other research groups.
- ✓ Comparison between GNRFET and CNTFET.

1.4 Outline of the Research Report

This thesis paper has been divided into four chapters including this one.

Chapter 1 thrashes out the overview and research incentive, the research objectives and the extents of work of this paper.

Chapter 2 gives a detailed overview of Silicon MOSFETs along with the limitation it faces due to scaling. Afterward there is a comprehensive discussion on Carbon Nanotube, the structure of CNT, chirality, single walled CNT (SWCNT), multi walled CNT (MWCNT) and properties of CNT are discussed. Subsequently the operational principles of carbon nanotube transistors are presented. Before ending, this chapter gives an elaborate discussion on graphene and graphene nanoribon, their synthesis procedures and their properties.

Chapter 3 contains the results and analysis of our focal works where we generated the I-V curves for both Schottky barrier GNRFET and CNTFET. This chapter largely deals with the transfer and output characteristics of both GNRFET and CNTFET. The result and analysis section exhibits and discusses the effects of relative dielectric constant, chirality and channel length on the transfer and output characteristics for different temperatures.

Chapter 4 brings to a closure of our entire research and discusses about our future projections and realistic researches.

Chapter 2

MOSFET, CARBON NANOTUBE, CNTFET, GRAPHENE AND GNRFET

2.1 Evaluation of the Silicon MOSFET

In 1930, Lilienfeld [7] patented the basic concept of the field effect transistor (FET). After thirty years in 1959, the concept was finally materialized in Si-SiO_2 by Kahng and Atalla [8] [9]. The first MOSFET was invented in 1959 and since then it has completely changed the world of digital electronics. MOSFETs have dominated all fronts of digital applications especially modern computers; because it offers many advantages to the user. MOSFETs are relatively small in size and this contributes to the fact that they can be packed in large numbers on a single integrated circuit. It is also very reliable and offers low consumption of power. The progress up to now is well described by "Moore's law." Gordon Moore predicted in 1965 that for each new generation of memory chip and microprocessor unit on the market, the device size would reduce by 33 percent, the chip size would increase by 50 percent, and the number of components on a chip would quadruple every three years. So far this trend has shown no signs of stopping [10].

Several properties of silicon have made these developments in microelectronics possible. Silicon can be grown in single crystals that are more than 1 m long and 30 cm across. The purity of the crystal and the number of electrically active defects can be controlled. The number of atomic crystal defects in sub-micrometresized MOSFETs is now limited to individual centers that act as traps for electrons. Such traps may be identified, individually characterized, and counted, so that single-electron transistors are possible. The reason behind Silicon being the semiconductor of choice for MOSFET is its native oxide. Silicon dioxide (SiO_2) is an almost perfect insulating material with a resistivity in excess of 1016 Vcm. The insulating films of SiO_2 grown on silicon are smooth and coherent with no holes, in a thickness ranges down to single atomic layers [10].

The metal–oxide–semiconductor field-effect transistor (MOSFET) is a transistor used for amplifying or switching electronic signals. Although the MOSFET is a four-terminal device with source (S), gate (G), drain (D), and body (B) terminals; [11] the body (or substrate) of the MOSFET often is connected to the source terminal, making it a three-terminal device like other field-effect transistors. The gate terminal is a metal electrode that controls the current flow from source to drain [12]. The gate voltage needs to be higher than the threshold voltage in order for the current to flow in MOSFET. The source terminal is usually grounded and the drain voltage applied is relatively very small. As the gate voltage rises above the threshold voltage; an inversion layer or channel is created. This causes electrons to flow from source to drain terminal and as a result of which the current flows from drain to source terminal. There is no current flow to gate terminal since there is an oxide barrier which acts as an insulator. Figure 2.1 shows the structure of MOSFET.

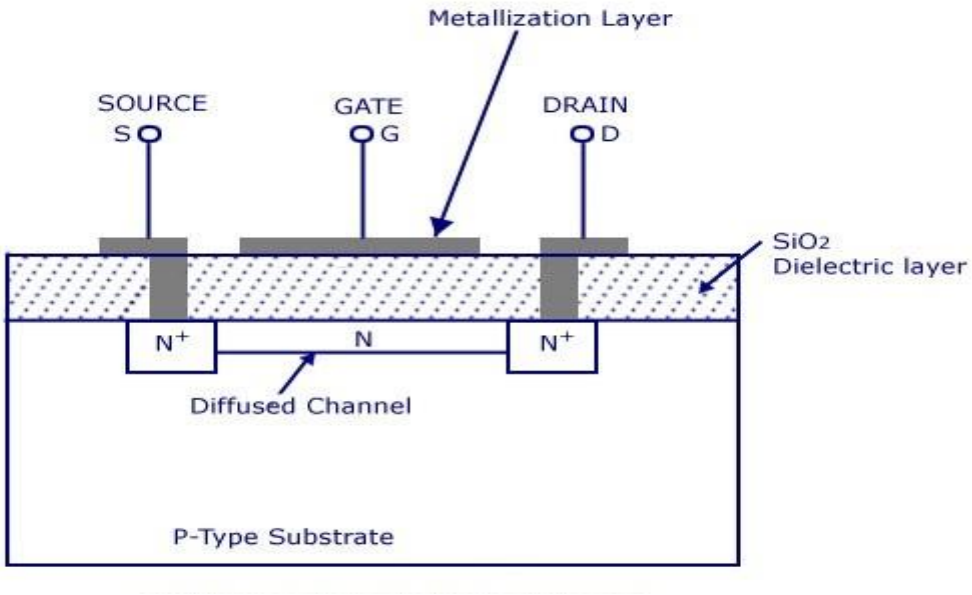

Figure 2.1: Structure of MOSFET

2.1.1 Scaling of the Silicon MOSFET

Scaling is a process which involves reducing the size of MOSFET and at the same time improving its performance. The first method was introduced in 1974 in which by reducing the MOSFET dimension, the device density, switching speed and energy was also improved. Each new generation has approximately doubled logic circuit density and increased performance by about 40% while the memory capacity has increased by four times. In ideal scaling, as the dimension and the operating voltage is reduced by a factor of 0.7, the area density doubles, switching delay decreases by a factor of

0.7 and the switching energy is halved. The switching speed can be estimated when the gate capacitance, operating voltage, and drive current are known. Switching energy is reduced as a result of the lower total combination parasitic capacitance due to smaller device size and lower operating voltage. Reduction of switching energy is very important since the overall circuit power is very crucial especially if the system is used for a long period continuously [12].

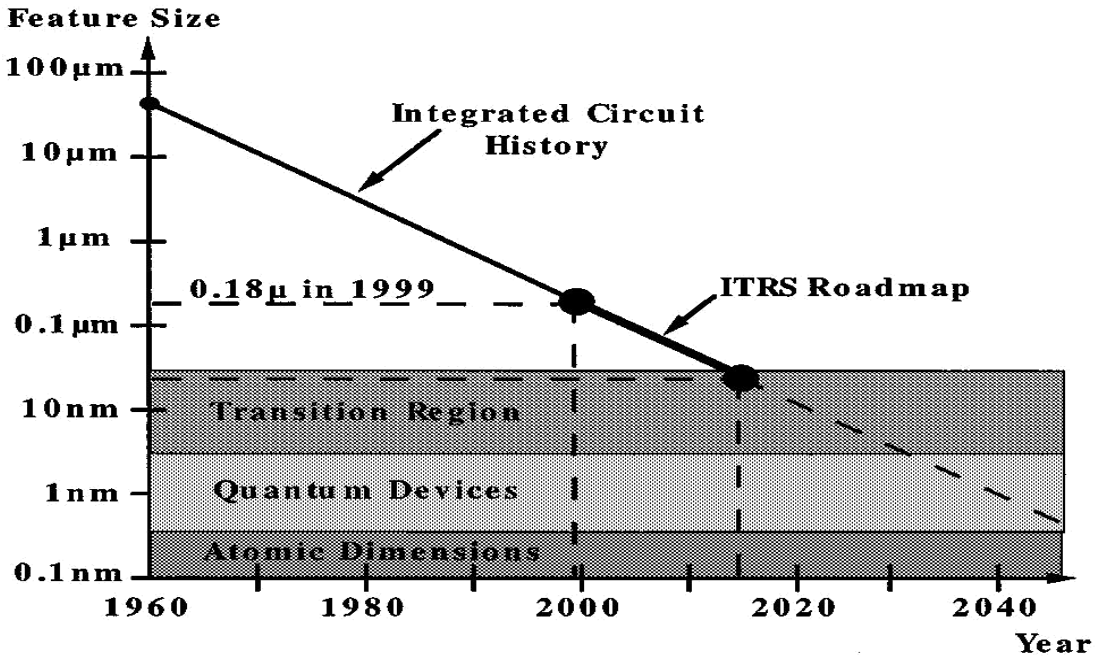

Figure 2.2: Feature size versus time in silicon ICs [13]

2.1.2 Limitations of Scaling

There have been many articles and papers on the current situation and future prospects for Si-MOSFETs; many different scaling limits for MOSFETs have also been discussed and proposed [8]. There are a number of factors which needs to be taken under consideration with continued MOSFET scaling that present challenges for the future and, ultimately, fundamental limits. There are quite a few problems which arise as the MOSFET size reaches nanometer scale and ultimately limits the performance of the MOSFET itself. These problems are crucial and must be taken under consideration if the MOSFET is to survive in the near future.

2.1.2.1 Short Channel Effect

The first factor to be considered is the short channel effect. The short channel effect introduces several leakage currents in MOSFET which are discussed below and shown in the figure- 2.3[14].

- ✓ Reverse bias p-n junction current occurs due to the minority carriers, diffusion near the depletion region and also due to the generation of electron-hole pairs.
- ✓ Weak reverse current occurs when gate voltage is lower than threshold voltage.
- ✓ DIBL current is present when source's potential barrier is reduced as a result of the drain's depletion region interacting with the source. The existence of DIBL lowers the threshold voltage.
- ✓ Gate-Induced Drain Lowering (GIDL) current occurs in high electric field between gate and drain, and it also occurs along the channel width between gate and drain.
- ✓ Another leakage current mechanism, punchthrough, occurs when the drain and source depletion regions touch deep in the channel.
- ✓ Narrow-width current arises when the channel length is reduced to less than 0.5µm.
- ✓ Gate-oxide tunneling current occurs when the oxide layer is made very thin and also causes gate leakage current tunneling through oxide bands.
- ✓ Hot-carrier injection occurs when hot carriers is injected into the oxide.

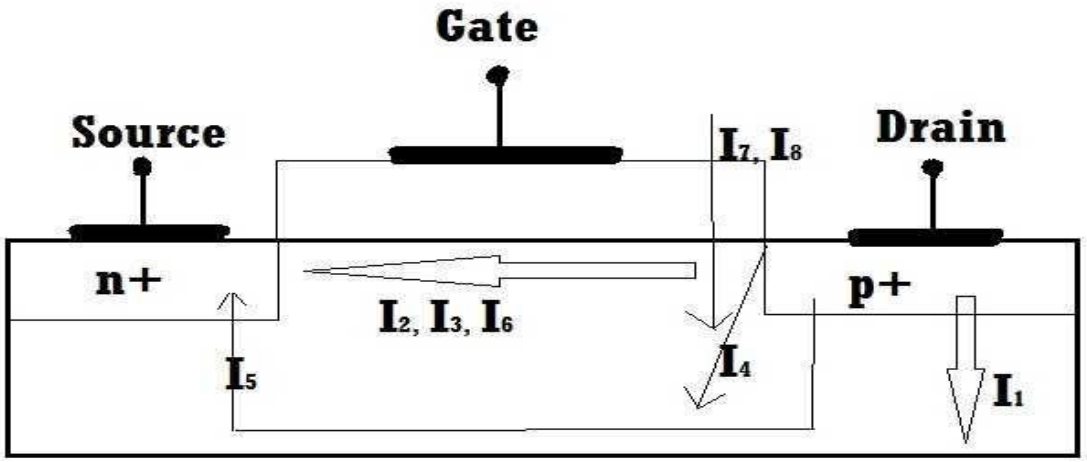

Figure 2.3: Short-channel-transistor leakage current mechanisms: reverse-bias p-n junction leakage (I_1), weak inversion (I_2), drain-induced barrier lowering (I_3), gate-induced drain leakage (I_4), punch-through (I_5), narrow-width effect (I_6), gate oxide tunneling (I_7), and hot-carrier injection (I_8).

Table 2.1: Schematically illustrates the MOSFET used in today's silicon chips. The basic fabrication process steps to manufacture such a device have been broadly described. The basic structure will continue to evolve to allow continued performance improvements, but fundamental changes are unlikely until 2015 [13].

Year of 1st DRAM Shipment	1997	1999	2002	2005	2008	2011	2014
Minimum Feature Size	250 nm	180 nm	130 nm	100 nm	70 nm	50 nm	35 nm
Isolated Gate Length	-	100 nm	70 nm	50 nm	35 nm	25 nm	18 nm
DRAM Bits/Chip	256M	1G	(3G)	8G	(24G)	64G	(192G)
DRAM Chip Size (mm^2)	280	400	460	530	630	710	860
Equivalent Physical Gate Oxide Thickness (nm)	3-5	1.9-2.5	1.5-1.9	**1.0-1.5**	**0.8-1.2**	**0.6-0.8**	**0.5-0.6**
Dielectric Constant of DRAM Capacitor		22	50	250	700	**1500**	**1500**
Max Gate Electrode Resistivity ($\mu\Omega$ cm)		60	43	33	**23**	**16**	**11**
Max Silicide/Si Contact Resistivity ρ_C (Ω cm^2)		$30x10^{-8}$	$17x10^{-8}$	$\mathbf{10x10^{-8}}$	$\mathbf{5x10^{-8}}$	$\mathbf{2.5x10^{-8}}$	$\mathbf{1.5x10^{-8}}$
S/D Extension Sheet Resistance (Ω/sq)		350-800	250-700	**200-625**	**150-525**	**120-450**	**100-400**
S/D Extension x_J (nm)	50-100	42-70	25-43	**20-33**	**16-26**	**11-19**	**8-13**
S/D Extension Lateral Abruptness (nm/decade)		14	8.5	6.5	**4.5**	**3.2**	**2.2**
Minimum Supply Voltage (volts)	1.8-2.5	1.5-1.8	1.2-1.5	0.9-1.2	0.6-0.9	0.5-0.6	0.5

2.1.2.2 Threshold Voltage Effect

A notable limitation to MOSFET is that the threshold voltage is not proportionally decreasing with respect to transistor scaling. The threshold voltage is maintained at a constant level when the channel length is between 0.1µm-1µm and it deviates further when the channel length is below 0.1µm [12], [7]. If the transistor is scaled below 0.1µm, the threshold voltage current does not drop to zero immediately but it decreases exponentially, and is inversely proportional to the thermal energy [12]. There are some thermally distributed electrons at source terminal that have enough energy to overcome the barrier potential regulated by gate terminal. This behavior is independent of channel length and power supply. So, higher threshold voltage causes higher leakage current. Denoting leakage current as I_{off} gives:

$$I_{off} = I_o (-qV_t / mKT) \quad (2.1)$$

I_{off} = Extrapolated current per width at threshold voltage.
m= Dimensionless ideality factor
V_t= Threshold voltage.

Lower leakage current is essential for a transistor in order to reduce the power loss. However lower threshold voltage can reduce the leakage current. So, designing a transistor should be in such a way that its threshold voltage remains very low. According to Sanudin, the leakage current is reduced ten times for every 0.1V reduction of threshold voltage [12].

2.1.2.3 Oxide Thickness

The gate insulator in a MOSFET needs to be thin compared to the device channel length in order for the gate to exert dominant control over the channel potential. This avoids "short channel effects," which are largely the result of the drain electric field penetrating throughout the channel and influencing the channel potential at the source of the device [13].

Gate-oxide thickness causes two kinds of limitations. Firstly, the thin layer of oxide eventually increases leakage current. This effect is also related to quantum effect tunneling that dominates in MOSFET as the oxide thickness is reduced. The tunneling current due to thick oxide layer may look negligible in comparison with "on state" c urrent. However, it has a major effect when the chip is in standby mode. Secondly, due to the oxide thickness there is a loss of inversion charge and also the

transconductance as a result of inversion-layer quantization and polysilicon gate depletion effect [15]. The gate electrode itself also presents some significant challenges. Polysilicon has been used for more than 25 years as the gate electrode material. However, decreasing its resistivity, as shown in table-2.1, implies increasing the doping levels in the polysilicon, which minimizes the resistivity of the gate electrode. This aids in avoiding polysilicon depletion effects. However, this approach is limited by dopant solubility limits and by dopant out diffusion from the polythrough to the thin gate dielectric and into the silicon. This later problem is particularly acute with p-gates because boron diffuses rapidly through SiO_2. The likely solution is again new materials. But there are no known materials solutions that are known to work in manufacturing [13].

2.1.2.4 Tunneling Effect

Under normal conditions, in an operating or computational system integrated transistors are separated sufficiently enough so that operation of one transistor does not in any way affect the operation of another transistor. This separation is made by inserting a material that acts as a barrier between two transistors. However, the barriers are also scaling down along with the MOSFETs. So there is a possibility of carriers from one MOSFET crossing over to another and distorting the performance. This effect increases exponentially as the barrier distance decreases.

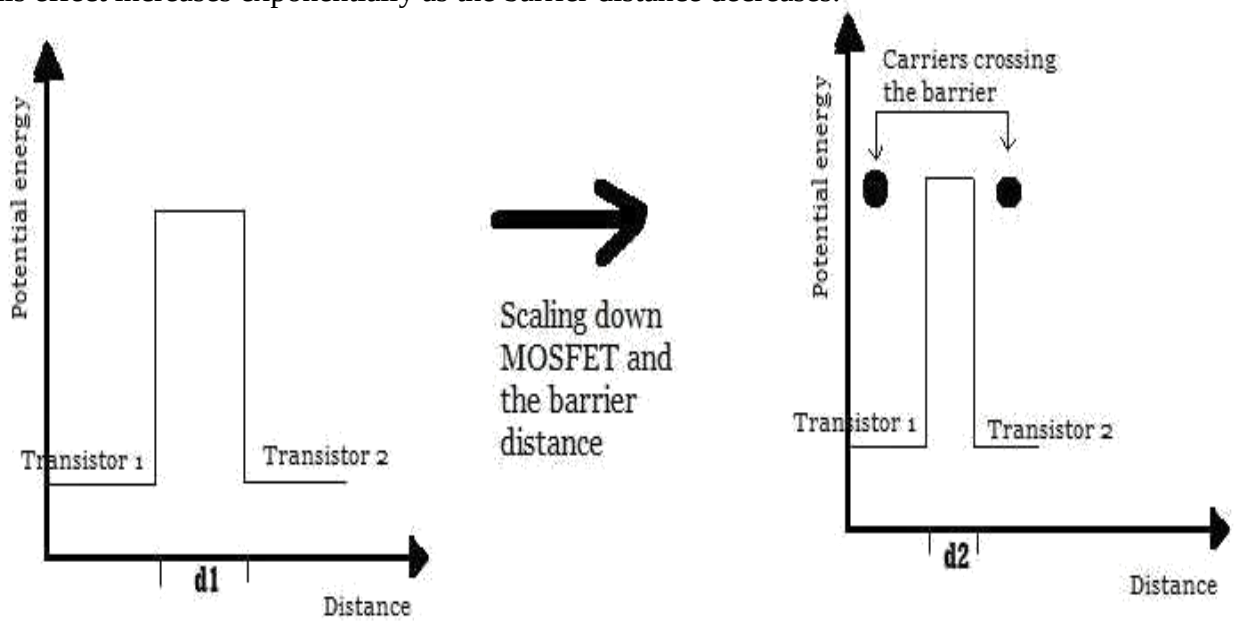

Figure 2.4: Potential barrier between two transistors.

2.1.2.5 Contact Resistance

Contacts are normally made by self-aligned silicides which are in contact with heavily doped silicon. This process provides an ohmic contact; which completely covers the area of the source/drain diffusions and this leads to the minimization or reduction of the contact resistance. Current flows in a distributed manner from the source/drain extension to the contact. The exact flow lines depend on the doping profile in the silicon and on the physical geometry. The contact resistance depends on the effective area of the contact. Current crowding on the leading edge of the contact can have a significant effect. In this structure, the contact resistance is given by:

$$R_{contact} = \sqrt{(\rho_c R_{SD})} / (W \times \coth (L_c / L_t)) \approx \rho_c / (WL_c) \qquad (2.2)$$

Where,

ρ_c= specific contact resistivity of the silicide/semiconductor contact ($\Omega\ cm^{-2}$);

R_{SD}= sheet resistance of the source/drain diffusion (Ω/square);

W= contact width;

L_c= contact length.

$L_t = \sqrt{(\rho_c / R_{SD})}$ is called the transfer length and is the average distance that carriers travel in the diffusion before entering the contact.

For typical values of ρ_c, R_{SD} and L_t, is greater than the physical contact length L_c, which results in the approximation shown above. In this case, the current flows into the entire length of the contact and current crowding effects are minimal. Thus, the contact resistance varies inversely with the contact area if ρ_c is constant.

The silicide formation process itself often consumes silicon since the metal component (Ti, for example) is usually deposited and then reacted to form the silicide. This has several important consequences. Firstly, some of the volume of the heavily doped source/drain regions is lost or consumed by the silicide formation. The portion of the source/drain region which is “lost” is the top portion, which is normally the most heavily doped and, therefore, the most conductive. This increases the sheet resistance of the remaining diffusion in which current can flow to the contact and, therefore, increases the effective contact resistance [13].

2.1.2.6 Power Consumption and Heat Dissipation

Power consumption and heat dissipation are two obstacles for further advancement in Si-based transistors. For the past three years power density has grown with the rate of 0.7 for every generation [16]. Large amount of power consumption boosts up the heat generation, increasing the possibility of transistors interfering with each other. As MOSFETs are scaling down these small transistors consume small amount of power but IC chips are becoming denser because of large number of transistors on each of them. So it uses large amount of power to drive all transistors and therefore generates more heat. Heat dissipation and power consumption are two major limitations. Therefore, there is the need of searching for alternative media, which can overcome the limitations of conventional Si based MOSFET. And this is where the idea of using carbon nanotubes instead of Silicon is conceived.

2.1.2.7 Theoretical Limitations

Thermal limit and quanta limit are a major problem. Amount of energy needed to write a bit must be greater than the thermal function in order to avoid the bit error to occur. This is called the thermal limit. Currently CMOS needs 10-13 J to write a bit and the trend is to reduce it, in order for the power dissipation to reduce [12].

Quantum limit is associated with E/f where, E is the thermal energy and f is the frequency. Currently CMOS is operating higher than the quantum limit and if the scale reaches to 100nm then it is expected the limit is approached as E is decreased and f is increased.

2.1.2.8 Design Limitations

Due to the scaling down of MOSFETs lead to the discovery of its design limitations. MOSFET does not work effectively when it is scaled to only around 30nm. The limit is because of the fact of Zener breakdown at source/substrate junction [12]. Leakage at gate also starts to surface and it becomes very difficult to have control over the channel.

2.2 Carbon Nanotube (CNT)

Carbon nanotubes were first discovered in 1991 by S. Lijima, also known as the father of carbon nanotubes. Carbon nanotubes are formed when graphene layers are folded into a seamless cylindrical form. Carbon nanotubes are quasi-one-dimensional and look like long thin cylinders of carbon with diameters of about 1nm. There are two types of carbon nanotubes depending on their composure. When the nanotube is composed of several shells of carbon, it is known as multi wall nanotube (MWNT). On the other hand, when only one shell composes the nanotube it is known as single wall nanotube (SWNT). Carbon nanotubes display a versatile range of properties which has attracted researchers all around the globe. They are good conductors of heat, electricity and also display semiconducting characteristics. Carbon nanotubes can be metallic, semiconducting or insulating depending on their rolling helicity most importantly and then on its length and diameter. What is fascinating is the fact that carbon nanotubes require no doping. The bandgap can also be varied just by changing the diameter of the nanotube. Bandgap decreases with increasing diameter. Carbon nanotubes have a very high current density; individual tubes are able to carry currents at a higher density than most metals and other semiconductors. Carbon nanotubes are also inert and this makes them very compatible with other materials. Currently, SWNTs are synthesized by one of three different techniques: pulsed laser vaporization, arc discharge growth, or chemical vapor deposition (CVD) on supported or gas phase catalysts. Transition metals in their nanoscales are used as catalysts in the processes. Pure carbon nanotubes are highly polarizable, smooth-sided structures, they tend to aggregate into parallel bundles that are held together by non-covalent interactions of approximately 0.5 eV per nanometer. These substantial Van der Waals cohesive forces are sufficient to bundle the nanotubes in raw samples. This makes it really difficult to separate and collect individual tubes for further research or device construction. One of the greatest needs in nanotube research and commercialization is the development of effective methods for obtaining samples of SWNTs with uniform electronic character. Ultrasonic agitation in surfactant solution followed by ultracentrifugation can often give stable suspensions that are rich in individual nanotubes. However, physical separation of the semiconducting and metallic species is much more difficult particularly for larger batch sizes. Obtaining SWNT samples of specific (n, m) types is the most difficult goal and it is one of the major factors disrupting the commercialization of carbon nanotubes [17].

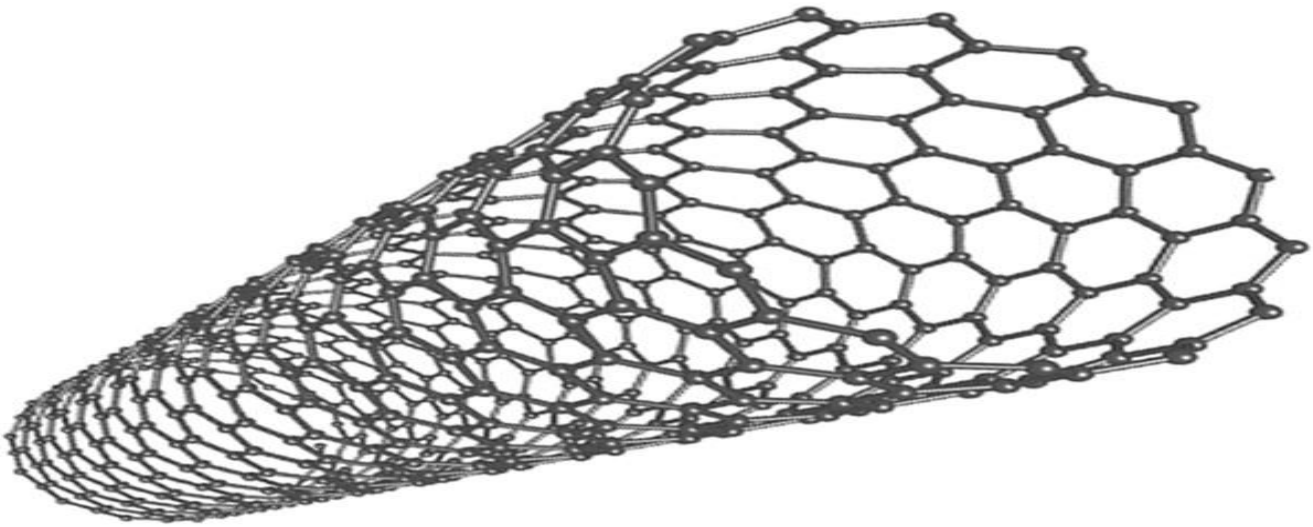

Figure 2.5: Single Wall Nanotube (SWNT)

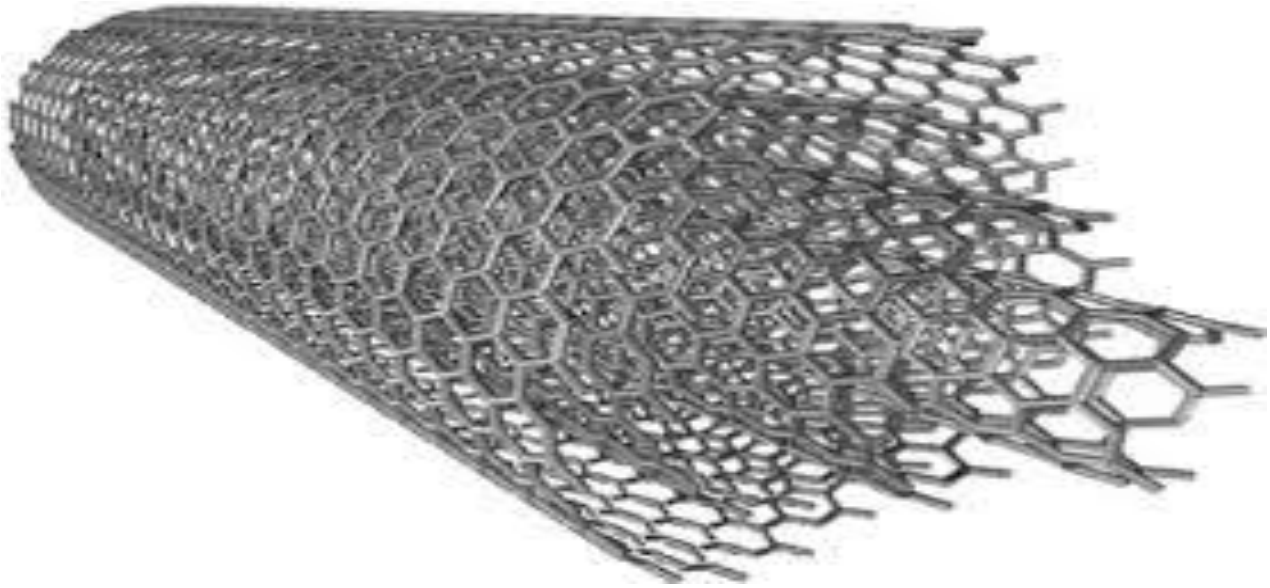

Figure 2.6: Multi Wall Nanotube (MWNT)

2.2.1 Physical Structure of CNT

SWNTs are more pliable than their multi-walled counterparts and can be twisted, flattened and bent into small circles or around sharp bends without breaking [18]. They can be conducting, like metal or semiconducting, which means that the flow of current through them can be controlled by varying an electrical field. Whereas, multi-walled carbon nanotubes are basically like Russian dolls made out of

SWNTs concentric cylindrical graphitic tubes. In these more complex structures, the different SWNTs that form the MWNT may have quite different structures (length and chirality). MWNTs are typically 100 times longer than they are wide and have outer diameters mostly in the tens o f nanometers. Although it is easier to produce significant quantities of MWNTs than SWNTs, their structures are less well understood than single-wall nanotubes because of their greater complexity and variety. Multitudes of exotic shapes and arrangements, often with imaginative names such as bamboo-trunks, sea urchins, necklaces, or coils, have also been observed under different processing conditions. The variety of forms may be interesting but also has a negative side—MWNTs always (so far) have more defects than SWNTs and these diminish their desirable properties [18].

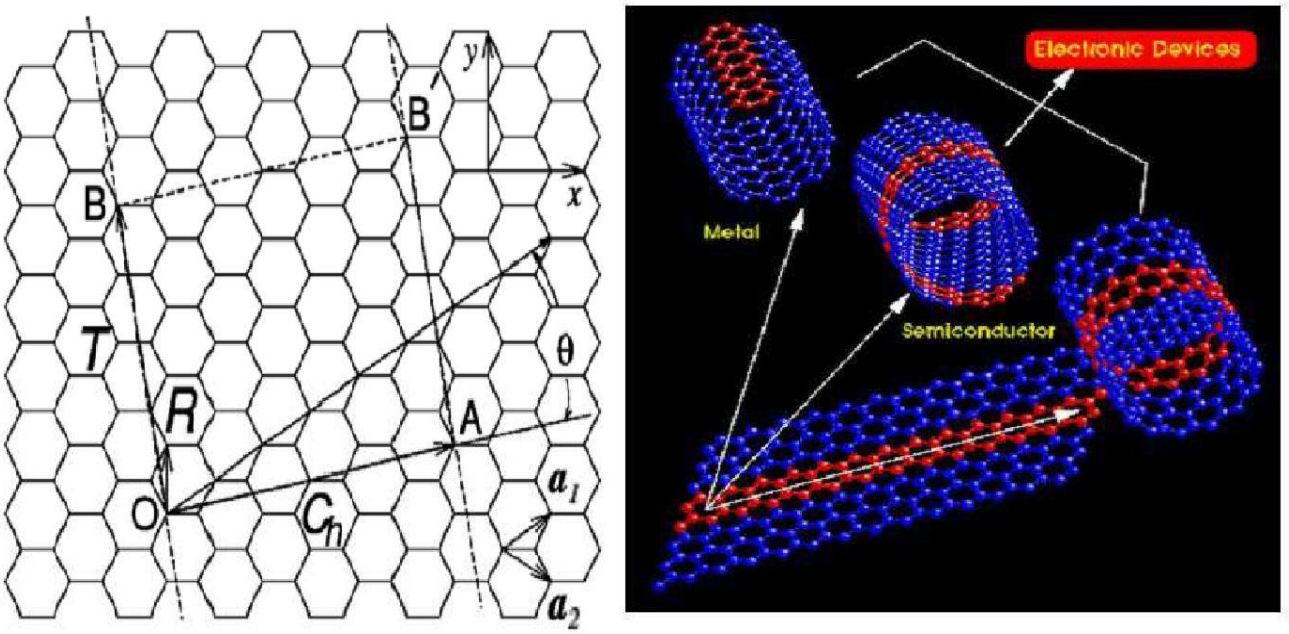

Figure 2.7: Graphene sheet [14] and rolling graphene sheet to create carbon nanotube [19].

A SWNT is described as a graphene sheet rolled up into a cylindrical shape with axial symmetry, exhibiting a spiral conformation called chirality [18]. Graphene has a hexagonal structure, and rolling up the graphene sheet in different directions and diameter would yield the nanotubes with different symmetries, which induces different electronic structures. Since electronic properties of SWNTs depend on their structures, it is very important to find a way to specify the geometric structure of a SWNT. As shown in Fig. 2.7, we can roll up the graphene sheet alone vector OA, which is perpendicular to the nanotube axis in the direction of OB. Here, we can see that O, A, B and B' are four crystallographically equivalent sites. By rolling up the paper plane and making OB overlap with AB', we get a seamless single-walled tubular structure. Then it would be straightforward to define the

vectors C_h =*OA* as chiral vector and *T*=*OB* as translational vector. If we use a1 and a2 as the base vectors of graphene 2-D crystal lattice, we can have the chiral vector as [20]:

$$C_h = na_1+ma_2 = (n, m) \quad (2.3)$$

$$0 \leq m \leq n.$$

The way the graphene sheet wraps can be represented by a pair of indices (n, m) called the chiral vector. The relationship between n and m defines three categories of CNTs. Arm chair (n = m) and chiral angle equal to 30°); zigzag (n = 0 or m = 0 and chiral angle equal to 0°); and chiral (other values of *n* and *m* and chiral angles lie between 0 and 30°) [21] [22] [23]. These are shown in figure 2.8

$$C_h= a/\sqrt{n^2 +m^2 +n} \quad (2.4)$$

Where, a = 2.49 Å.

$$d_t(\text{diameter})= C_h / \pi \quad (2.5)$$

$$\theta(\text{chiral angle})=\arccos (2n+m/2\sqrt{n^2 +m^2 +nm}) \quad (2.6)$$

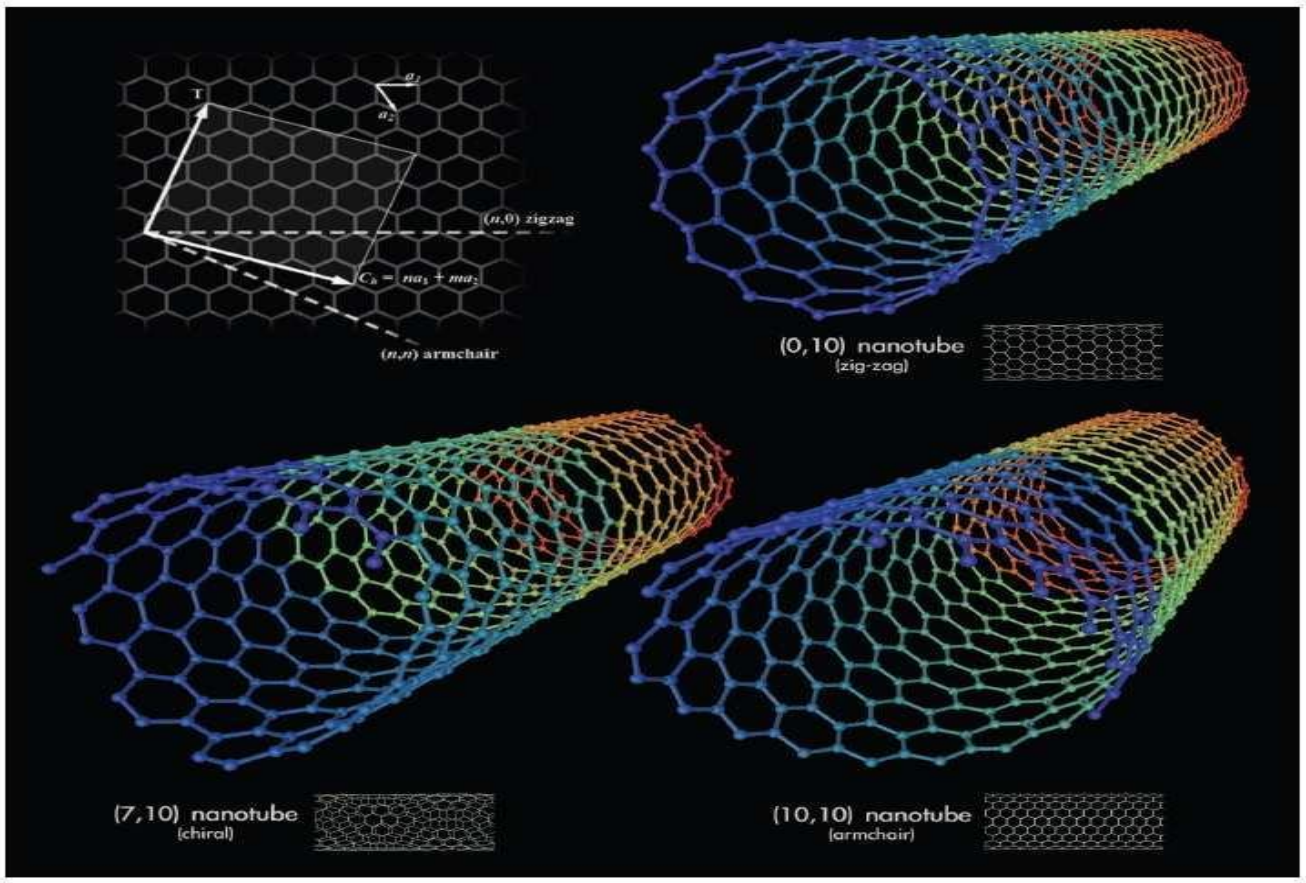

Figure 2.8: 3D model of the three types of single walled carbon nanotubes [21].

Table 2.2: Young's modulus, Tensile strength, and density of carbon nanotubes compared with other materials [21]

Material	Young's Modulus(Gpa)	Tensile Strength (Gpa)	Density (g/cm3)
Single wall nanotube	1054	150	
Multi wall nanotube	1200	150	2.6
Steel	208	0.4	7.8
Epoxy	3.5	0.005	1.25
Wood	16	0.008	0.6

Table 2.3: Some parameters for carbon nanotubes [21]

Average diameter of SWNTs	1.2-1.4 nm
Distance from opposite carbon atoms (Line 1)	2.830 Å
Analogous carbon atom separation (Line 2)	2.456 Å
Parallel carbon bond separation (Line 3)	2.450 Å
Carbon bond length (Line 4)	1.420 Å
C-C tight bonding overlap energy	~ 2.50 eV
Group symmetry (10, 10)	C5V
Interlayer spacing:	
(n, n) Armchair	3.380 Å
(n, 0) Zigzag	3.410 Å
(2n, n) Chiral	3.390 Å
Optical properties	
Fundamental gap:	
For (n, m); n-m is divisible by 3 [Metallic]	0 eV
For (n, m); n-m is divisible by 3 [Semiconducting]	~0.5 eV
Maximum current density	1013 A/m2
Thermal transport	
Thermal conductivity (room temperature)	~ 2000 W/m K
Phonon mean free path	~ 100 nm
Relaxation time	~ 10-11 s
Elastic behavior	
Young's modulus (SWNT)	~ 1 TPa

2.2.2 SWNT Characteristics of Electrical Transport

A determination of the band structure allows for the calculation of an energy dependent Drude conductivity for the graphene sheet that constitutes a nanotube surface, as $\left(\frac{2e^2}{h}\right)\frac{E}{\hbar v_F}\, l_e$. Here the elastic scattering length (l_e) of the carriers is proportional to the electron-phonon scattering and generally increases with decreasing temperature .One characterize the electrical conductivity in two regimes:

- Low temperatures (kBT<EF), where in the conductivity equation above, the energy (E) replaced by EF (the Fermi energy).The conductivity in this regime is metallic. A finite zero-temperature value, the magnitude of which is determined by the static disorder, is obtained.
- High temperatures (kBT>EF), where in the conductivity equation, the energy (E) is replaced by kBT. The conductivity, and the carrier density, is then directly proportional to T.

At the very outset, it is not trivial to measure the intrinsic resistance of a SWNT. Any contact in addition to those at the two ends of the tube can destroy the one-dimensional nature of the SWNT and make a true interpretation difficult. Theoretically, for a strictly one-dimensional system the Landauerm formula predicts an intrinsic resistance, independent of the length is equal to $h/e^2\ (1/T\ (E_f))$. Assuming perfect transmission through ideal Ohmic contacts, i.e., T (E_F) equal to one. This contact resistance arises from an intrinsic mismatch between the external contacts to the wire (which are of higher dimensionality) and the one-dimensional nanotube system and is always present. When one takes individually into account both the two-fold spin and band degeneracy of a nanotube the intrinsic resistance (R_{int}) now becomes: $(R_{int})= h/4e^2(1/T(E_f))$, which again seems length independent [24] [25].

However, in the above discussion, we have not yet considered the contribution of the external contacts. When we consider the transmission (T) through the contacts into the one dimensional channel and then to the next contact, $T=l_e/l_e+L$, where l_e is the mean free path length for scattering and L is the length of the one-dimensional conductor. The resistance is now equal to:

$$\frac{h}{4e^2}\,\frac{l_e+L}{l_e} \equiv \frac{h}{4e^2}\,\left(1+\frac{l_e}{L}\right) \qquad (2.7)$$

The first term represents *Rint* while the second term denotes an Ohmic resistance *(ROhmic)* associated with scattering. In the presence of dynamically scattering impurities, such as acoustical or optical phonons, which are inevitably present at any temperature above 0 K, the Ohmic resistance should definitely be considered. It is interesting to consider the limiting cases of a large mean free path ($l_e\rightarrow$ infinity) or a small tube (L→ 0) i.e., in the ballistic regime, when the Ohmic resistance is seen to

vanish. Finally, the material resistance of the contacts contributes an additional term: Rc. The total resistance as measured in an external circuit would now be: *R = Rint +ROhmic +Rc.* These considerations imply that a minimum resistance of *h/4* (~6.5 kohm) is present in a SWNT with a single channel of conduction. In practice however, imperfect contacts (which lead to T<1) and the presence of impurities lead to larger resistance values, while deviations from strict one-dimensionality or multiple channels of conduction (as in a MWNT) could lead to smaller numbers for the resistance[24].

2.3 Carbon Nanotube field effect Transistor

2.3.1 Structure of CNTFET

The first carbon nanotube field-effect transistors were reported in 1998. These were simple devices fabricated by depositing single-wall CNTs (synthesized by laser ablation) from solution onto oxidized Si wafers which had been pre-patterned with gold or platinum electrodes. The electrodes served as source and drain, connected via the nanotube channel, and the doped Si substrate served as the gate. A schematic of such a device is shown in Fig. 2.9 Clear p-type transistor action was observed, with gate voltage modulation of the drain current over several orders of magnitude. The devices displayed high on-state resistance of several MΩ, low transconductance (-Ins) and no current saturation, and they required high gate voltages (several volts) to turn them on [1] [12].

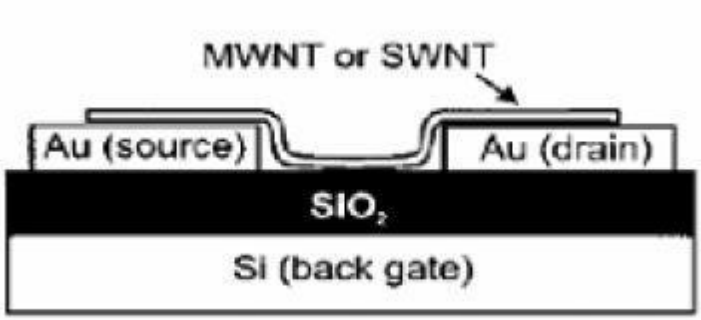

Figure 2.9: Early CNTFET structure [12].

Following these initial CNTFET results advances in CNTFET device structures and processing yielded improvements in their electrical characteristics. Rather than laying the nanotube down upon the source and drain electrodes, relying on weak van der Waals forces for contact, the electrodes were patterned on top of previously laid down CNs [2]. In addition to Au, Ti and CO were used, with a thermal annealing step to improve the metal/nanotube contact. In the case of Ti, the thermal

processing leads to the formation of TiC at the metal/nanotube interface, resulting in a significant reduction in the contact resistance - from several MΩ to – 30 kΩ. On-state currents ~1 μA were measured, with transconductance - 0.3 μS. All early CNTFET were p-type, i.e., hole conductors.
Whether this was due to contact doping or doping by the adsorption of oxygen from the atmosphere was initially unclear. N-type conduction was achieved by doping from an alkali (electron donor) gas and by thermal annealing in vacuum. Doping by exposure to an alkali gas involves charge transfer within the bulk of the nanotube, analogous to doping in conventional semiconductor materials [25]. On the other hand, annealing a CNTFET in vacuum promotes electron conduction via a completely different mechanism: the presence of atmospheric oxygen near the metal/nanotube contacts affects the local bending of the conduction and valence bands in the nanotube by way of charge transfer, and the Fermi level is pinned close to the valence band, making it easier for injection of holes. When the oxygen is desorbed at high temperatures, the Fermi level may line up closer to the conduction band, allowing injection of electrons. Contrary to the case of bulk doping, there is no threshold voltage shift when going from p-type to n-type by thermal annealing. In addition, it is possible to achieve an intermediate state, in which both electron and hole injection are allowed, resulting in ambipolar conduction. The ability to make both p-type and n-type CNTFETs enabled the first carbon nanotube CMOS circuits. These were demonstrated by Derycke et al., who built simple CMOS logic gates, including an inverter in which the two CNTFETs were fabricated using a single carbon nanotube. Subsequently, more complex CN-based circuits have been built as well [1]. Carbon nanotube field effect transistor (CNTFETs) uses semiconducting carbon nanotube as the channel. Both p-channel and n-channel devices can be made from nanotubes. The physical structure of CNTFETs is very similar to that of MOSFETs and their I-V characteristics and transfer characteristics are also very promising and they suggest that CNTFETs have the potential to be a successful replacement of MOSFETs in nanoscale electronics. Of course, there are some distinct properties of CNTFETs, such as:

- The carbon nanotube is one-dimensional, which greatly reduces the scattering probability. As a result the device may operate in ballistic regime.
- The nanotube conducts essentially on its surface where all the chemical bonds are saturated and stable. In other words, there are no dangling bonds which form interface states. Therefore, there is no need for careful passivation of the interface between the nanotube channel and the gate dielectric, i.e. there is no equivalent of the silicon/silicon dioxide interface.
- The Schottky barrier at the metal-nanotube contact is the active switching element in an intrinsic nanotube device.

Because of these unique features CNTFET becomes a device of special interest. The field effect transistors made of carbon nanotubes so far can be classified into two types:

a) Back gate CNTFET
b) Top gate CNTFET

2.3.2 Back Gate CNTFET

CNTFET was first demonstrated in 1998 by Tans et al. [26] to show a technologically exploitable switching behavior and this work marked the inception of CNTFET research progress. In this structure a single SWNT was the bridge between two noble metal electrodes on an oxidized silicon wafer. The silicon oxide substrate can be used as the gate oxide and adding a metal contact on the back makes the semiconducting CNT gateable. Here the SWCNT plays the role of channel and the metal electrodes act as source and drain. The heavily doped silicon wafer itself behaves as the back gate. These CNTFETs behaved as p-type FETs with an I (on) / I (off) ratio~10^5 [27]. This suffers from some of the limitations like high parasitic contact resistance (≥1Mohm), low drive currents (a few nanoamperes), and low transconductance gm ≈ 1nS. To reduce these limitations the next generation CNTFET developed which is known as top gate CNTFET.

2.3.3 Top Gate CNTFET

To get better performance Wind et al. proposed the first top gate CNTFET in 2003 [27]. In the first step, single-walled carbon nanotubes are solution deposited onto a silicon oxide substrate. Then by using either atomic force microscope or scanning electron microscope the individual nanotubes are located. After which, source and drain contacts are defined and then patterned using high resolution electron beam lithography. High temperature annealing reduces the contact resistance and also increases union between the contacts and CNT. A thin top-gate dielectric is then deposited on top of the nanotube, either via evaporation or atomic layer deposition. Finally, the top gate contact is deposited on the gate dielectric. Arrays of top-gated CNTFETs can be fabricated on the same Silicon wafer, since the gate contacts are electrically isolated from each other, unlike in the back-gated case. Also, due to the thinness of the gate dielectric, a larger electric field can be generated with respect to the nanotube using a lower gate voltage. These advantages mean top-gated devices are generally favored over back-gated CNTFETs, regardless of their more complex fabrication process [28].

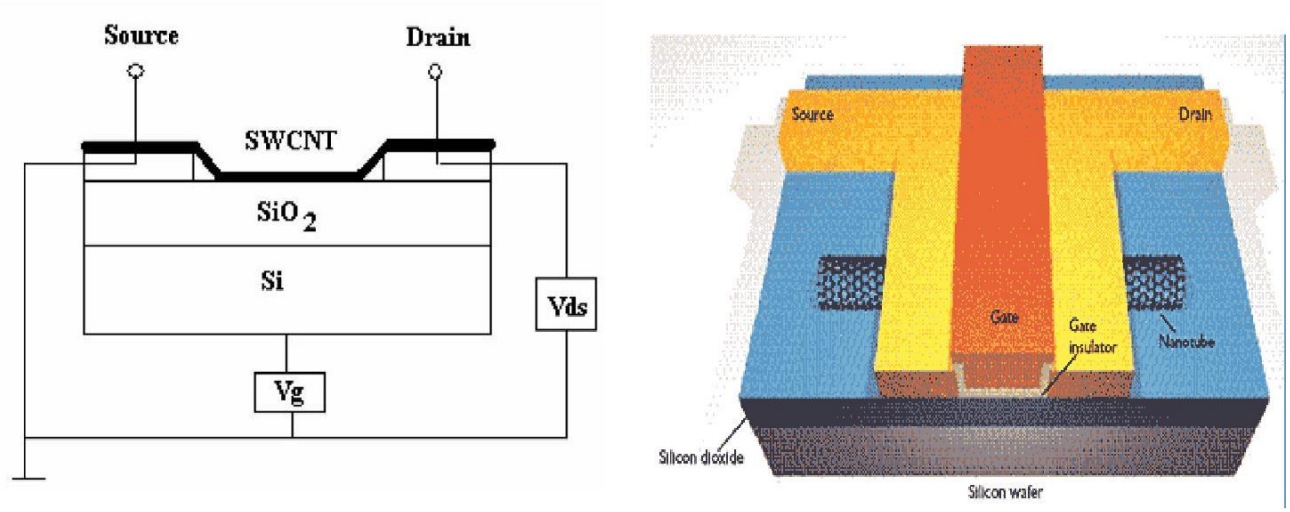

Figure 2.10: (a) Back gate CNTFET [29], **(b)** Top gate CNTFET [Source- Internet image].

Table 2.4: Comparison between Back gate CNTFET and Top gate CNTFET [29]

Parameters	Back gate CNTFET	Top gate CNTFET
Threshold voltage	-12V	-0.5V
Drain current	Of the order of nanoampere	Of the order of microampere
Transconductance	1nS	3.3μS
I(on)/I(off)	10^5	10^6

2.3.4 Schottky-barrier (SB) CNTFET

Normally, a potential barrier known as Schottky barrier (SB) exists at every contact between metal and semiconductor. The barrier height is determined by the filling of metal-induced gap states. These states become available in the energy gap of semiconductor due to interface formed with the metal. The SB is controlled by the difference of the local work functions of the metal and the carbon nanotube. SB is also extremely sensitive to changes of local environment at the contact [30]. For example, gas adsorption changes the work function of metal surfaces. Since this device employs metal as its source/drain terminals and has Schottky barrier at its terminal contact between nanotube and metal, therefore it is called Schottky-barrier CNTFET (SB-CNTFET). Diagram of SB-CNTFET is shown in Figure 2.11.

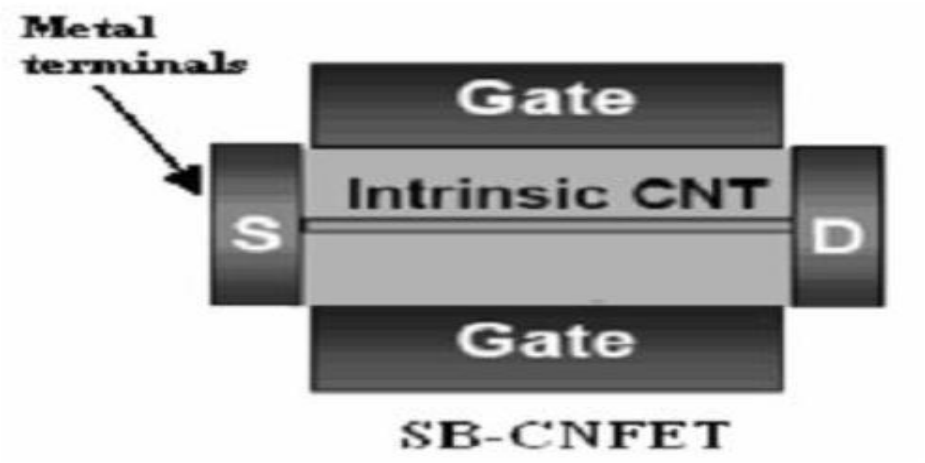

Figure 2.11 Diagram of a SB-CNTFET [12].

SB-CNTFET works on the principle of direct tunneling through the Schottky barrier at the source-channel junction. The barrier width is controlled by the gate voltage and hence the transconductance of the device depends on the gate voltage. At low gate bias, large barrier limits the current in the channel. As gate bias is increased, it reduces the barrier width, which increases quantum mechanical tunneling through the barrier, and therefore increases current flow in transistor channel. In SB-CNTFET, the transistor action occurs by modulating the transmission coefficient of the device [4] [10] [31] [32].

SB-CNTFET shows very strong ambipolar conduction particularly when the gate oxide thickness is reduced even the Schottky barrier is zero [31]. This type of conduction causes leakage current to increase exponentially with supply voltage especially when the nanotube diameter is large, which results in limiting device potential. Thus, ambipolar conduction must be reduced in order to improve the performance of SB-CNTFET. One of the solutions is to increase the gate oxide thickness. If the gate oxide thickness is high, there is no ambipolar conduction exists when Schottky barrier is zero. Hence, the leakage current is reduced and as a result, the transistor performance is improved. Another alternative is to build asymmetric gate oxide, which is has been proposed recently, in order to suppress the ambipolar conduction [32] [30].

Another issue regarding on SB-CNTFET is that this type of transistor suffers from metal-induced-gap states which limit minimum channel length and thus increases source to drain tunneling. SB-CNTFET is also unable to place gate terminal close to source because it can increase parasitic capacitance.

2.3.5 MOSFET-like CNTFET

The structure of this device is slightly dissimilar to SB-CNTFET since it uses heavily doped terminals instead of metal. This was formed in order to overcome problems in SB-CNTFET and operates like MOSFET. Unlike SB-CNTFET, source and drain terminals are heavily doped like MOSFET and hence it is called as MOSFET-like CNTFET. This device, as shown in Figure 2.12, operates on the principle of modulation the barrier height by gate voltage application. The drain current is controlled by number of charge that is induced in the channel by gate terminal.

This type of transistor has several advantages over SB-CNTFET. This device is able to suppress ambipolar conduction in SB-CNTFET. It also provides longer channel length limit because the density of metal-induced-gap-states is significantly reduced. Parasitic capacitance between gate and source terminal is greatly reduced and thus allows faster operation of the transistor. Faster operation can be achieved since length between gate and source/drain terminals can be separated by the length of source to drain, which reduces parasitic capacitance and transistor delay metric. It operates like SB-CNTFET with negative Schottky barrier height during on-state condition and thus it delivers higher on-current than SB-CNTFET. Previous work has shown that this type of device gives higher on-current compared to SB-CNTFET and therefore it can justify the upper limit of CNTFET performance. Based on the device performance, it is obvious that this device can be used to investigate the ballistic transport in CNTFET [33] [34].

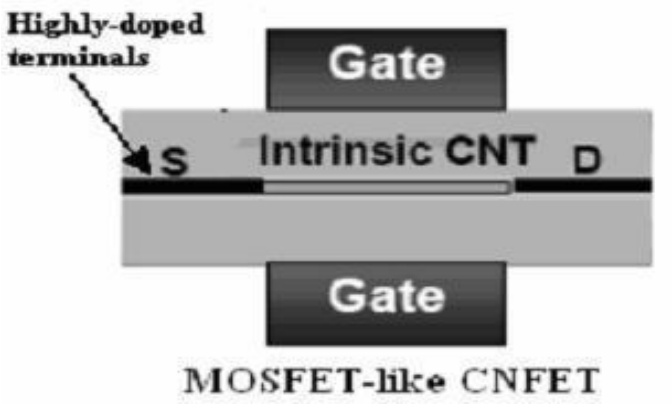

Figure 2.12: MOSFET-like CNTFET [35].

2.3.6 Vertical CNTFET (V-CNTFET)

The latest development in CNTFET progress could be the initiation of vertical CNTFET. This structure with surround-gated is suggested by Choi *et al.* in 2004 [12]. The transistor size can be as small as the diameter of carbon nanotube which corresponds to tera-level CNTFET and density of 10^{12} elements per cm^{-2}.The vertical CNTFET is prepared through the following steps: nano-pore formation by anodization followed by synthesizing the carbon nanotube, metal-electrode formation, oxide deposition and patterning and finally gate electrode formation. The silicon oxide was deposited at the top of aligned carbon nanotube by electron gun evaporation and followed by holes formation of e-beam patterning and chemical etching. The silicon oxide deposition process is then followed by deposition of top gate electrode. The structure of vertical CNTFET is illustrated in Figure 2.13. In this structure, each carbon nanotube is electrically attached to bottom electrode, source, upper electrode (drain) and gate electrode is put around the carbon nanotube. Each cross point of source and drain electrodes corresponds to a transistor element with a single vertical carbon nanotube. The number of carbon nanotube in transistor depends on the hole-diameter of gate oxide. The vertical CNTFET allows higher packing densities that can be achieved since source and drain areas can be arranged on top of each other [36]. On the other hand, real 3-D structures can be made possible because the active devices are no longer bound to the surface of mono-crystalline silicon wafer.

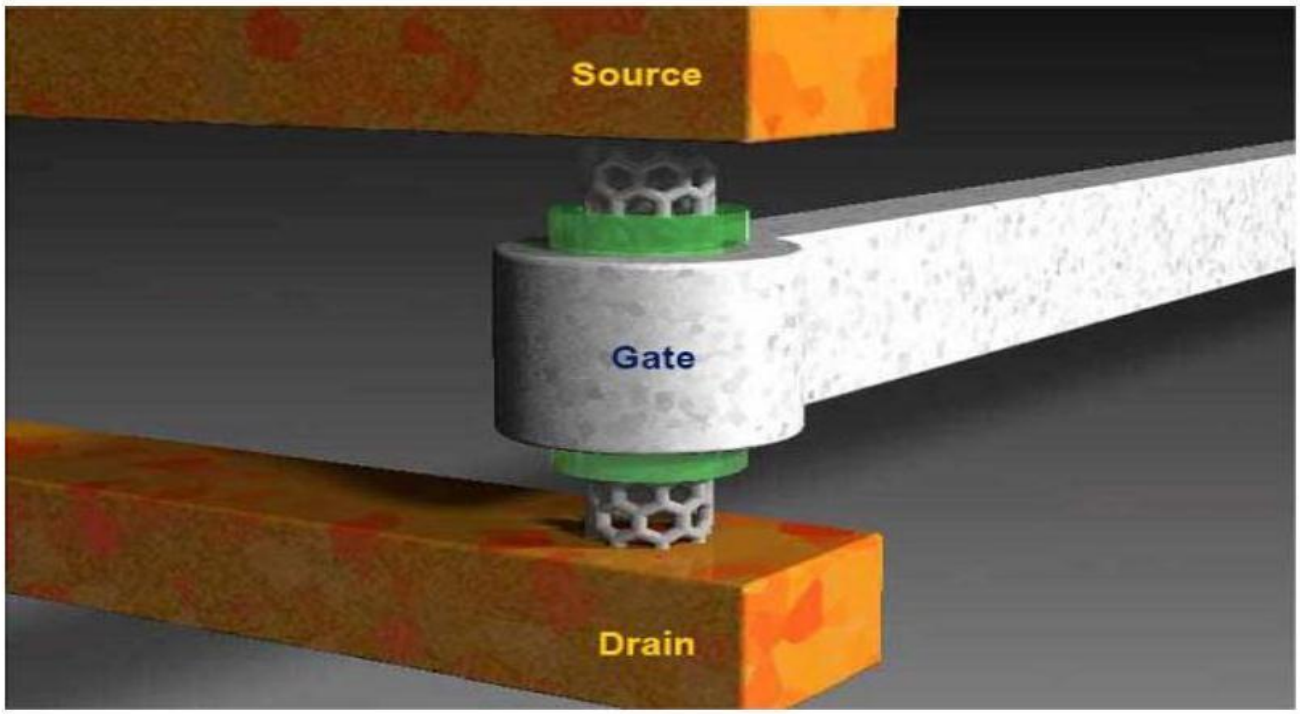

Figure 2.13: Structure of Vertical CNTFET [2]

2.4 Introduction to Graphene

Taking the shape of sheer thin, almost transparent like one atom thick Graphene composed of pure carbon. It has extraordinary tensile strength being 100 times compared to that of steel despite of being so light [37]. It also possesses sheer electrical and thermal conductivity [38]. First isolated in a lab in 2004 [39]. Such qualities as mentioned herewith make it highly potential for flexible conductors.

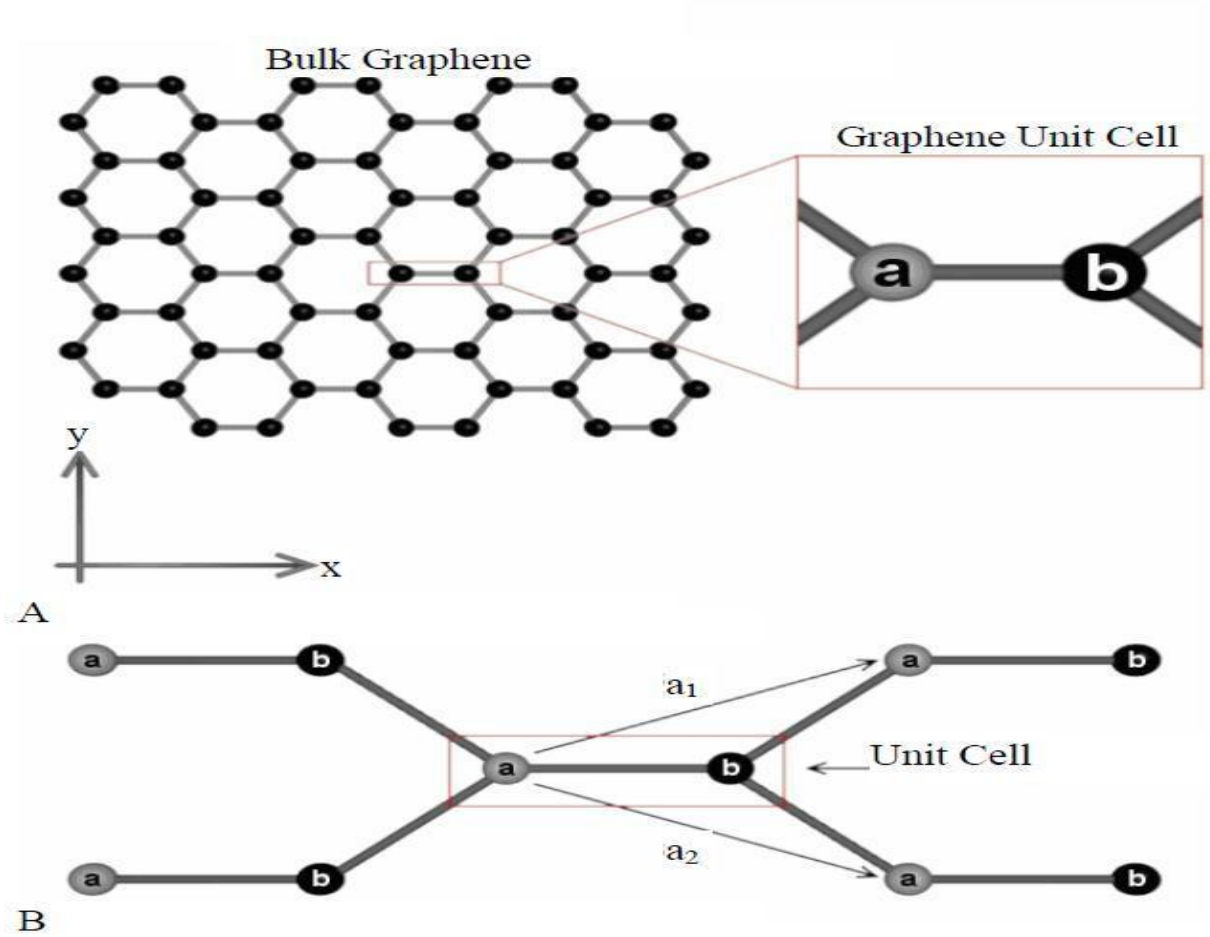

Figure 2.14: Unit cell of graphene. A) Image of bulk graphene, with a unit cell show in the inset. B) Unit cell of graphene demonstrating its four nearest neighbors [40].

The allotrope of carbon, graphene has a 2-dimensional property. Mainly it consists of a lattice structure of carbon atoms in the sp^2 hybridization state. As depicted in figure 2.14 [41] each unit of graphene lattice cell contains two carbon atoms that contributes one extra electron each to this vast ocean of electron. In the atomic lattice the carbon atoms are closely packed in a typical sp^2 bonded atomic-scale chicken wire (hexagonal) pattern. If stated plainly graphene is just a thick one-atom layer of graphite. The basic structure of other allotropes of carbon, charcoal, carbon nanotube and fullerenes constitute are the same.

Scientists initially were not atoned with the idea of separating graphene sheets despite of it being known that graphite comprised of hexagonal carbon sheets layered on top of one another. A revolution was brought about by Konstantin Novoselov, Andre Geim when they along with their collaborators put forward that a layer could be separated from graphite and such few layers could electrically characterized. Their electrical measurement for a single layer was published in July 2005 and as such introduced the scientific fraternity to the graphene concept. [34] Figure 2.15 shows three separate structures made of honeycomb lattice.

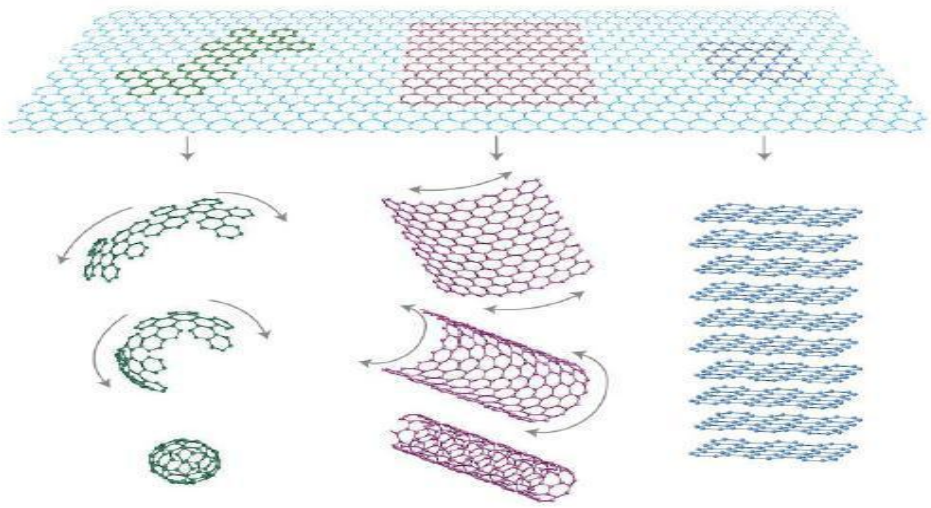

Figure 2.15: Structures made of graphene - fullerene molecules, carbon nanotubes, and graphite can all be thought of as being formed from graphene sheets, i.e. single layers of carbon atoms arranged in a honeycomb lattice [42].

2.4.1 Synthesis of Graphene

For decades in order to improve mass production techniques to generate high quality graphene rigorous research has been going on [43]. Since the invention of x-ray diffraction crystallography the graphite structure is widely known. Solution based exfoliation of graphite gave a unreasonable idea about the atomic planes of carbon [44]. In order to get monolayers in solution Boehm put forward the concept of lowering exfoliated graphite oxide [45]. Several successful venture accounts of producing monolayers of carbon in graphitic structures, on various carbides [46] [47] [48] and transition metal surfaces, [48-53] are there, of which the most praiseworthy is Van Bommel's journey with SiC [54]. Since the tightly bound metallic surfaces interrupt the perpendicular pi-orbitals, with SIC being a special case, these studies did not reinforce the observation for any electronic properties. Synthesis techniques can be categorized into micromechanical exfoliation, solution-based and chemically assisted exfoliation, chemical synthesis, epitaxial growth through sublimated SiC surfaces, and the

pyrolysis of hydrocarbons on metal surfaces. In aspect of quality, processability, scalability & cost each has its own pros, cons and distinctive features.

2.4.1.1 Exfoliation

2.4.1.1.1 Mechanical Cleavage

Using this technique bulk graphite can be isolated into single atomic planes. Before the 'Scotch tape Method" [54-57] was introduced scrutinizing isolated layers of graphene was nonviable. Micromechanical cleavage of bulk graphite often been used to produce graphene samples of high quality also termed peeled graphene. To pare layer off highly oriented pyrolytic graphite it uses adhesive tape, which is then pulverized onto a proper substrate which is generally oxidized silicon. This technique induce low output and largely used for the study of underlying properties of ballistic transport, carrier mobility, thermal conductivity and the likes. This method is not feasible and efficient although it produces quality graphene layers [57-63].

2.4.1.1.2 Solution and Chemical Exfoliation

This particular technique has the capability of producing graphene in bulk. By installing reactants between layers than causes the cohesive Van Der Waals force [64] to weaken, bulk graphite is intercalated. Successful high-quality, single-layer graphene sheets, stably suspended in organic solvents were produced by Dai's group in steps of chemical intercalation, reintercalation, and sonication[65]. Expandable graphite firstly is suspended in sulfuric & nitric acid, where the exfoliated particles are still thick. This step is subsequently followed by oleum treatment with tetra-butyl alcohol reintercalation to ensure the graphene is of high quality. Next sonification is done based on AFM measurement immersed in a surfactant solution. Sonicating graphite powder in N-methylpyrroidone[66] a liquid exfoliation process came into being which helps produce graphene. Weeks of low power sonification to avoid damage to graphene sheets generate high concentration (up to 1.2 mg/mL up to 4 wt %) of monolayer graphene [67]. Sonication-free, mild dissolution of graphite by synthesizing well-documented GICs bearded large graphene flakes and ribbon [68].

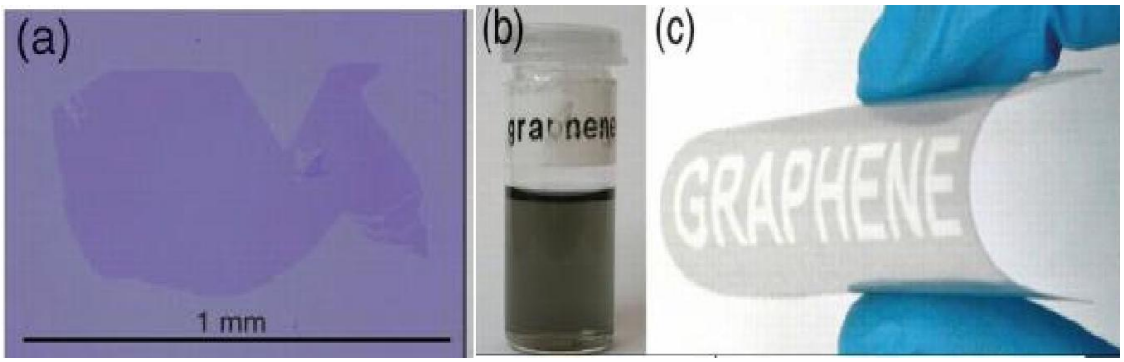

Figure 2.16: Exfoliated graphene. a) Optical microscopy image of a very large micromechanically exfoliated (tape method) monolayer of graphene. Note the considerable contrast for the single atomic layer. b) Photograph of dispersed graphene by ultrasonic exfoliation of graphite in chloroform and (c) that deposited on a bendable film [69].

2.4.1.1.3 Oxidation and Reduction

A more potent technique which provides high yields of graphene is to synthesize graphite oxide first followed with exfoliation into monolayers, followed by the removal of oxygen groups by reduction[71- 72]. Huge numbers of negative charges are carried by every single oxidized flake that repel each other. The Brodie, Staudenmeier and Hummers methods are the three most familiar ways to oxidize graphite. Of all these the Hummers method has become the most popular subject to some slight modification in producing graphite oxide, for its comparatively lesser reaction time and the absence of toxic byproducts[72]. As a result of oxidation the interlayer gap increases from 0.34 nm to more than 0.6 nm, with delicate van der Waals forces in between layers. Exfoliation is generally suplemented with sonication[73], generating single layers of graphene oxide[74] which are water soluble without aid of surfactants to form unfaltering colloidal system. Using chemical [75], thermal [76], electrochemical [77] or electromagnetic flash [78], laser-scribe techniques [79], etc the GO is then minimized.

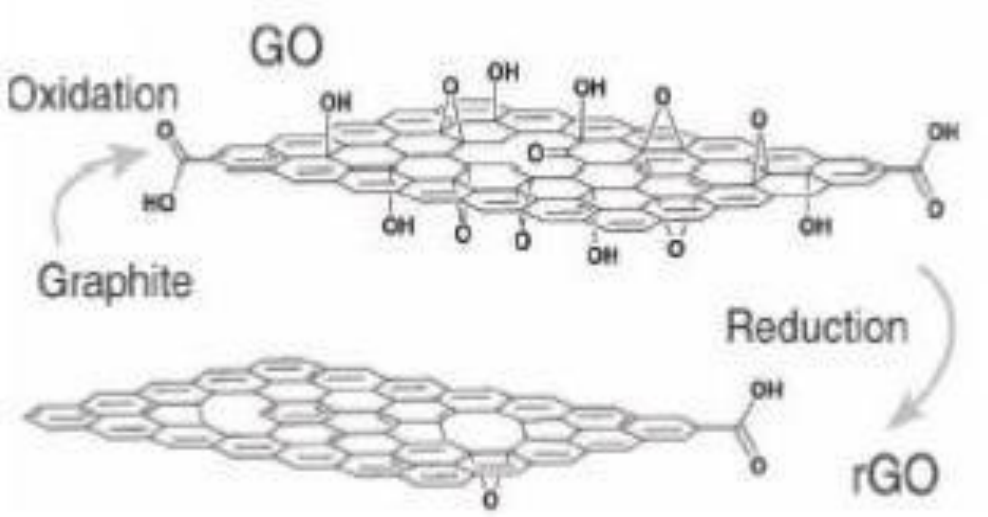

Figure 2.17: Synthesis of graphene by oxidation and reduction. Graphene oxide and reduced graphene oxide showing the remaining oxygen-rich functional groups after reduction [69].

2.4.1.2 Chemical Vapor Deposition

The Chemical vapor deposition technique demonstrates great potential of scalability for production of single and multi layered graphene films. Wafer size graphene films have developed on both single and poly crystalline, invariably, in transition metal surfaces in high temperature such as of methane[80-84] a result of pyrolysis of hydrocarbon precursors. Layers of graphene are variably dependent on carbon solubility of the substrate. Metals with high carbon solubility, the atoms of carbon can disintegrate at high temperature and as a result precipitate onto the surface of the metal to form develop into single or multilayered graphite films upon cooling. Films with such non uniform structures ranging from 1-10 layers along with mono layer domain integrate up to several micrometers in diameters on nickel [85-87] substrate [88].The rate of cooling and hydrocarbon gas concentration dictates the thickness and crystal ordering. Moreover, low carbon solubility in few transition metals like copper [89] and platinum [90] allows complete monolayer presentation [91].

2.4.1.3 Chemical Synthesis

Through bottom-up organic synthesis a controlled production of graphene can be achieved. It can be composed of as a interconnected pattern of polycyclic aromatic hydrocarbons (PAHs) which are tiny two dimensional segments of graphene. Due to its high flexibility and compatibility with different organic synthesis techniques [92] this way of doing is appealing. The pioneers in this field are Mullen & his coworkers announcing synthesis of nanoribbon like PAHs with lengths over 30 nm [93-94]. Lately the biggest stable colloidal graphene quantum dots were synthesized with the help of a

benzene-based chemical route which composed of 132, 168 & 170 mixture of carbon atoms [95-96]. Due to the decreasing solubility however the graphene dots are inhibited in size resulting in increased size and more side reactions which are still now the main hurdle for organic synthesis of controllable shapes, sizes and edge structured graphene molecules.

2.4.2 Properties of Graphene

2.4.2.1 Structure

Due to a closely packed periodic aray of atoms and of carbon a sp^2 orbital hybridization - a combination of orbitals p_x and p_y that constitute the σ-bond graphene is basically a steadfast material. It has three σ-bonds and one π-bond. Final pz electron makes up the π-bond, and is key to the half-filled band that allows free-moving electrons[98].The structure of isolated single layered graphene i.e atomic structure was studied with the help of transmission electron microscopy (TEM) suspended on a metallic bar grid[98] upon sheets of graphene. The expected honeycomb lattice resulted the electron diffraction patterns.

2.4.2.2 Electronic

Graphene is a semi-metal or zero-gap semiconductor. It is distinguished from other condensed matter systems as a result of four electronic properties.

2.4.2.2.1 Electronic spectrum

Electrons that proliferate due to graphenes honeycomb lattice structure produce quasi-particles by losing their mass and that which is illustrated by a 2D analogue of the Dirac equation rather than the Schrödinger equation for spin-1⁄2particles[99][100].

2.4.2.2.2 Dispersion Relation

Using a conventional tight-bonding model given the electron energy with wave vector k the dispersion relation is [101][102].

$$E = \pm\sqrt{\gamma_0^2(1 + 4\cos^2\frac{k_y a}{2} + 4\cos\frac{k_y a}{2}.\cos\frac{k_x\sqrt{3}a}{2}} \qquad (2.8)$$

With the nearest-neighbor hopping energy $\gamma 0 \approx 2.8$ eV and the lattice constant $a \approx 2.46$ Å. The conduction and valence bands equate to the different signs; touch each other at six points, "K-values"

of the two-dimensional hexagonal Brillouin zone. Of these six points two are independent which the rest are symmetrical. Around the K points the energy relies directly on the wave vector as is the case to a relativistic particle [101][103].Since an elementary cell of lattice has a two basis atom, the wave function has an effective 2-spinor structure.

As a matter of which even the true spin,at low energy, the electrons can be stated by an equation that is equivalent to the massless Dirac equation. Thus, the holes and the electrons are are known as Dirac fermions and the six corners are called Dirac points.As a consequence, at low energies, even neglecting the true spin, the electrons can be described by an equation that is formally equivalent to the massless Dirac equation. Hence, the electrons and holes are called Dirac fermions and the six corners are called the Dirac points[98].This pseudo-relativistic description is restricted to vanishing rest mass *M*0, which leads to interesting extra features[101][105]:

$$v_F \vec{\sigma} \cdot \nabla \psi(\mathbf{r}) = E\psi(\mathbf{r}). \qquad (2.9)$$

The Fermi velocity in graphene here is illustrated as *vF* ~ 106 m/s (.003 c) which in the Dirac theory substitutes the velocity of light; $\vec{}$ is the vector of the Pauli matrices, is the two-component wave function of the electrons, and *E* denotes their energy[99].

The equation is as describing the linear dispersion relation is:

$$E = \hbar v_F \sqrt{k_x^2 + k_y^2}; \qquad (2.10)$$

the wavevector *k* is measured from the Dirac points. The equation uses a pseudospin matrix formula that describes two sublattices of the honeycomb lattice [103].

2.4.2.2.3 Single-atom wave propagation

Waves of electron in a graphene proliferate within a single layer of atom thus making them vulnerable in the vicinity of materials such high-κ dielectrics, superconductors and ferromagnetic.

2.4.2.2.4 Electronic Transport

Results derived from transport measurement imply that at room temperature graphene has tremendous high electron mobility, with values exceeding 15,000 $cm^2 \cdot V^{-1} \cdot s^{-1}$[106].Moreover the measured symmetrical conductances highlights that hole and electron mobilities are almost the same [100].This mobility is free of temperature in between the range of 10k and 100k [107-109] pointing that the main scattering mechanism is defect scattering. Intrinsically room temperature mobility is limited to

200,000 $cm^2 \cdot V^{-1} \cdot s^{-1}$ at a carrier density of 1012 cm^{-2} by the scattering of the acoustic phonons of graphene, later on which was presented and exceeds that of copper[111].

The peripheral resistivity should be in order of 10^{-6} Ω·cm for the graphene sheet. This is lower than the familiar resistivity at room temperature. The corresponding resistivity of the graphene sheet should be in the order of 10^{-6} Ω·cm. this is lowered than the typical resistivity at room temperature. Graphene on SiO2 substrates, scattering of electrons by optical phonons of the substrate, however, is greater in effect than scattering by phonons of graphene. Thus limiting the mobility to 40,000 $cm^2 \cdot V^{-1} \cdot s^{-1}$ [109].

In epitaxial graphene of 40-nanometer wide nanoribbons the change in electrical resistance is distinct. The predictions are surpassed by a factor of 10 by the conductance of the ribbon. Like the optical waveguides or quantum dots the ribbons behave in much similar way, facilitating the undisrupted flow of electrons along the ribbon edges. For copper the resistance improves in proportion to length as electrons jolt into impurities [113- 114].
Dominated by two modes transport basically of which one being ballistic and temperature independent whereas the other thermally agile. The ballistic electrons replicate those in cylindrical carbon nanotubes. Transport is dominated by two modes. One is being ballistic and temperature independent, while the other is thermally activated. Ballistic electrons resemble those in cylindrical carbon nanotubes. at a particular length- ballistic mode at 16 micrometers and the other at 160 nanometers (1% of the former length) [113] there is a sudden increase in resistance.

By encraving into silicon carbide wafers on the edge of the 3-dimensional structure the ribbons were natured. When these wafers are heated as a preference the silicons are washed away along the edges, ideally at 1000 degree Celsius, forming nanoribbons the structure of which is determined by the motif of the 3-dimensional surface. The nanoribbons had the ideal edges, tempered y the fabrication process. Measurement of electron mobility exceeding one million is equivalent to a sheet resistance of one ohm per square which is two orders lower in magnitude compared to 2-dimensional graphene [113]. Even at room temperature graphene electrons can connect micrometer distances without scattering [99].

Graphene demonstrates the least conductivity on the order of $4e^2/h$, despite of zero carrier density at the Dirac points. However the cause of this minimum density is still vague, although, taking ruffling of the graphene sheets or ionized impurities in the SiO2 substrate may result local carrier puddles that aid conduction [100]. Numerous theories imply that the minimum conductivity should be $4e^2/(\pi h)$;

however most measurement are of the order $4e^2/h$ or greater[106] and relies on impurity concentration[115].
Graphene with near zero carrier density shows positive while negative photoconductivity at high carrier density. Induced by changes of both Drude weight and carrier scattering rate such interplay mainly controls it [116].

Graphene can be withdraw to an undoped state by gently heating [115][117] Graphene doped with different gaseous species (both acceptors and donors). For concentrations of more than 1012 cm^{-2} for dopant carrier mobility shows no identifiable change [114]. Mobility can be reduced 20 times [115][118] if graphene is doped with potassium in ultra-high vacuum at low temperature. The reduction in mobility is reversible on heating the graphene thus getting rid of the potassium.

As Graphene is two dimensional, there are chances of charge fractionalization to take place (In low dimensional system where the usual charge of single pseudoparticles is less than a single quantum [119]). Thus it may be an ideal material for constructing quantum computers with the help of anionic circuits [121].

2.4.2.3 Thermal

In terms of thermal conductivity graphene is perfect. Recently its thermal conductivity was measured and is way higher than the values observed for other carbon structures like carbon nanotubes, graphite and diamond (> 5000 $W \cdot m^{-1} \cdot K^{-1}$) in room temperature. Graphenes ballistic thermal conductance is isotropic that is same in every direction. Being a 3D version of Graphene, graphite demonstrates thermal conductivity which is 5 times smaller (1000 $W \cdot m^{-1} \cdot K^{-1}$). Elastic waves propagating in the graphene lattice termed phonons generally guide the whole phenomenon. Thermal conductivity studies have crucial implications in electronic devices that are graphene based. Thermal conductivity reaches 600 $W \cdot m^{-1} \cdot K^{-1}$ on a substrate too [111].

2.4.3 Energy Bandstructure of Graphene

In contrast to the regular three dimensional structure graphenes electronic structure is very much unorthodox. The sic double cones on the Fermi surface is characteristic at illustrated in fig 2.18. Fermi surface as such is found at the cones adjoining points in undoped graphene. As the density of material is zero at that point, the intrinsic electrical conductivity is usually lower of the conductance quantum $\sigma \sim e^2/h$; exact prefactor still debatable. However, with the means of an electric field the Fermi level can

be adjusted so that the material shifts either to p-doped(with holes) or n-doped(with electrons) dependent on the applied fields' polarity. Graphene too can be dopped applying the adsorption process. For doped graphene the electrical conductivity can be largely high and probably may be higher than copper at room temperature [70].

The dispersion relation in case of electrons and holes is linear in proximity to the Fermi Level. The curvature of the energy bands gives the effective masses; this equals to zero effective mass. The equation is similar to the Dirac equation for describing the excitation in graphene for mass less fermions which travel at constant speed. The cones connecting points are thus termed Dirac points [70].

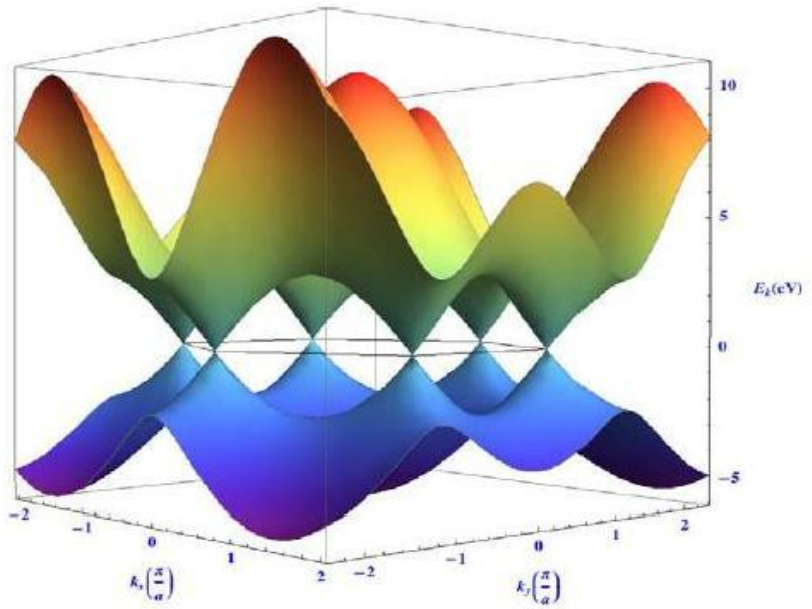

Figure 2.18: E-k diagram of graphene. The energy, E, for the excitations in graphene as a function of the wave numbers, kx and ky, in the x and y directions. The black line represents the Fermi energy for an undoped graphene crystal. Close to this Fermi level the energy spectrum is characterized by six double cones where the dispersion relation (energy versus momentum, ħk) is linear. This corresponds to massless excitations [70].

2.4.4 Band gap opening in Graphene devices

Several ways that can be taken into consideration before inducing a bandgap in graphene. i)lateral confinement, i.e, utilizing grpahene nanoribbons as material for FET channels, II)the usage of bilayer

graphene that has a perpendicular electric field consisting of a gap tunable iii) utilizing epitaxial graphene on SiC iv) graphene functionalization or doping.

There are a number of different ways that can be considered for inducing a bandgap in graphene: *i)* lateral confinement, i.e., using graphene nanoribbons as material for FET channels, *ii)* the use of bilayer graphene, that has a gap tunable with a perpendicular electric field, *iii)* the use of epitaxial graphene on SiC, *iv)* graphene functionalization or doping. Through evaluation by modeling we will further discuss the possibilities of these options. [123]

2.4.4.1 Graphene nanoribbons

As can be inferred from from fig 2.19 Nanocarbons offer a remarkable upperhand over carbonnanotubes: by virtue of relaxation, all nanoribbons have a semiconducting gap [122].

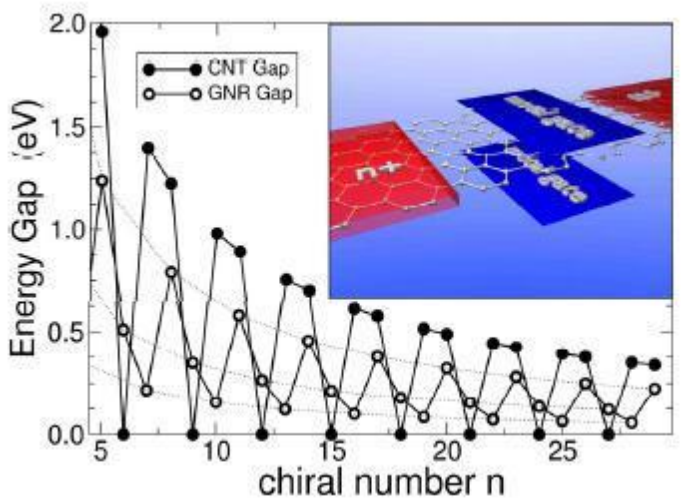

Figure 2.19: Energy gap as a function of the chiral number in zigzag carbon nanotubes (2n,0) [black] and in zigzag carbon nanoribbons (2n, 0) [white] [123].

2.4.4.2 Bilayer graphene FETs and Tunnel FETs

By applying a vertical electric field as suggested theoretically [124,125] the bandgap in bilyaer graphene can be altered and observed [126,127]. This aspect opens a new prospect: the bandgap for any device becomes large when required can be made possible i.e. the device should be turned off.

2.4.4.3 Epitaxial graphene on SiC

Graphene layer grown as a result of epitaxy on a SiC substrate if measured by angle-resolved photo-emission spectroscopy can demonstrate a gap of around 0.26 eV as evident in recent experiments [128]. However, there is still need of further experiment but the point made is promising as epitaxial graphene on SiC is good for wafer scale fabrication. By exploring design with semi-analytical model [129]. The chances of putting the material to use have been evaluated. For Vdd = 0.25 V An ION/IOFF ratio of up to 60 is attainable but the channel bandgap (in eV) has to be more than the supply voltage (in V), or else strong interband tunneling will take place. For smaller Vds large current modulation is quite possible but considering digital applications the Vgs swing must be equivalent to the applied Vds.

2.4.4.4 Functionalized Graphene

Of the many vitalizing options chemical functionaliztion of Graphene sheets or nanoribbons are encouraging for tuning bandstructure and electronic properties. Conductance variations of up to six orders in magnitude are attainable through reversible chemical modifications (probably hydrogenation) as per latest experiments indicating the possibility of realizing memory elements [130]. The experimental demonstration of Graphene [131], a two-dimensional hydrocarbon with a gap of 4-5 eV attained by hydrogenation of graphene via plasma treatment further manifested that chemical functionalizing is a feasible route toward bandgap engineering of graphene based materials. However, suitable technique to achieve good ohmic contains and to preserve high mobility (exceeding 100 cm^2/Vs) are still required.

2.5 Graphene Nanoribbon

Graphene nanoribbon (GNR) can be considered as a cut off from a graphene sheet. A chirality vector defines how the stripr is to be cut off and this vector is distinct from CNT's. Like CNT's GNR's do have periodic boundary conditions, as matter of which GNR has no closed form solution and thus must be numerically determined. The following examples are based on armchair edge and zigzag edge GNRs, which are similar to zigzag and armchair CNTs [132].

2.5.1 GNR Structure

The plainest way to define a graphene nanoribbon is to take of it as strip cut off from a graphene sheet with a specific chiral vector as previously mentioned. With the chiral vector it would point out the direction and magnitude of the GNR's width. For Graphene the basis vectors are a1 and a2, and these basis vectors too makes it up for the CNT chirality vector. Although the origin of these vectors are not critical for CNT, but is for the GNR's for conditions of absence periodic.

As it has been mentioned already, the simplest way of defining a graphene nanoribbon is to think of it as a strip cut off from a graphene sheet that follows a specific chiral vector. The chiral vector would indicate the direction and magnitude of the width of the GNR. The basis vectors for graphene are **a1** and **a2**, and that these vectors make the basis vectors for the CNT chirality vector. Although the origin of these vectors is not very important for CNT, it is crucial for GNRs due to the absence periodic boundary conditions. The following figure would demonstrate this fact [132].

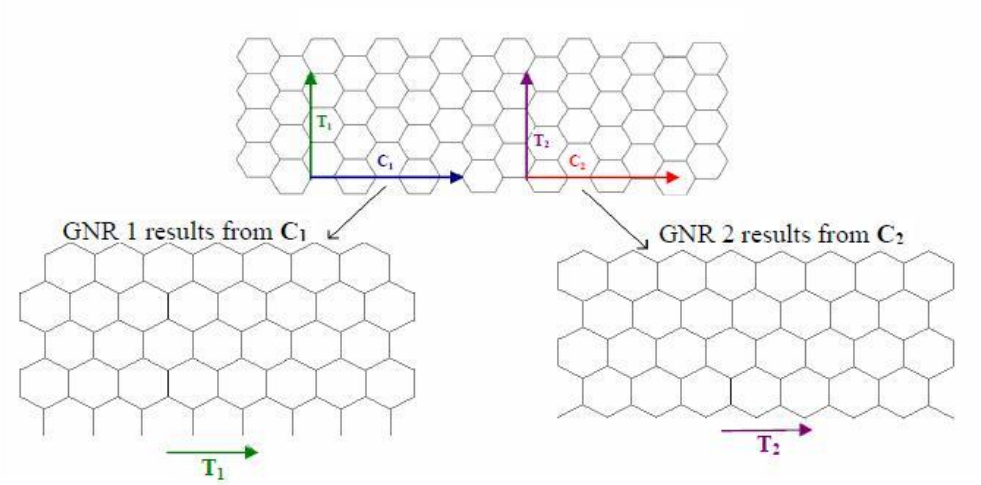

Figure 2.20: Affect of the origin of the GNR chiral vector [132].

A continuous infinite set of chiral vectors and their origins define every GNR. Here a specific genre of GNR will be discussed which with the aid of integer GNR chiral vectors can be defined with basis a1/2 and a2/2 with origin at either atom a or atom b of a graphene unit cell. A is the left-hand atom whereas b is the right-hand atom for a graphene unit cell. Consider these GNRs as A-type and B-type in case of this example. In Fig 2.20, GNR 1 is A-type, and GNR 2 is B-type. With the same convention, the GNR chiral vector can be defined as:

$$\vec{C} = n\frac{\vec{a_1}}{2} + m\frac{\vec{a_2}}{2} = (n,m)_{A/B} \qquad (2.10)$$

In Equation 2.10 the subscript A/B represents the origin of the GNR chirality vector and is either value A or B. The quantities n and m in this equation must be integers. The *transport vector* of the GNR is perpendicular and equal in magnitude to the chiral vector. Fig 2.21 shows examples of the GNR chiral and transport vectors. It is indispensible that there are few constraints on the indices that will result stable structures. In most situations, n & m must be even. The chiral vector will not identify to a carbon atom in case n & m are not even. If m is equal to zero, then n may be odd or even. Secondly, if n is equal to m, then they may be odd or even [132].

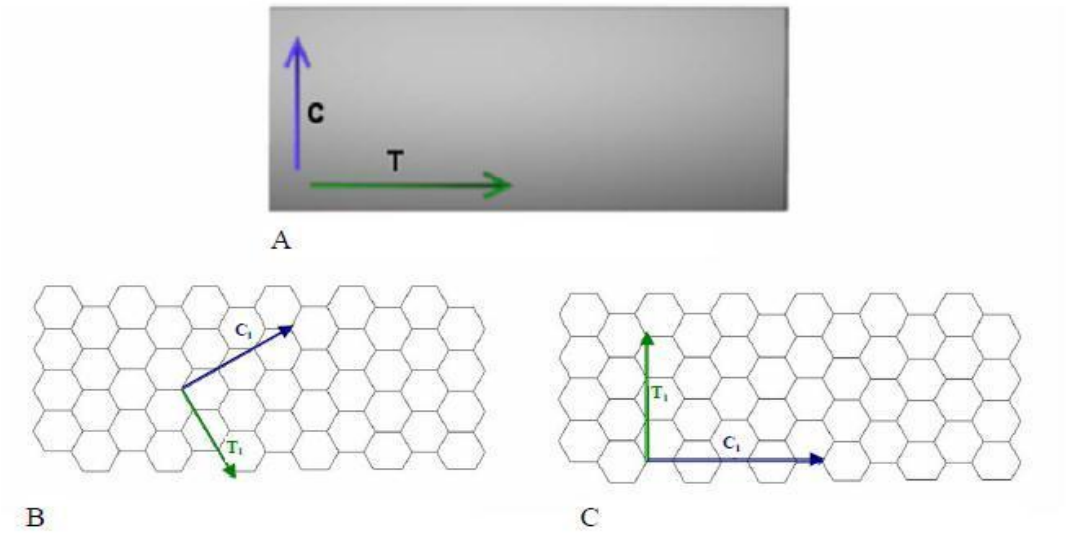

Figure 2.21: Examples of GNR chiral and transport vectors [132].

As numerous methods are used, it is crucial not to point out that this is the undeniable method for defining GNR. One popular method as proposed by Ezawa does a good job of defining physically realizable GNRs. With these method two zigzag lines in a zigzag edge GNR which is m hexagons long is firstly defined. An integer multiples of translation vector supersede the chain to create the ultimate nanoribbon structure. Direct comparison has not been made in this paper as no definite relationship to the simple indexing method exists [132].

2.5.2 Production of Graphene nanoribbon

Large volume of width controlled GNRs [133] can be produced by a process known as graphite nanotomy. Applying sharp diamond knife on graphite nanoblock are fabricated. These blocks later on can be exfoliated to yield GNRs. Another way would be 'unzipping' or cut open of the nanotubes [134]. Using the action of potassium permanganate and sulfuric acid solution multi-walled carbon nanotubes were unzipped [135]. Another method is through plasma etching of nanotubes partially

embedded in polymer film [136]. Lately using ion implantation followed by vaccum or laser annealing [137-139]. Graphene nanoribbons have been nurtured onto SiC.

2.5.3 Electronic Structure of GNR

The edge structures determine the electronic states of GNRs. The localized state with non-bonding molecular orbitals near the Fermi energy is made possible by zigzag edges. They are expected to have substantial changes in optical & electronic properties as a result of quantization.

As the tight binding theory anticipates based on computation that zigzag GNR are always metallic whereas armchairs can either be metallic or semiconducting, dependent on the armchair nanoribbons width. When it comes Discrete Fourier Transforms calculations it shows armchair nanoribbons are semiconducting consisting of an energy gap inversely proportional to the GNR width [143]. With decreasing GNR width experiments corroborate that energy gaps increase. Control edge oriented graphene nanoribbons have been created by scanning tunneling microscope (STM) lithography [142]. It revealed energy gaps up to 0.5 eV in a 2.5 nm wide armchair ribbon.

Zigzag nanoribbons exhibit spin polarized edges and are metallic. Due to an unusual antiferromagnetic coupling at carbon atoms of opposite edge this gap opens up. The size of this gap is inversely proportional to the width of the ribbon and can be recounted to the spatial distribution properties of edge wave functions in terms of behavior, and the exchange characteristics that creates the spin polarization is mostly local character. As a result in zigzag GNR the quantum confinement, inter-edge super exchange, and intra-edge direct exchange interactions are critical mostly for magnetism and its bandgap is controlled by alkaline adatoms [144]. Zigzag GNRs edge magnetic moment and bandgap are inversely proportional to the electron concentration.

Numerical simulation [145] of tight binding derived via ViDES [146] demonstrates transistors are affected by field harnessing GNR for its compliance as channel material with ITRS stipulation for next generation devices.

Graphene nanoribbons high electrical, thermal conductivity and 2D structure & low noise make GNRs considerate alternative for integrated circuit interconnects to copper. By changing the width of GNRs at certain points along the ribbon researchers are investigating the creation of quantum confinement [147]. As graphene nanoribbons contains semi conductive properties it can be taken as a alternative to silicon semiconductors [148] capable of sustaining microprocessor clock speeds in the vicinity of 1

THz [149]. with width less than 10 nm field-effect transistors came into being with GNR – "GNRFETs" – with an ION/IOFF ratio $>10^6$ at room temperature [150,151].

2.5.4 Graphene Transistors

In 2004 Manchester group reported a graphene MOS device. Doped silicon substrate as the black gate and a 300-nm SiO2 layer underneath the graphene are used as black-gate dielectric. To manifest concepts such back gate devices are useful but are susceptible to large parasitic capacitances and thus cannot be integrated with various components. Thus, graphene transistor requires a top gate structure. The top gate for a graphene MOSFET was first reported in 2007, and since then there has been immense progress. Research in graphene is still in its premature days; graphene MOSFETs has the potential to compete with devices that are result of years of research and investment.

Top gated graphene MOSFETs have been created with the help of exfoliated graphene, the ones that grow on nickel and copper and epitaxial graphene. Channels for these top-gated graphene transistors have been created by making use of large area graphene, which does not contain a bandgap so that these transistors can be switched off.

As shown in fig 2.23a large area graphene transistors demonstrate a distinct current-voltage transfer characteristic. The type of carrier and its density (electrons or holes) in the channel is largely controlled by the potential difference between channel and the gates (top-gate and/or back-gate). Electron accumulation in the channel (n-type channel) is a result of large positive gate voltages while the large negative gate voltages assist a p-type channel. Two branches of the transfer characteristics arise from this behavior segregated by the Dirac point (Fig. 2.23a). Several points determine the position of the Dirac point; the differentiation between the work functions of the gate and the graphene, the type and density of the charges at the interfaces at the top and bottom of the channel (Fig. 2.21), and any doping of the graphene. For MOSFET devices the reported on-off ratios with large area graphene channels are in 2-20 range.

Reports of graphene MOSFETs with gigahertz capabilities have come out lately where these transistors have large area channels of exfoliated and epitaxial graphene. Currently the fastest graphene transistor that Is in existence is a MOSFET that has a 240-nm gate with a cut off frequency fT = 100 GHz, which compared to best silicon MOSFETs having similar gate lengths is quite higher (as is the cut-off frequency of 53 GHz reported for a device with a 550-nm gate. A drawback of all

radio frequency graphene MOSFETs reported so far is the unsatisfying saturation behavior (only weak saturation or the second linear regime), which has an adverse impact on the cut-off frequency, intrinsic gain and other merits for radiofrequency devices. However, while operating with weakly saturated current to outdone silicon MOSFETs is undoubtedly splendid.

One way of introducing a bandgap into graphene for logic applications is the creation of graphene nanoribbons. Nanoribbon MOSFETs with back-gate control and having widths of even less than 5 nm, have been operated as p-channel devices and that showed on–off ratios of up to 106. Such high ratios have been obtained despite simulations showing that edge disorder leads to an undesirable decrease in the on-currents and a simultaneous increase in the off-current of nanoribbon MOSFET. This, and other evidence of a sizeable bandgap opening in narrow nanoribbons, provides sufficient proof that nanoribbon FETs are highly suitable for logic applications. However, due to their relatively thick back-gate oxide of these devices, voltage swings of several volts were needed for switching, which is significantly more than the swings of 1 V and less needed to switch Si CMOS devices. Additionally, CMOS logic requires both n-channel and p-channel FETs with well-controlled threshold voltages, and graphene FETs that has all these properties have not yet been reported [152].

Recently, the fabrication of the first graphene nanoribbon MOSFETs with topgate control has been reported. These transistors feature a thin high-dielectric-constant (high-*k*) top-gate dielectric (1–2 nm of HfO2), a room-temperature on–off ratio of 70 and an outstanding transconductance of 3.2 mS μm-1 (which is higher than the transconductance reported for state-of-the-art silicon MOSFETs and III-V HEMTs) [152].

Investigation of graphene bilayer MOSFETs have been carried out experimentally and also device simulation has been performed. Although the on–off ratios seen so far (100 at room temperature and 2,000 at low temperature83) are too small for logic applications, they note a significant improvement(of about a factor of 10) over MOSFETs in which the channel is made of large-area gapless graphene [152].

We now return to the discussion of two-dimensional nature of graphene. According to theory of scaling a thin channel region allows short-channel effects to be suppressed and thus makes it feasible to scale MOSFETs to very short gate lengths. The two dimensional nature of graphene means that the thinnest possible channel can be obtained by using graphene, so graphene MOSFETs should be more scalable than their competitors. However, it should be noticed that scaling theory is valid only for transistors with channels semiconducting in nature and does not apply to graphene MOSFETs with gapless channels. Thus, the scaling theory does describe nanoribbon MOSFETs, which not only have a bandgap but which have significantly lower mobility than large area graphene, as discussed. Given

that the high published values of mobility relate to gapless large-area graphene, the most attractive characteristic of graphene for use in MOSFETs, especially those required to switch off, is probably its ability to scale to shorter channels and higher speeds, rather than its mobility [152].

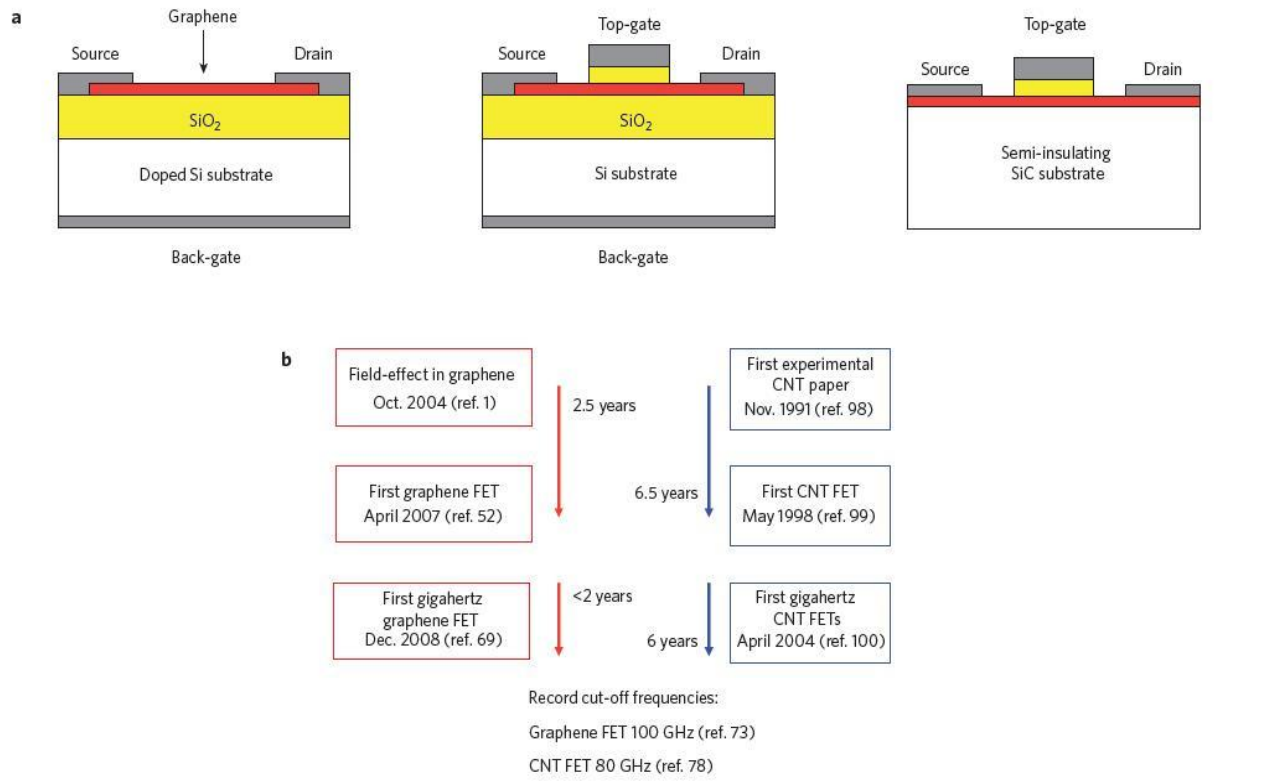

Figure 2.22: Structure and evolution of graphene MOSFETs. **(a)** Schematics of different graphene MOSFET types: back-gated MOSFET (left); top-gated MOSFET with a channel of exfoliated graphene or of graphene grown on metal and transferred to a SiO_2-covered Si wafer (middle); top-gated MOSFET with an epitaxial-graphene channel (right). The channel shown in red can consist of either large-area graphene or graphene nanoribbons. **(b)** Progress in graphene MOSFET development compared with the evolution of nanotube FETs [70].

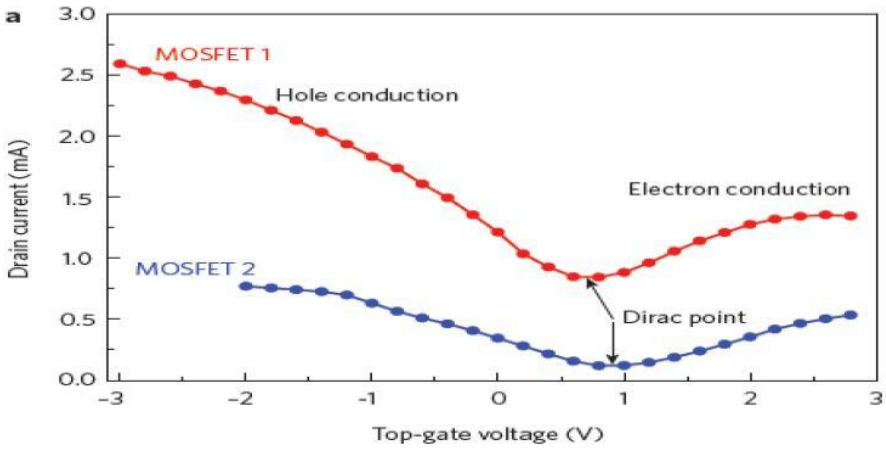

Figure 2.23: Direct-current behaviour of graphene MOSFETs with a large-area-graphene channel**.** Typical transfer characteristics for two MOSFETs with large-area-graphene channels. The on–off ratios are about 3 (MOSFET 1) and 7 (MOSFET 2), far below what is needed for applications in logic circuits. Unlike conventional Si MOSFETs, current flows for both positive and negative top-gate voltages [70].

2.6 Summary:

The limitation of conventional Si-MOSFET, properties of carbon nanotube, types of carbon nanotube, characteristics of Carbon nanotube, properties of graphene, synthesis of graphene, band structure of graphene and properties of graphene nanoribbon have already been discussed. The production techniques and electronic structure of GNR are also covered in this chapter. It is found that the performance properties of CNT and GNR have given a higher performance properties compared to conventional properties. Each type transistor is modeled in difference way based on the structure of the transistor. This discussion includes different types of CNTFET from starting CNT technology, operation of CNTFET and types of CNTFET based on this operation. Also, various types of graphene transistors are discussed in this chapter and some details about their operation and properties are also given.

Chapter 3

RESULTS AND CHARACTERIZATIONS OF CNTFET AND GNRFET USING NANOTCAD ViDES

This chapter will explain the methodology used in this project, simulation model used for simulation study, simulation result obtained, comparing those results with other reliable research group's results and finally making summary, analysis and discussion on the result.

3.1 The Model

This research implicates simulation based study to investigate the effect on I-V characteristic by changing different parameters of CNTFET and GNRFET. This python based simulation study is carried out based on the self-consistent solution of the 3-D Poisson and Schrödinger equations with open boundary conditions within the non-equilibrium Green's function formalism and a tight-binding Hamiltonian [155]. The model is built for a Schottky barrier field effective transistor in order to investigate ballistic transport in CNTFET and GNRFET. The goal is to modify the MATLAB code such a way to investigate the effect on I-V characteristics by changing major parameters of CNTFET and GNRFET and also focused the result on 2D plot.

3.1.1 Model Physics and the Process of Calculation

The potential profile in the 3-D simulation domain obeys the Poisson equation
[156]

$$\nabla[\in(\vec{r})\nabla\emptyset(\vec{r})] = -q\,[\,p(\vec{r}) - n(\vec{r}) + N_D^+(\vec{r}) - N_A^-(\vec{r}) + \rho_{fix}] \qquad (3.1)$$

Where, $\emptyset(\vec{r})$ is Electric potential, $\in(\vec{r})$ is dielectric constant, ρ_{fix} is fixed charge, N_D^+ is concentration of ionized donor and N_A^- is concentration of ionized acceptor.

The electron and hole concentrations (*n* and *p*, respectively) are computed by solving the Schrödinger equation with open boundary conditions by means of the NEGF formalism [157]. A tight-binding Hamiltonian with an atomistic (*pz* orbitals) real-space basis for CNT [158] and GNR [159] has been used with a hopping parameter t = 2.7 eV.

Green's function can be expressed as:

$$G(E) = [EI - H - \Sigma S - \Sigma D] - 1 \quad (3.2)$$

Where, E is the energy, I is the identity matrix, H is Hamiltonian, ΣS is self-energy of the source and ΣD is self-energy of the drain. Transport here is assumed to be ballistic.

The length and chirality of CNT or GNR are now defined and the coordinates in the 3-D domain of each carbon atom are then computed [160]. After that, the 3-D domain is discredited so that a grid point is defined in correspondence with each atom, while a user-specified grid is defined in regions not including the CNT or GNR.

A point charge approximation is assumed, i.e., all the free charge around each carbon atom is spread with a uniform concentration in the elementary cell including the atom. Assuming that the chemical potential of the reservoirs is aligned at the equilibrium with the Fermi level of the CNT or GNR, and given that there are no fully confined states, the electron concentration is

$$n(\vec{r}) = 2 \int_{E_i}^{+\infty} dE \left[|\psi_s(E,\vec{r})|^2 f(E - E_{F_s}) + |\psi_D(E,\vec{r})|^2 f(E - E_{F_D})\right] \quad (3.3)$$

While the hole concentration is

$$p(\vec{r}) = 2 \int_{+\infty}^{E_i} dE \left[|\psi_s(E,\vec{r})|^2 [1 - f(E - E_{F_s})] + |\psi_D(E,\vec{r})|^2 [1 - f(E - E_{F_D})]\right] \quad (3.4)$$

Where, $\vec{r}$ is coordinate of carbon site, f is Fermi-Dirac factor,

$|\psi_S|^2$ is probability that states injected by the source reach the carbon site ($\vec{r}$),

$|\psi_D|^2$ is probability that states by the drain reach the carbon site ($\vec{r}$),

E_{FS} is Fermi level of the source and E_{FD} is Fermi level of the drain.

The current is computed as

$$I = \frac{2q}{h} \int_{-\infty}^{+\infty} dE T(E)[f(E - E_{F_S}) - f(E - E_{F_D})] \quad (3.5)$$

Where q is the electron charge, h is Planck's constant, and $\mathcal{T}(E)$ is the transmission coefficient computed as

$$\mathcal{T} = -\mathrm{Tr}\left[\left(\Sigma_s - \Sigma_s^{\dagger}\right)G\left(\Sigma_D - \Sigma_D^{\dagger}\right)G^{\dagger}\right] \quad (3.6)$$

Where Tr is the trace operator. In the present model, we only deal with the one-dimensional (1-D) transport between source and drain reservoirs, while the leakage gate current has not be taken into account. For the considered devices with channel length of a few nanometers, it can be shown that the gate current is negligible with respect to the drain current.

Detail discussion about the physics and mathematical calculation of modeling is provided in Appendix A. Figure 3.1 describes the total calculation procedure that is done in the simulation.

Table 3.1: Parameters and physical constants used in the simulation.

Input Parameters	**Default Values**
Gate Insulator Thickness, t (nm)	Boltzmann's Constant, k= 1.8 10^{-23} J/K
	Planck's constant,h= 6.63 10^{-23}
Relative dielectric constant, ε_r	Reduced Planck's constant, ħ= 1.05 10^{-34}
Temperature, T (K)	
Gate Voltage, V_G(V)	Mass of electron, m_0= 9.11 10^{-31} kg
Drain Voltage, V_D(V)	Source Fermi level, E_f= 0.32eV
	Overlap integral of tight bonding C-C model,
	ς= 2.7 eV
Channel Length, L_{ch}(nm)	Charge of an electron, q=1.6 10^{-19} C
Chiral axis,(n,0)	Permittivity of free space, ε_0= 8.854 10^{-12}
	C-C bond length, $a_{c\text{-}c}$= 1.42 10^{-10} m

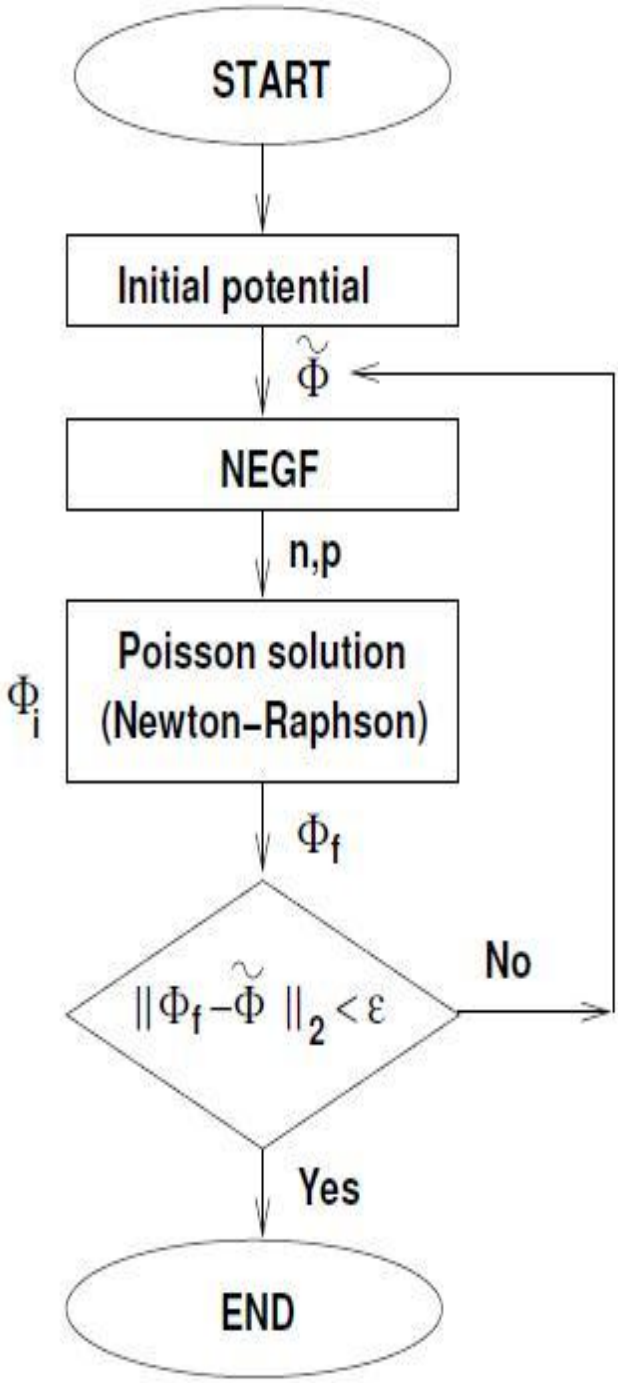

Figure 3.1: Flow-chart of the self-consistent 3D Poisson-Schrodinger solver [155].

3.2 Result and Analysis

From the simulation different parameter changing effect on I-V characteristics of CNTFET and GNRFET is shown. Result started with varying contact temperature effect, dielectric constant effect, and also chirality changing effect on Graphene nanoribbon field effect transistor and Carbon nanotube based field effect transistor. The GNRFET and CNTFET structure that considered for the simulation is shown in Fig 3.2.

For studying the various effects, perfectly patterned 15nm long N=12 armchair GNR having chirality (6, 0) and a 15nm long zigzag CNT having chirality (13, 0) are used as the default channel materials in the simulation due to their similar bandgaps. The default relative dielectric constant for both the FETs is taken to be 3.9. The default gate oxide thickness is 1.5nm and lateral spacing is 0.5nm. The default contact temperature is taken to be 300K. This default values are used in the simulation if the user does not specify the values of the parameters mentioned above.

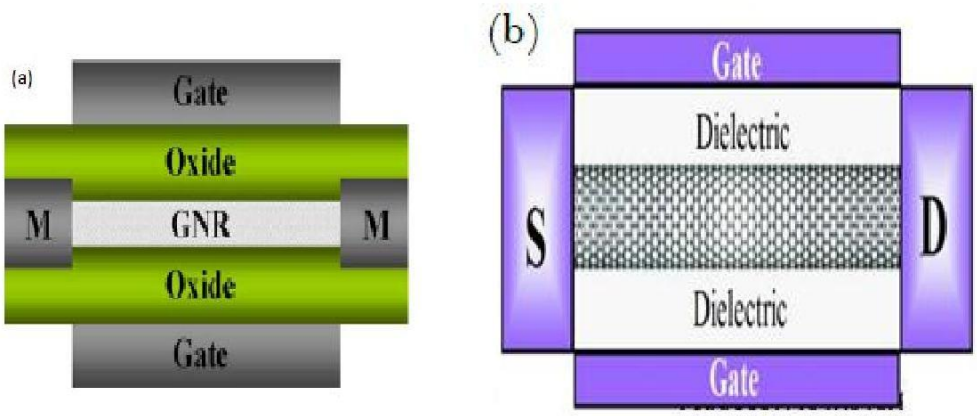

Figure 3.2: (a) Structure of GNRFET [179] (b) Structure of CNTFET [Source-internet image].

3.2.1 Effect of Contact Temperature

Now the concern is the effect of changing contact temperature on the transfer and output characteristics of graphene nanoribbon and carbon nanotube FET. Figure 3.3 and 3.4 deals with the contact temperature changing effect. The simulation is carried out at contact temperatures 77K, 100K, 200K, 300K, 350K and 400K.

In Fig 3.3, both GNR FET and CNT FET display ambipolar characteristics. The on-state drain currents are similar for both GNRFET and CNTFET. Both the FETS have off-state leakage currents which are almost of the same order of magnitude. It is observed that for different contact temperatures the drain current remains same for different gate voltages because of the ballistic consideration of the model.

The effect of changing contact temperatures on the output characteristics for both the FETs is shown in Fig 3.4. As the contact temperature varied between 77K and 400K, there is a small increase in the on-state drain current for each FET. This is increase is due to the decrease in channel resistance of the channel materials. Fig 3.5 shows the how the resistance of graphene nanoribbon decreases as contact temperature is increased from 198K to 373K studied by Huaqing Xie *et al* [161]. At any particular contact temperature, the on-state drain current of GNRFET is higher compared to the on-state drain current of CNTFET. The GNRFET has drain current in the order of 10^{-6} and the drain current of CNTFET has an order of 10^{-7}. In Figure 3.4, At V_D=0.35V, GNRFET has a current of 1.93×10^{-6} A at T=400K while the CNTFET has a current of 7.63×10^{-7} A. Thus, we can conclude that the channel resistance of graphene nanoribbon is lower compared to the channel resistance of carbon nanotube at any particular contact temperature resulting in a higher on-state drain current for GNR. The off-state leakage current for both GNRFET and CNTFET can be found by extrapolation of the output characteristics graphs and it can be concluded that the GNRFET will have a higher off-state leakage current than CNTFET.

Fig 3.6 shows the schematic of a FET based on GNR arrays patterned by BCP lithography [162].Fig 3.6 (c) and (d) shows its transfer and output characteristics recorded by Son *et al* in the contact temperature range 100K-300K. It is observed in the figure that as the contact temperature of the patterned FET increases, its ambipolar behavior decreases. It is seen in Fig 3.3 (a) that for the GNR SBFET simulated in this thesis paper, the ambipolar behavior decreases with increasing contact temperature. Thus it can be concluded that ambipolar behavior decreases with increasing contact

temperature.

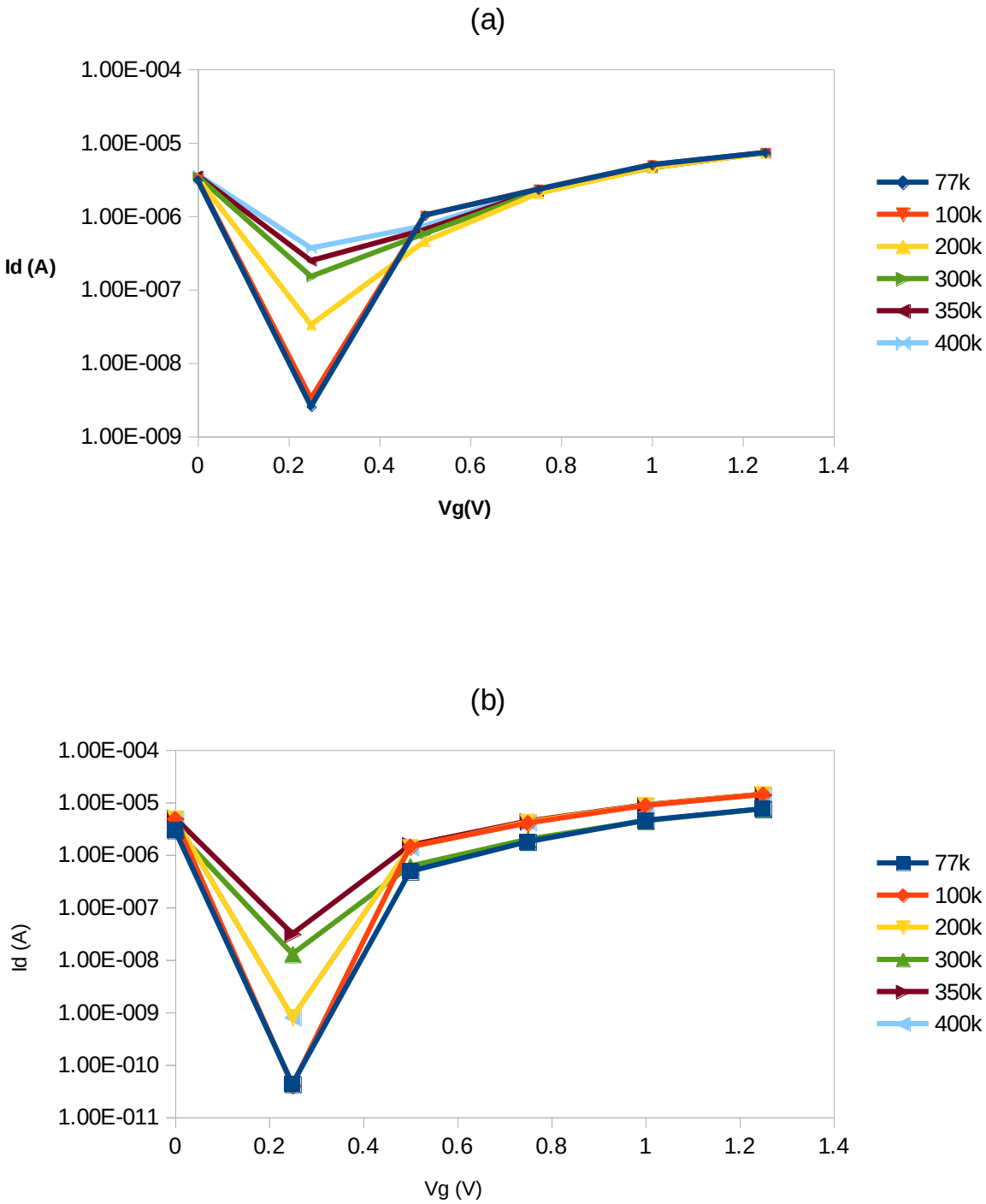

Figure 3.3: I_D vs. V_G characteristics of (a) Graphene Nanoribbon FET (b) Carbon Nanotube FET for different contact temperatures at V_D = 0.5 V.

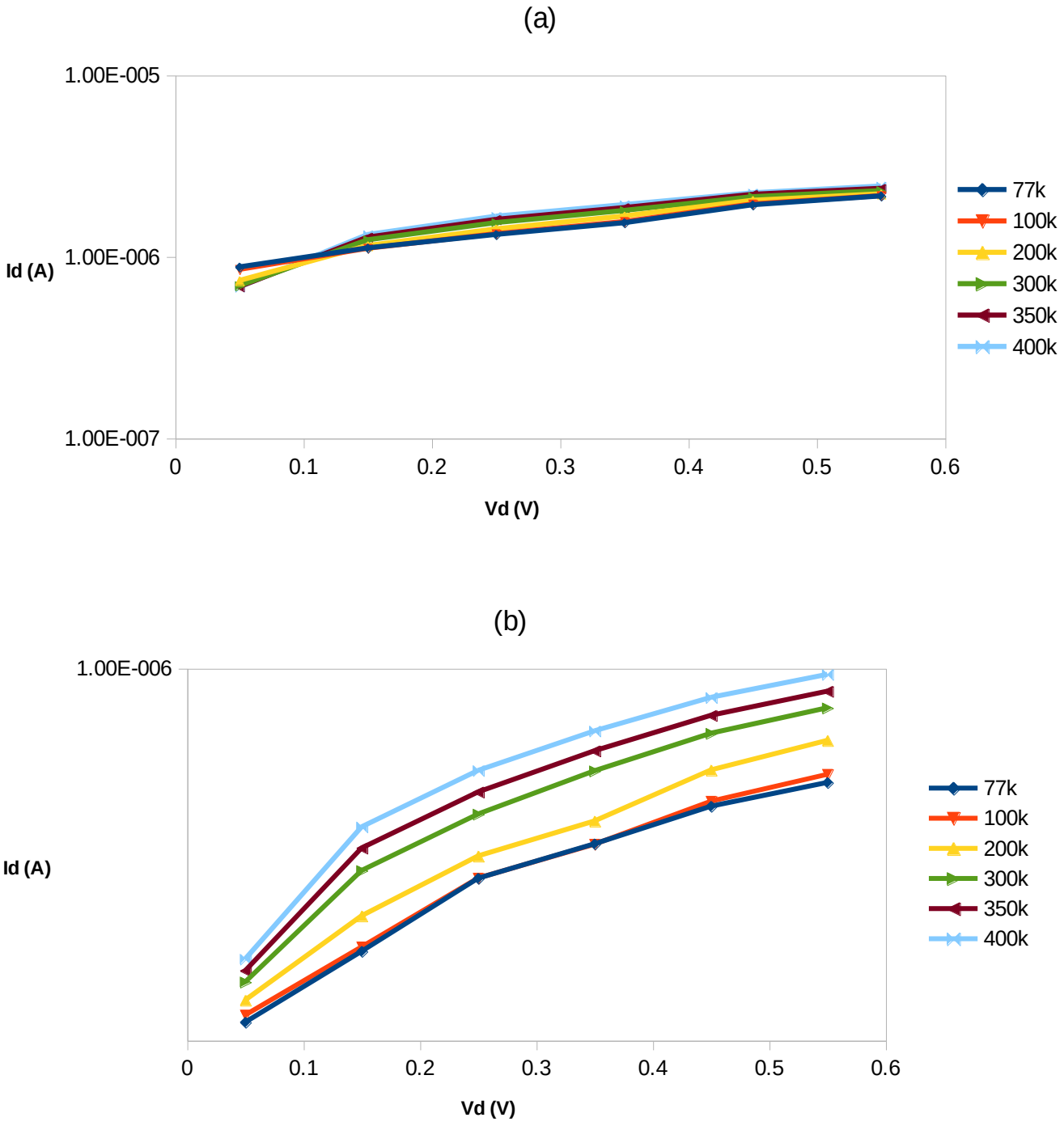

Figure 3.4: I_D vs. V_D characteristics of (a) Graphene Nanoribbon FET (b) Carbon Nanotube FET for different contact temperatures at V_G = 0.5 V.

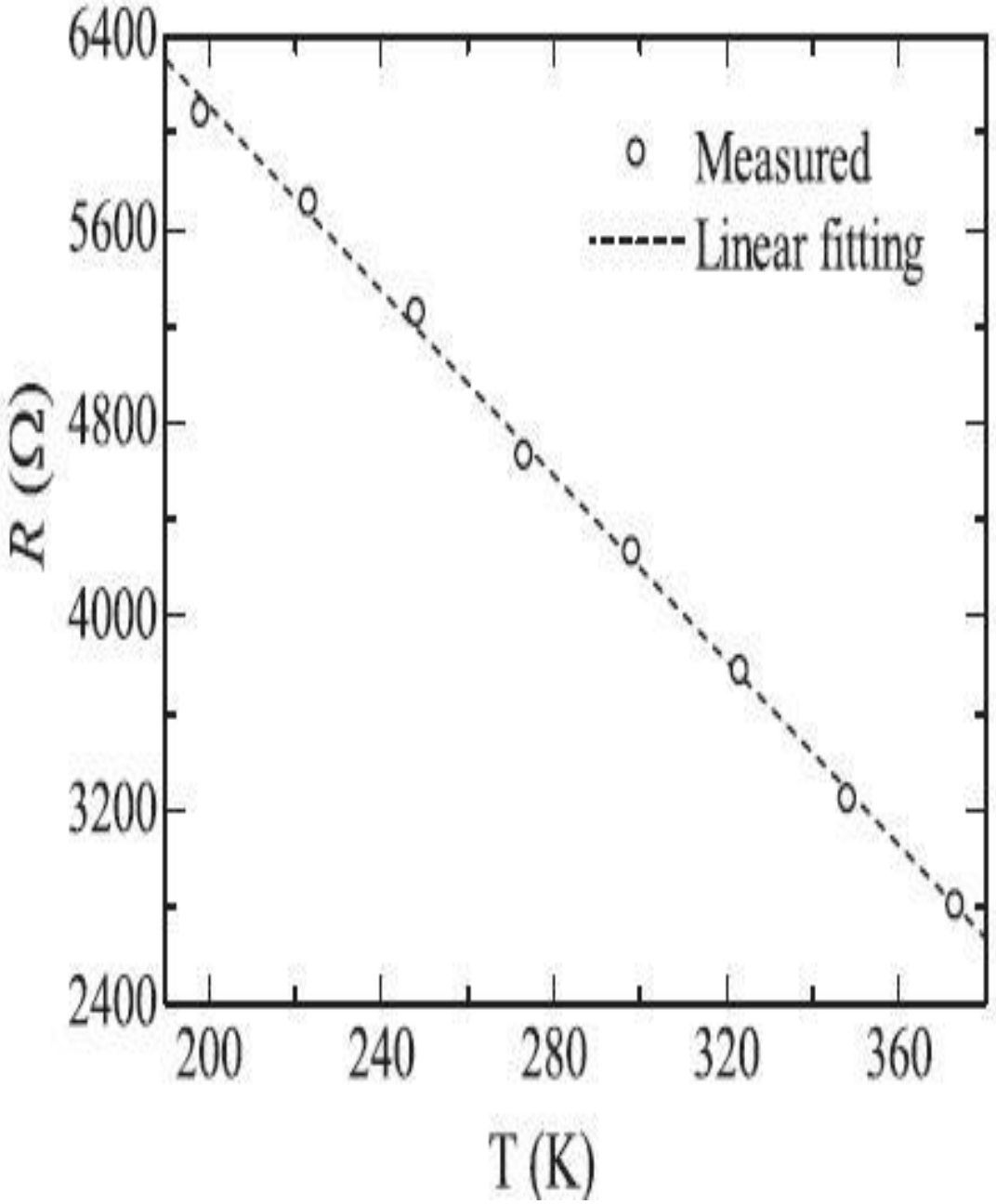

Figure 3.5: Dependence of resistance on contact temperature of graphene nanoribbon [161].

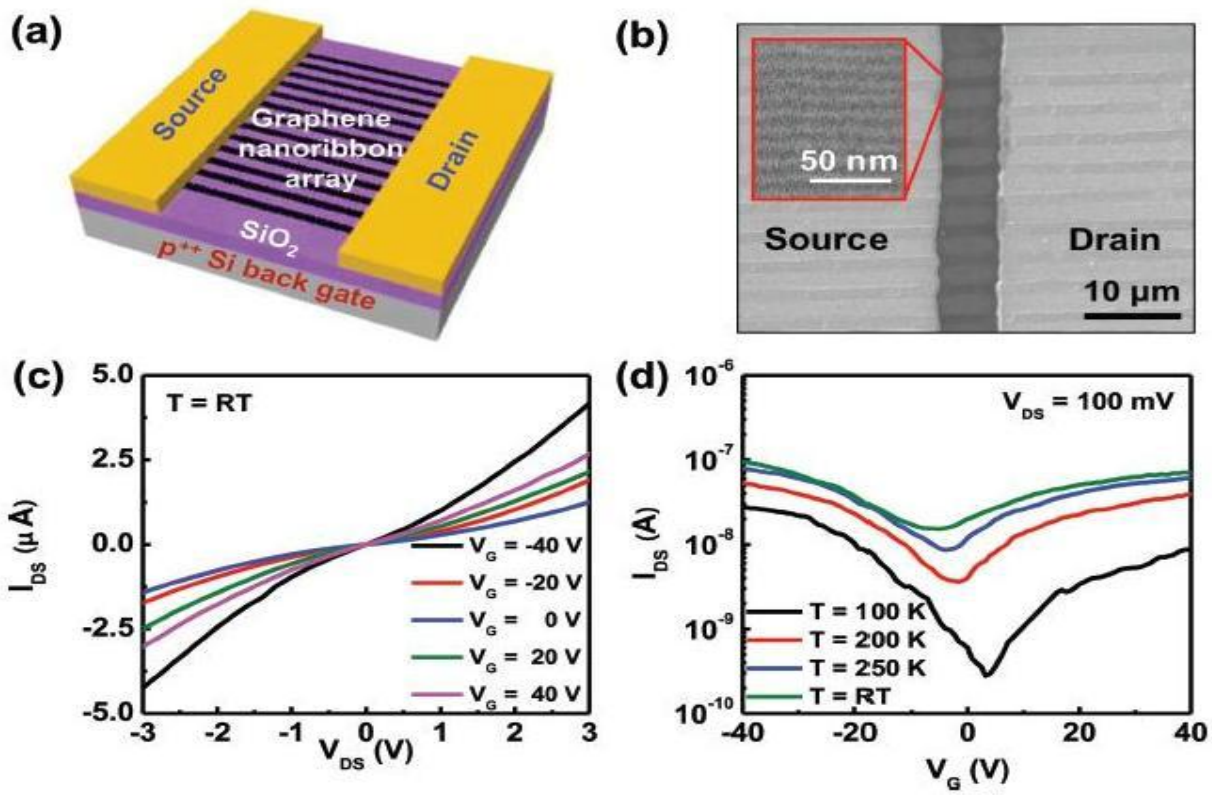

Figure 3.6: (a) Schematic of a FET based on GNR arrays patterned by Block Copolymer lithography and (b) the corresponding SEM image. In (b), the contrast difference in the channel between the GNR arrays and the bare silica is evident. (c) *I* DS - *V* DS curves of the GNR array FET with a 9 nm ribbon width recorded at different gate voltages. (d) *I* DS - *V* G curves of the GNR array FET with a 9 nm ribbon width recorded at *V* DS = 100 mV in the contact temperature range of 100–300 K [162].

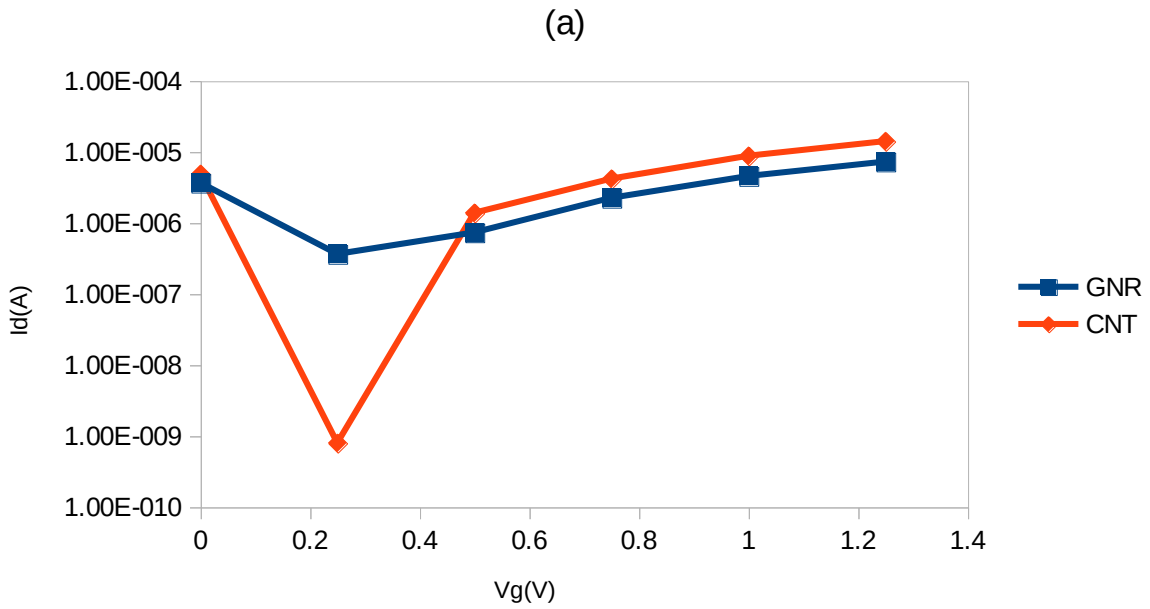

Figure 3.7: Combined I_D vs. V_G characteristics of Graphene Nanoribbon FET and Carbon Nanotube FET at T= 400K and V_D = 0.5 V.

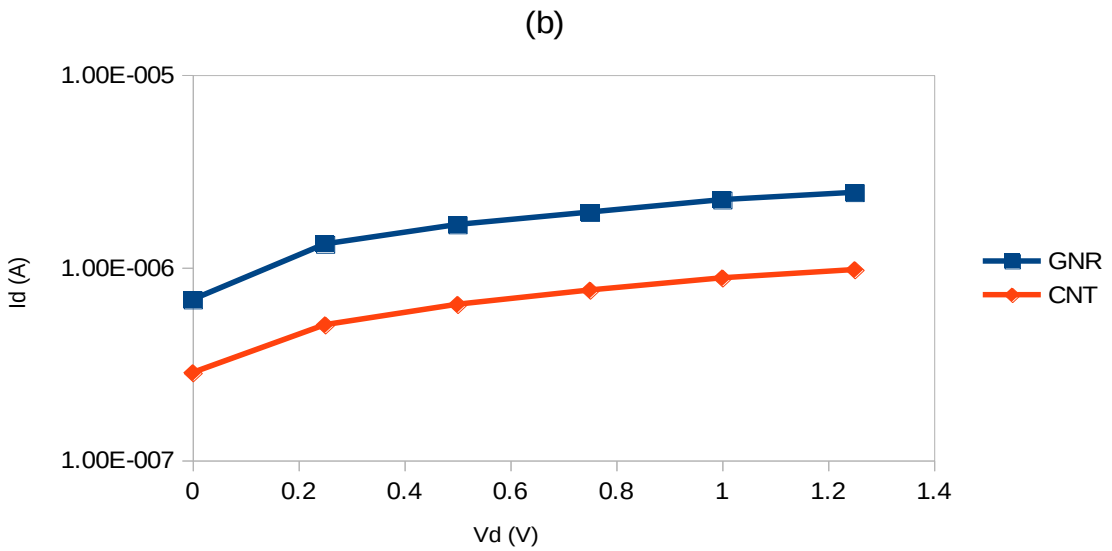

Figure 3.8: Combined I_D vs. V_D characteristics of Graphene Nanoribbon FET and Carbon Nanotube FET at T= 400K and V_G = 0.5 V.

3.2.2 Effect of Relative Dielectric Constant

At this stage of report now the concern is to investigate the effect on GNRFET and CNTFET transfer and output characteristics by changing the dielectric constant. Naturally SiO_2 is used as a gate oxide material which has a dielectric constant of 3.9. But other material can be used as an oxide material for better performance. At this case dielectric constant will change definitely. Figure 3.9 shows the results of changing dielectric constant studied by Rasmit Sahoo *et al* [164].

Because of scaling, bulk Si MOSFET suffers from many limitations like short channel effect, tunneling etc. To overcome these limitations many solutions were proposed by different researchers. Use of high dielectric material as gate insulator was one of the proposed solutions [163-167]. Keeping this in eye it is tried to see the effect of using different dielectric materials as gate insulator in GNRFET and CNTFET. In this case the dielectric constant is changed within a range of 3.9 to 15.9 and interval is 4 keeping other parameter constant. At this inspect the temperature is kept at 300K which was a subject of change in our previous experiment. In Fig 3.10, the transfer characteristics of GNRFET and CNTFET are shown for different values of relative dielectric constant. Both the FETs show ambipolar characteristics. From the figure, it is observed that transfer characteristics for both GNRFET and CNTFET are similar. It is seen that as the relative dielectric constant is increased, the on-state drain current at any particular voltage increases. For GNRFET, at V_G=0.5V the value of drain current at k=3.9 is 5.72×10^{-7} A and at k=15.9 is 2.56×10^{-6} A. For CNTFET, at V_G=0.5V the value of drain current at k=3.9 is 6.08×10^{-7} A and at k=15.9 is 1.57×10^{-6} A.

Fig 3.11 shows the output characteristics of the FETs for different values of relative dielectric constant. When the value of relative dielectric constant is 3.9, the off-state leakage current of CNTFET is observed to be lower than the off-state current of GNRFET. The on-state drain current of GNRFET at k=3.9 is of the order of 10^{-6}A and that of CNTFET is of the order of 10^{-7}A. As the value of relative dielectric constant increases, both the off-state leakage current and the on-state drain current increases for both GNRFET and CNTFET. The GNRFET has a higher saturation current compared to the CNTFET. For k=15.9, the current in the GNRFET is 5μA and the current in the CNTFRT is 2.33 μA at V_D=0.55V. It is clear from the plot is that the saturation current increases for increasing dielectric constant but degree of this positive effect reduces as going for higher dielectric material [166] . This means that going for higher and higher dielectric material the increment in I_D with respect to k reduces. These results also match with the result of Rasmita Sahoo *et al* Fig 3.9 [164].

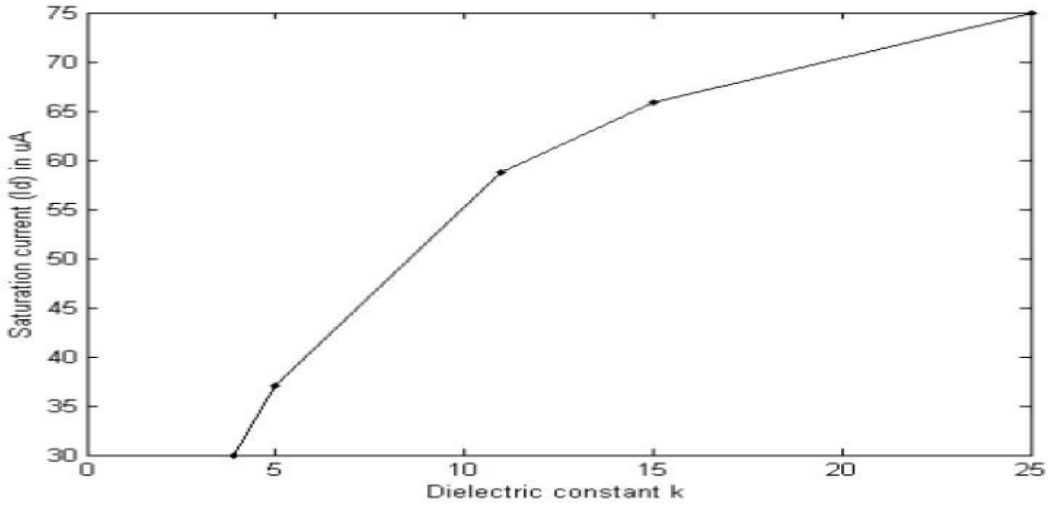

Figure 3.9: Dielectric constant changing effect investigated by Rasmita Sahoo *et al.* which satisfied simulation result [164].

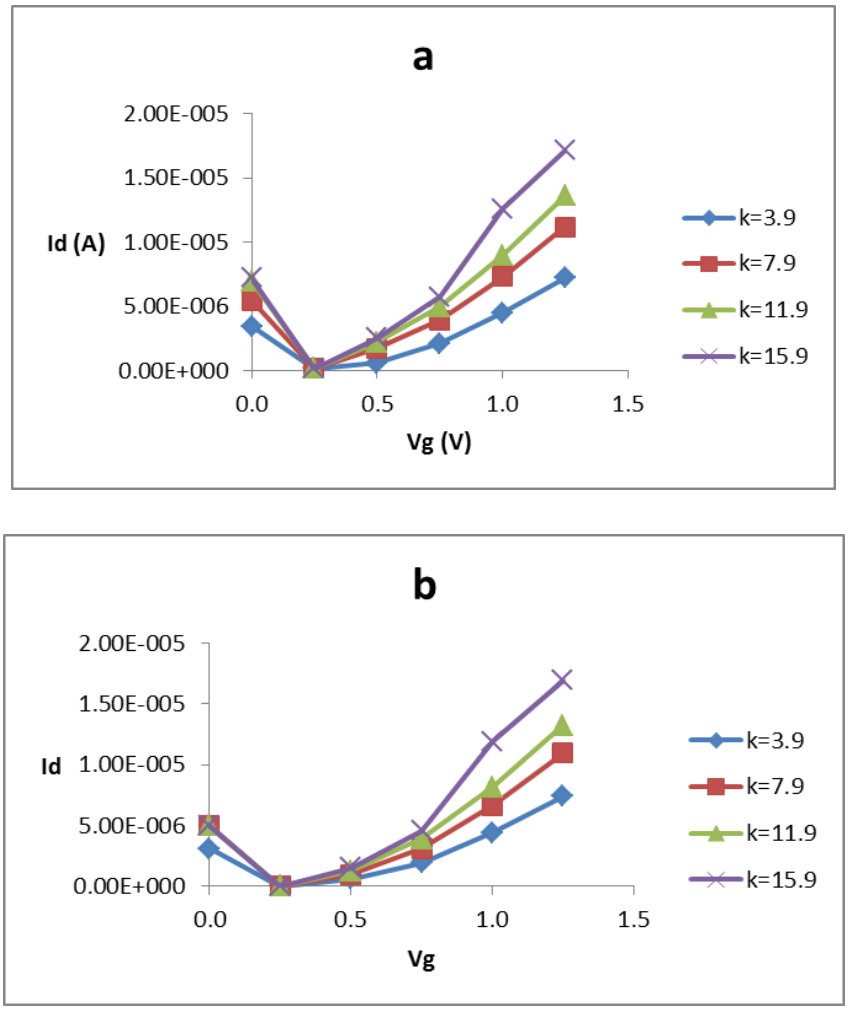

Figure 3.10: I_D vs. V_G characteristics of (a) Graphene Nanoribbon FET (b) Carbon Nanotube FET for different relative dielectric constant at V_D = 0.5 V.

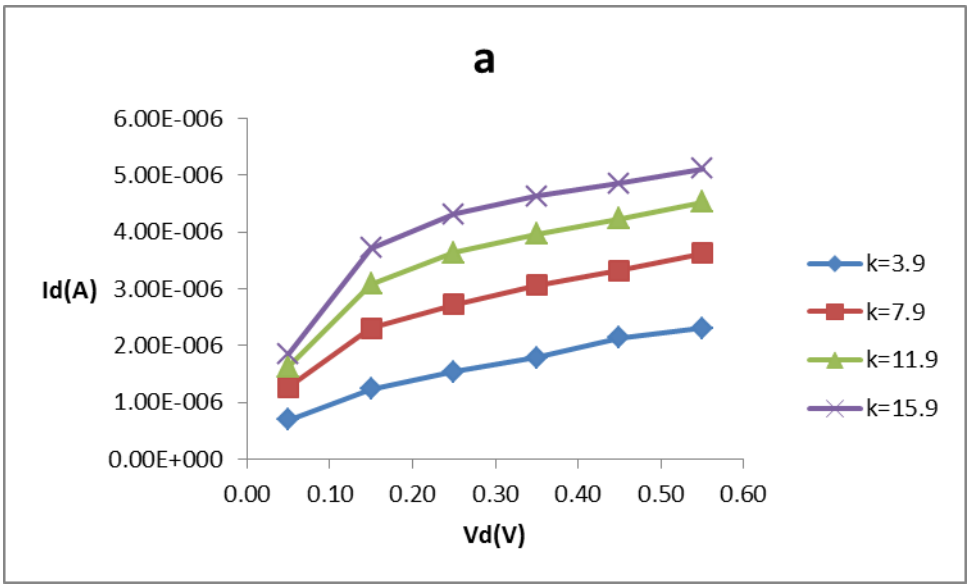

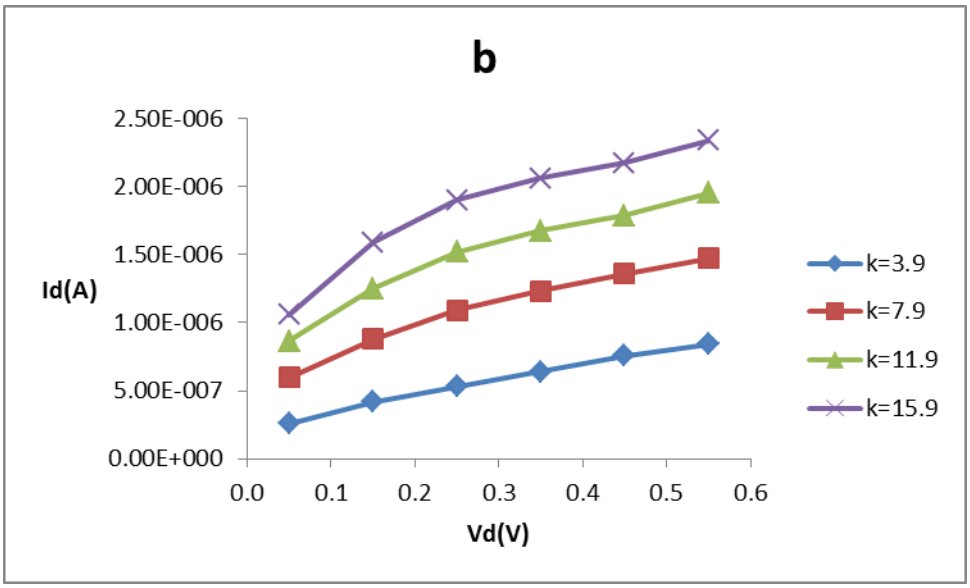

Figure 3.11: I_D vs. V_D characteristics of (a) Graphene Nanoribbon FET (b) Carbon Nanotube FET for different relative dielectric constant at V_G = 0.5 V.

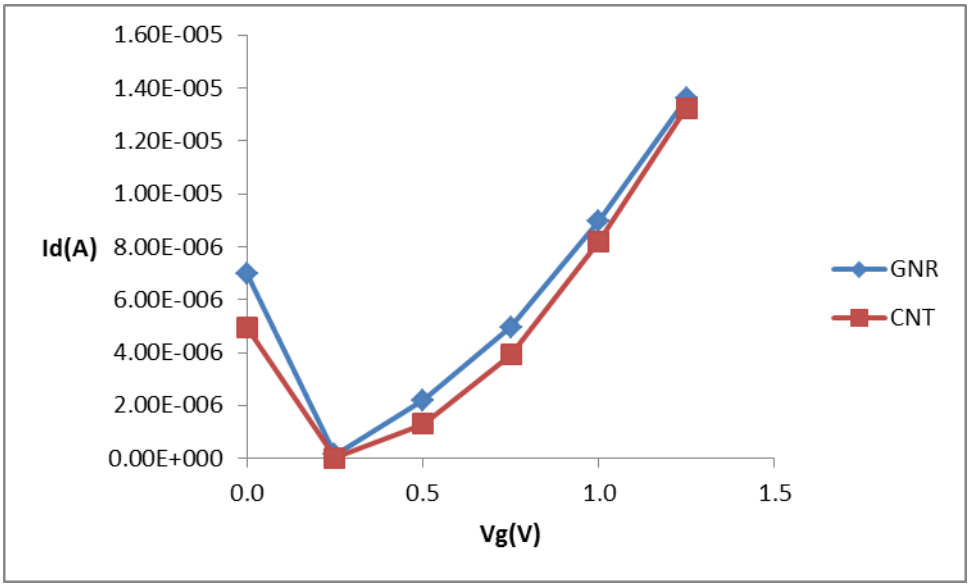

Figure 3.12: I_D vs. V_G characteristics of Graphene Nanoribbon FET and Carbon Nanotube FET for relative dielectric constant of 11.9 at V_D = 0.5 V.

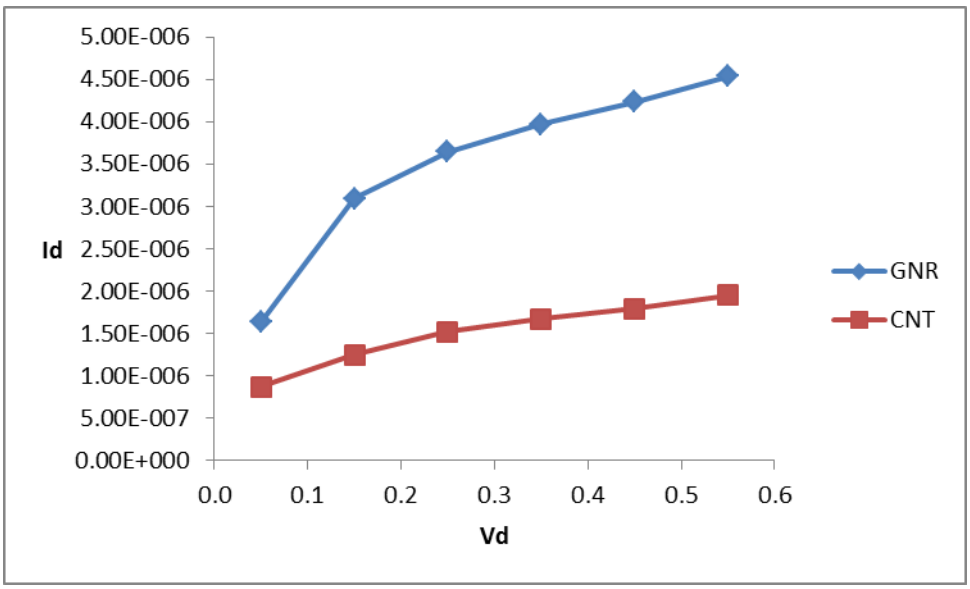

Figure 3.13: I_D vs. V_D characteristics of Graphene Nanoribbon FET and Carbon Nanotube FET for relative dielectric constant of 11.9 at V_G = 0.5 V.

Again we check the dielectric effect by varying contact temperature and observed that, as the contact temperature increases on state drain current and off state leakage current also increase for both GNRFET and CNTFET.

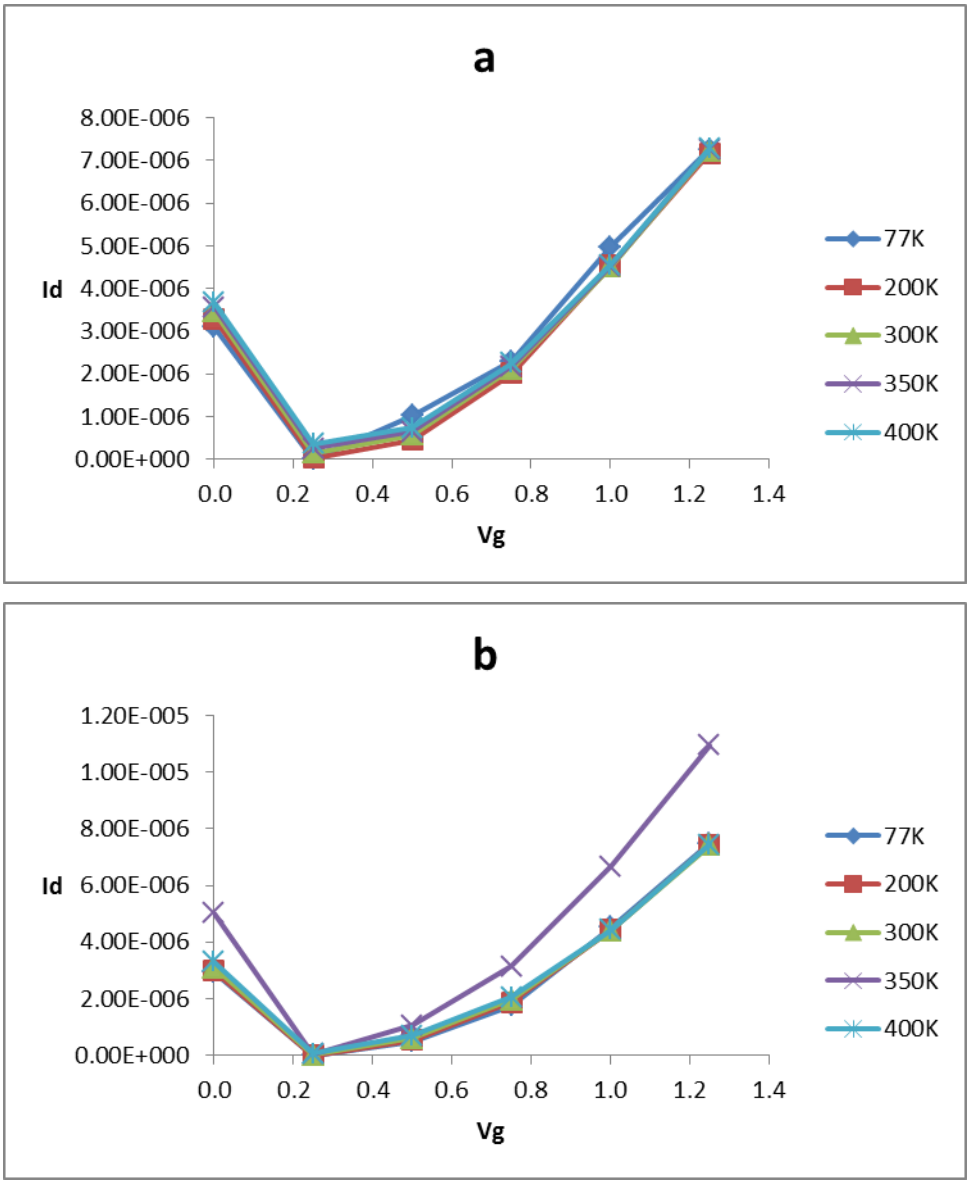

Figure 3.14: I_D vs. V_G characteristics of (a) Graphene Nanoribbon FET (b) Carbon Nanotube FET in different contact temperatures for relative dielectric constant k = 3.9 at V_D = 0.5 V.

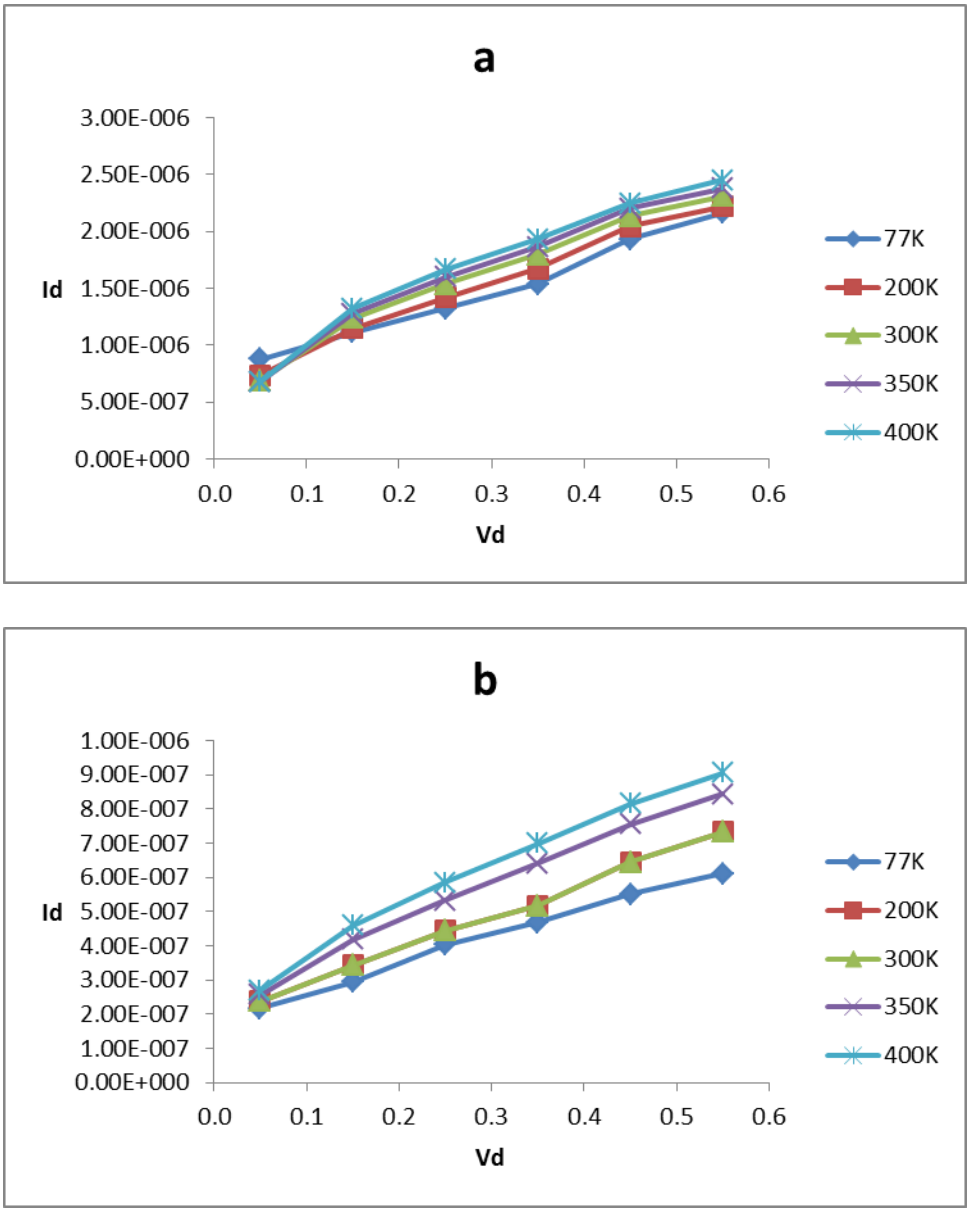

Figure 3.15: I_D vs. V_D characteristics of (a) Graphene Nanoribbon FET (b) Carbon Nanotube FET in different contact temperatures for relative dielectric constant k = 3.9 at V_G= 0.5 V.

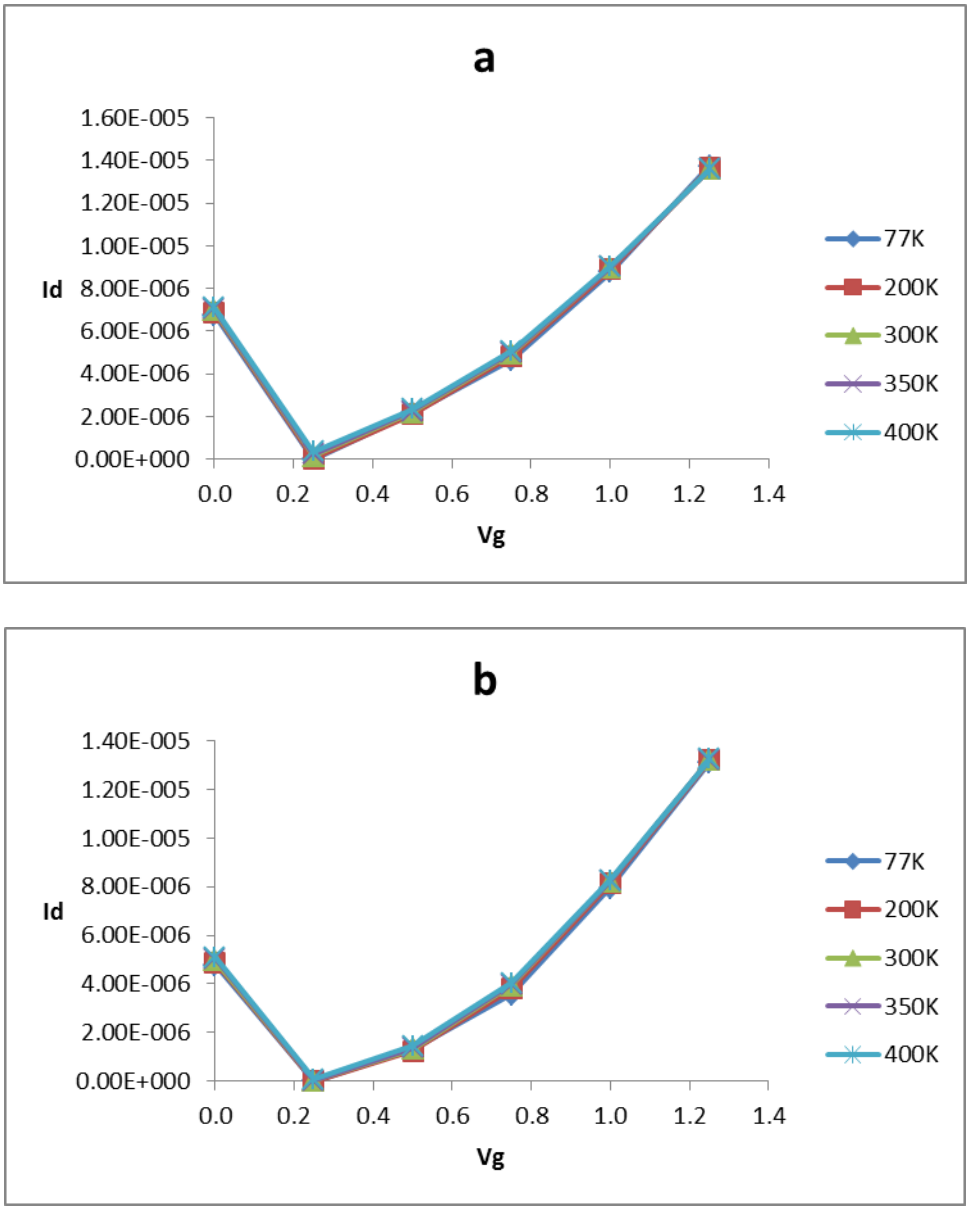

Figure 3.16: I_D vs. V_G characteristics of (a) Graphene Nanoribbon FET (b) Carbon Nanotube FET in different contact temperatures for relative dielectric constant k = 11.9 at V_D = 0.5 V.

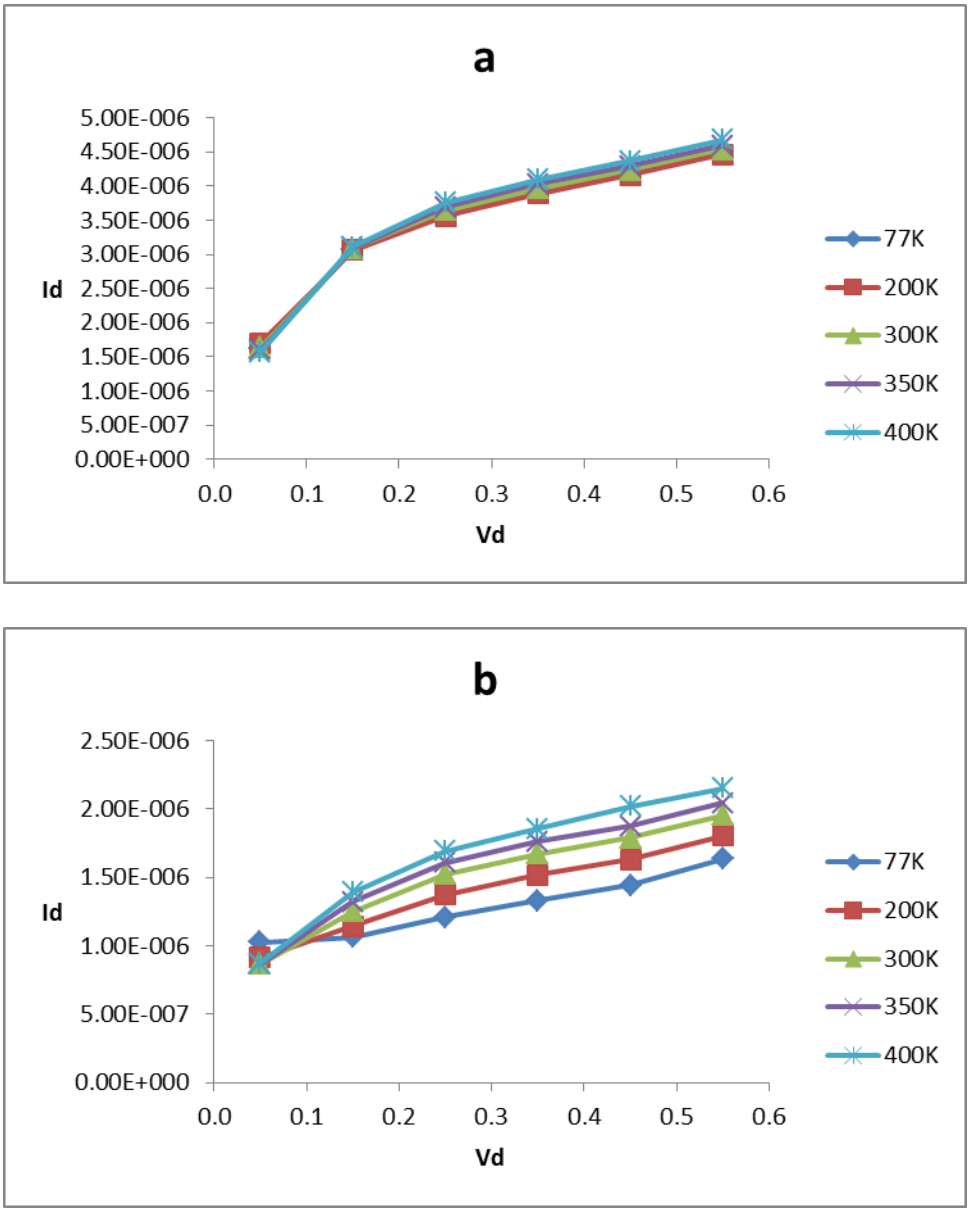

Figure 3.17: I_D vs. V_D characteristics of (a) Graphene Nanoribbon FET (b) Carbon Nanotube FET in different contact temperatures for relative dielectric constant k = 11.9 at V_G = 0.5 V.

3.2.3 Effect of Chirality

Now the discussion will relate the changing effect of chirality on GNRFET and CNTFET. Actually chirality relates with the diameter and diameter changing effect is very important for FET. That's why chirality changing effect is very important for any Graphene Nanoribbon or Carbon Nanotube based design. The equation that relates chirality and diameter is:

$$d_t = a\sqrt{n^2 + m^2 + nm}/\pi \qquad (3.7)$$

Where, m and n is the chiral axis (n, m). Here n should be always greater than m. The width of Graphene Nanoribbon is equal to the perimeter of the Carbon Nanotube [168].

The energy bandgap of the CNT is inversely proportional to the nanotube diameter (Egap α 1/Diameter) and also inversely proportional to the width of the GNR (Egap α 1/Width). Since the drain current of CNFET is dependent on the total charge that filled up the first subband, therefore it is possible that the drain current too depends on the diameter of CNT [169]. So ultimately the drain current depends on the chirality. In this experiment it will observe one chiral axis changing effect that is n. When it is changing n we will keep m value constant and the range of n value should be such a value that is always greater than m value to observe the effect on output. Other parameter will maintain their default value as like previous experiment.

Fig 3.18 shows the transfer characteristics of both GNR FET and CNT FET for different chirality. In Fig 3.18 (a), variation in I_D vs. V_G graph is seen for different chiralities of Graphene Nanoribbon. Graphene Nanoribbon can be metallic or semiconducting [170]. It is metallic when *N*= 3M-1, where *M* is an integer and N=2n. Hence, the gate voltage has little control over the drain currents as shown in in Fig 3.18(a). It is observed that for semi-conducting GNRs, the bandgap decreases with increasing chirality as width increases. In Fig 3.18(b) the ambipolar characteristics decreases and drain current increases as CNT diameter increases with increasing chirality. Comparing Fig 3.18(a) and Fig 3.18(b) it is seen that the order of the drain current of GNR FET is greater than the order of the drain current of CNT FET.

The output characteristics of GNRFET and CNTFET for different chirality are shown in Fig 3.19. In Fig 3.19 (a) the Graphene Nanoribbons have significantly higher off-state leakage currents compared to the Carbon nanotubes shown in Fig 3.19 (b).

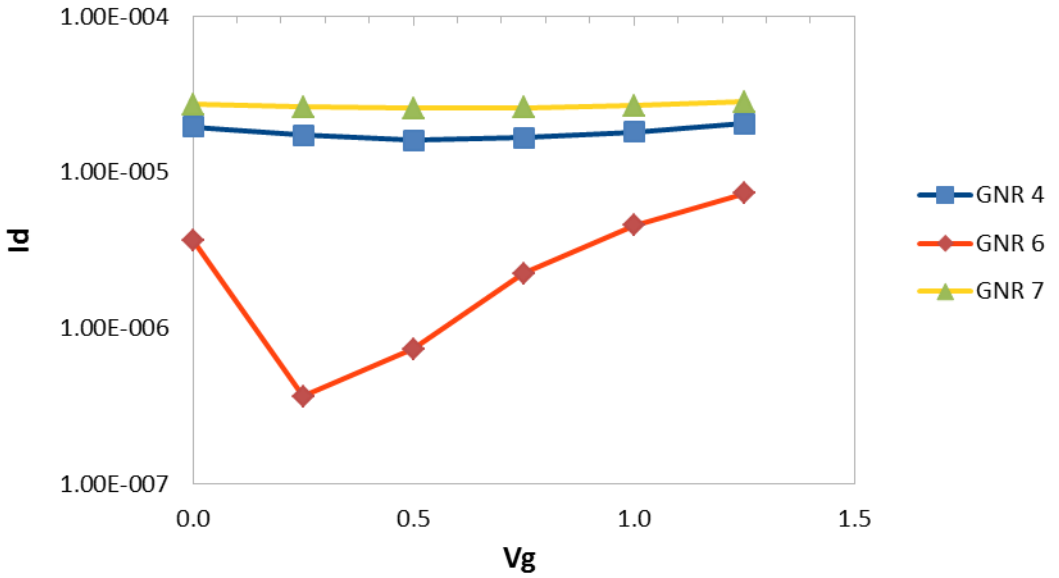

(a)

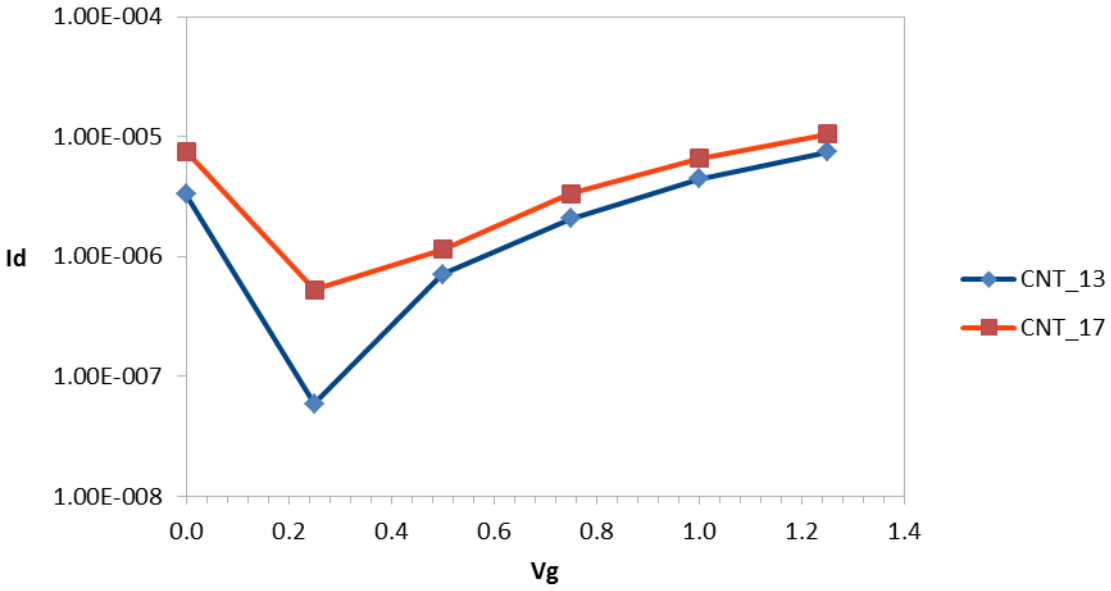

(b)

Fig 3.18 I_D vs. V_G characteristics of (a) Graphene Nanoribbon FET (b) Carbon Nanotube FET for different chirality at 400K V_D = 0.5 V.

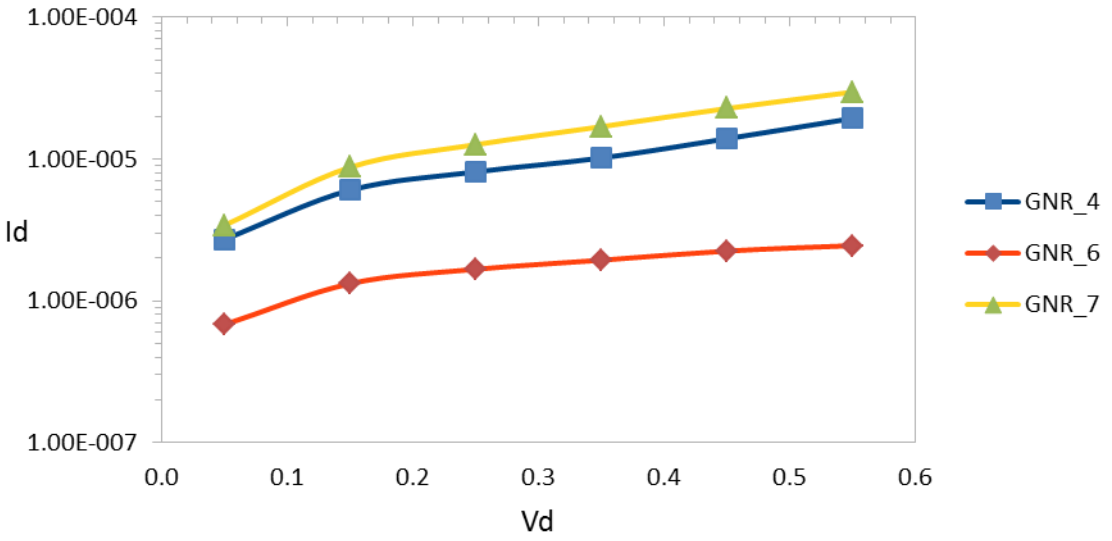

(a)

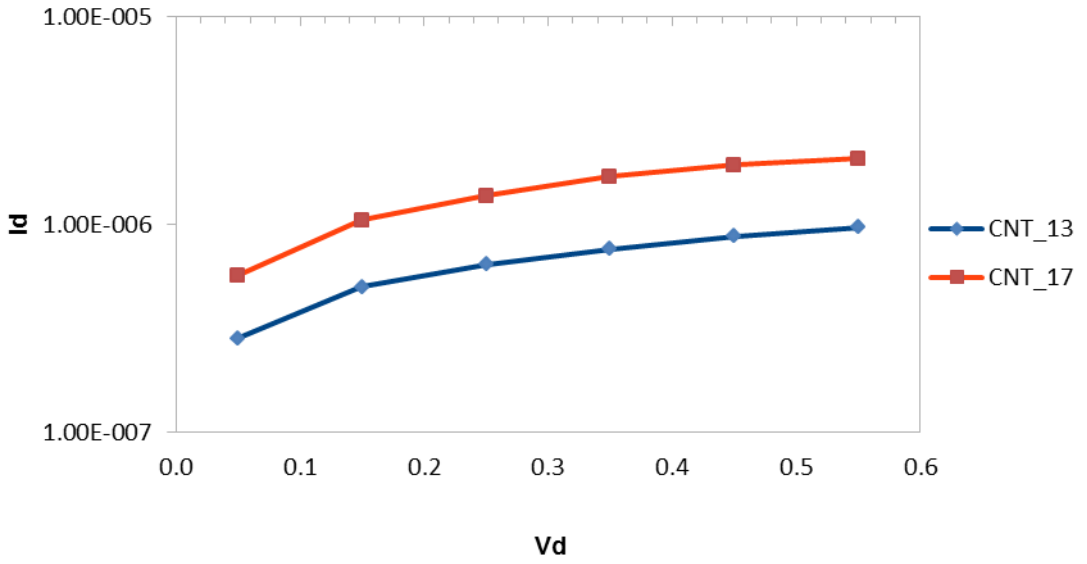

(b)

Fig 3.19: I_D vs. V_G characteristics of (a) Graphene Nanoribbon SBFET (b) Carbon Nanotube SBFET for different chirality at 400K and V_G = 0.5 V.

3.3 Summary

This research primarily investigates the dependence of the transfer and output characteristics of GNRFET and CNTFET with respect to contact temperature, relative dielectric constant and chirality. A comparative analysis of the transfer and output characteristics between the GNRFET and CNTFET is done in this chapter. Also, the results of contact temperature dependence of sub-10 nm Graphene Nanoribbon Array Field-Effect Transistors Fabricated by Block Copolymer Lithography are given in this paper and are compared to the contact temperature dependence of the GNRFET simulated in this research paper. The results of changing chirality of both GNRFET and CNTFET are observed. The transfer and output characteristics of the simulated GNRFET and CNTFET for relative dielectric constant with respect to contact temperature also observed in this chapter.

So, to summarize the results:

- The drain current increases only slightly with respect to contact temperature for both GNRFET and CNTFET.

- For both the transistors, the saturation current increases with respect to relative dielectric constant.

- For a specific relative dielectric constant, on state drain current increases with increasing contact temperature for both GNRFET and CNTFET.

- Ambipolar behavior decreases with respect to diameter of CNT and width of GNR for semiconducting transistors.

- The drain current is directly proportional to the diameter (CNT) or width (GNR) for both semiconducting GNRFET and CNTFET

- GNRFET has comparatively higher drain current than CNTFET.

Chapter 4

CONCLUSION

4.1 Conclusion

Of the most promising nanoscale device transistors currently grapheme and carbon nanotube are leading the way. Substantial research has been carried out on these materials and their accompanying devices. As a result the understanding of these devices has improved and has thus led to drastic improvements. The drawback faced by the present silicon MOSFESTs on the face of scaling has opened up avenues for a new range of devices and their application in logic circuit device which can significantly produce improved performance. Grapheme and carbon transistors that are of ideal quality are capable of providing significant performance and energy utility over regular CMOS technology. However high defect rates and material irregularity due to confinement of fabrication techniques are the setbacks faced by such nanoscale devices. Graphene and carbon nanotube exhibit electronic properties like high mobility which is remarkable and due to its scale it makes it possible to design high performance standard devices.

A detailed comparative analysis is undertaken between grapheme nanoribbon field-effect transistor and carbon nanotube field-effect transistor as part of this research paper. In this analysis three distinct parameters set are varied for each transistor. They are contact temperature, relative dielectric constant, and chirality. For each parameter varied for each transistor ID vs.V_G curves and ID vs. V_D curves are obtained for comparison purpose.

When it comes to the results the initial analysis demonstrates the effect of changing contact temperature on both transistor types. The transfer characteristic for contact temperature is very much similar since a ballistic transport has been assumed in our model. Additionally the output characteristics for GNRFET and CNTFET here a slight increase in drain current is visible with a rise in contact temperature. In contrast to CNTFET a higher drain current is observed for GNRFET.

The effects of changing relative dielectric constant on GNRFET and CNTFET are demonstrated in the second analysis. On-state drain current rises in relation to dielectric constant for both the FETs in

terms of both transfer and output characteristics. For both the transistors the transfer characteristics are the same whereas when it comes to output characteristics grapheme nanoribbon transistor possess a drain current that is higher. Thus we can infer from this analysis that performance of both grapheme nanoribbon and carbon nanotube transistors will improve with materials of higher relative dielectric constant.

The third part of our result and analysis section compares the changing effects of chirality of the two transistors. The diameter increases with respect to chirality. For GNR and CNT it is observed that gate voltage has only slight control over the drain current. For semiconducting FETs, it is observed that bandgap decreases with increasing diameter or width. As a result, drain current increases with respect to diameter or width. Lastly, the results obtained in this simulation are compared to the results of other research groups.

The changing effects of chirality of two transistors are compared in the third part of our outcome. Moreover the diameter increases in terms of chirality. In terms of semiconducting FETs it is evident that bandgap reduces with increase in diameter or width as a result of which the drain current also increases in that respect.

In the end after examination it can be said that grapheme nanoribbon and carbon nanotube field effect transistors has remarkable potential in the electronic industry and can be used to embark in a new era of electronics.

4.2 Future work:

There remain a large number of areas of graphene nanoribbon and carbon nanotube transistor modeling that can be explored further and which offer further scopes for improvement and development. The following would be the future prospects of this research:

- ✓ In future, the study can expand our study to the effects of varying transconductance and conductance of GNRFET and CNTFET.
- ✓ GNRFET and CNTFET with doped reservoirs can be modeled and simulate these transistors to make comparative analysis between these two transistors.
- ✓ In the future the performances of the GNRFET and CNTFET and GNRFET and CNTFET with doped reservoirs can be compared to determine which type of structure is better.

- ✓ Expanding comparison of GNRFET and CNTFET to traditional MOSFET to get a clearer picture of the performance of these transistors compared to MOSFET.
- ✓ Lastly, GNRFET and CNTFET can be modeled using different model physics and make simulation for each structure and make comparison between each model performances.

References

[1] Heng Chin Chuan, “Modeling and Analysis of Ballistic Carbon Nanotube Field Effect Transistor (CNTFET) with Quantum Transport Concept” MAY 2007, Unpublished.

[2] M P Anantram, and FL ´Léonard, “Physics of carbon nanotube electronic devices” Institute of Physics Publishing, Rep. Prog. Phys. 69, pp: 507–561, 2006.

[3] P. Avouris, J. Appenzeller, R. Martel, and S. J. Wind, “Carbon nanotube electronics”, Proceedings of the IEEE, Vol. 91, pp. 1772-1784, 2003.

[4] P. L. McEuen, M. S. Fuhrer, and H. K. Park, “Single-walled carbon nanotube electronics”, IEEE Transactions on Nanotechnology, Vol. 1, pp. 78-85, 2002.

[5] Zhu, Y., Murali, S., Cai, W., Li, X., Suk, J. W., Potts, J. R. and Ruoff, R. S. Graphene and Graphene Oxide: Synthesis, Properties, and Applications. Adv. Mater., 22: 3906–3924. doi: 10.1002/adma.201001068, 2010.

[6] Gianluca Fiori; Giuseppe Iannaccone, "NanoTCAD ViDES," https://nanohub.org/resources/vides, 2009. (DOI: 10.4231/D3RJ48T8X)

[7] Compano, R. ed. “Technology Roadmap for Nanoelectronics,” Microelectronics Advanced Research Initiative, 2000.

[8] David J. Frank et al, “Device Scaling Limits of Si MOSFETs and Their Application Dependencies,” proceedings of the IEEE, vol. 89, no . 3, march 2001.

[9] Chen, Z. et. al. “IDDQ Testing for Deep-Submicr on ICs: Challenges and Solutions,” IEEE Design and Test of Computers. pp: 24-33, 2002.

[10] Max Schulz, “The end of the road for Silicon?” Nature, Vol 399, 24 June, 1999.

[11] Yuhua Cheng, Chenming Hu (1999). “MOSFET classification and operation,” MOSFET modeling & BSIM3 user's guide. Springer. p. 13. ISBN 0-7923-8575-6.

[12] Rahmat Bin Sanudin, “Characterization of Ballistic Carbon Nanotube Field-Effect Transistor,” Thesis report, University Technology Malaysia, November 2005.

[13] James D. Plummer, Peter B. Griffin (2001).”Mate rial and Process Limits in Silicon VLSI Technology,” PROCEEDINGS OF THE IEEE, VOL. 89, NO. 3, MARCH 2001.

[14] Taur, Y., “CMOS design near the limit of scaling,” IBM J. Ref. & Dev., Volume: 46(2): pp: 213-220, 2002.

[15] T Surukai, “Perspectives on power aware electronics”, Keynote presentation, F, ISSCC Conference, pp.26-29, 2003.

[16] John L. Hennessy and David A. Patterson, “Computer Architecture, A Qualitative Approach”, Ed. 3, pp. 14. 55 Carbon Nanotube Field Effect Transistors

[17] J. Guo, S. Datta, and M. Lundstrom, "A numerical study of scaling issues for Schottky-Barrier carbon nanotube transistors," IEEE Transactions on Electron Devices, vol. 51, pp. 172-177, 2004.

[18] Paul Holister, Tim Harper and Christina Roman Vas, “Nanotubes White Paper,” CMP Cientifica, January 2003.

[19] T.Grace, “An Introduction to Carbon Nanotubes, ” Summer, Stanford University, 2003.

[20] Xiaolei Liu,“Synthesis, Devices and Applicatio ns of Carbon Nanotubes,” Thesis report, University of Southern California, January 2006.

[21] Jaldappagari Seetharamappa, Shivaraj Yellappa and Francis D’Souza, “Carbon Nanotubes: Next Generation of Electronic Materials,” The Elect rochemical Society Interface, Summer 2006.

[22] P.R. Bandaru., “Electrical Properties and Appl ications of Carbon Nanotube Structures,” Journal of Nanoscience and Nanotechnology Vol.7, 1– 29, 2007.

[23] T. W. Odom, J. L. Huang et al.,“Atomic structu re and electronic properties of single-walled Carbon Nanotubes,” Nature, Volume 391, January, 1998.

[24] Xiaolei Liu,“Synthesis, Devices and Applications of Carbon Nanotubes,” Thesis report,

University of Southern California, January 2006.
[25] J.Seetharamappa et al., “Carbon Nanotubes Next Generation of Electronic Materials,” summer, The Electrochemical Society Interface, 2006.
[26] Forro, L. and Schoenberger, C. “Physical Properties of Multi-wall Nanotubes”, Berlin, Germany: Springer-Verlag Berlin Heidelberg, pp: 329-390; 2001.
[27] Rasmita Sahoo and R. R. Mishra, “Simulations of Carbon Nanotube Field EffectTransistors,” International Journal of Electronic Engineering Research ISSN 0975- 6450 Volume 1 Number 2, pp. 117–125, 2009.
[28] Avouris et al., "Vertical scaling of carbon nanotube field-effect transistors using top gate electrodes," Applied Physics Letters, 2002.
[29] Paul Holister, Tim Harper and Christina Roman Vas, “Nanotubes White Paper,” CMP Cientifica, January 2003.
[30] Chen, Z. et. al. “IDDQ Testing for Deep-Submicron ICs: Challenges and Solutions,” IEEE Design and Test of Computers.pp: 24-33, 2002.
[31] Choi, W. B. et. al. “Aligned carbon nanotubes for nanoelectronics,” Institute of Physics Publishing, Volume: 15, pp: 512-516, 2002.
[32] Derycke, V. et. al. “Carbon Nanotube Inter- and Intramolecular Logic Gates,” Nano Letters, Volume:1(9), pp: 453-456, 2001.
[33] W. Shockley and G.L. Pearson, Phys. Rev. 74, 232, 1948.
[34] S.J. Tans, A.R.M. Verschueren, and C. Dekker, Nature 393, 49, 1998.
[35] D. Kahng and M.M. Atalla, Silicon-Silicon Dioxide Field Induced Surface Devices, IRE Solid-State Device Research Conference, Carnegie Institute of Technology, Pittsburgh, PA, 1960.
[36] D. Jiménez, X. Cartoixà, E. Miranda, J. Suñé, F. A. Chaves, and S. Roche, “A simple drain current model for Schottky-barrier carbon nanotube field effect transistors” Bercelona,Spain pp: 1-18, 2007.
[37] Andronico, Michael (14 April 2014). "5 Ways Graphene Will Change Gadgets Forever". Laptop.
[38]"Graphene properties". www.graphene-battery.net. 2014-05-29. Retrieved 2014-05-29.
[39]"This Month in Physics History: October 22, 2004: Discovery of Graphene".APS News. Series II 18 (9): 2. 2009.
[40]Fodor, J. K. Simulations involving carbon nanotubes and nanoribbons. Gainesville, Fla.: University of Florida, 2007.
[41]"This Month in Physics History: October 22, 2004: Discovery of Graphene".APS News. Series II 18 (9): 2. 2009.
[42]Wu, Yudong. Simulation of graphene electronic devices. Ph.D. thesis, University of Birmingham, 2011.
[43]"The Nobel Prize in Physics 2010 - Advanced Information". Nobelprize.org.Nobel Media AB 2014. Web. 22 Aug2014. http://www.nobelprize.org/nobel_prizes/physics/laureates/2010/advanced.html
[44] A. K. Geim and K. S. Novoselov, Nature Materials 6, 183, 2007.
[45] D. R. Dreyer , R. S. Ruoff , C. W. Bielawski , Angew. Chem. Int. Ed.2010 , 49 , 9336.
[46] M. S. Dresselhaus , G. Dresselhaus , Adv. Phys. 1981 , 30 , 139.
[47] V. H. P. Boehm , A. Clauss , G. O. Fischer , U. Hofmann , Z. Naturforschg.1962 , 17 , 150 .
[48] P. M. Stefan , M. L. Shek , I. Lindau , W. E. Spicer , L. I. Johansson , F. Herman , R. V. Kasowski , G.Brogen , Phys. Rev. B 1984 , 29 , 5423 .
[49] T. Aizawa , R. Souda , S. Otani , Y. Ishizawa , C. Oshima , Phys. Rev. Lett. 1990 , 64 , 768 .
[50] A. Nagashima , K. Nuka , H. Itoh , T. Ichinokawa , C. Oshima , S. Otani , Surf. Sci. 1993 , 291 , 93 .
[51] Chuhei Oshima et al 1977 Jpn. J. Appl. Phys. 16 965. doi:10.1143/JJAP.16.965
R. Rosei , M. De Crescenzi , F. Sette , C. Quaresima , A. Savoia ,P. Perfetti , Phys. Rev. B 1983 , 28 , 1161 .
[54] N. R. Gall , S. N. Mikhailov , E. V. Rut’kov , A. Y. Tontegode , Sov. Phys.Solid State 1985 , 27 , 1410.

[55] H. Zi-Pu , D. F. Ogletree , M. A. Van Hove , G. A. Somorjai , Surf. Sci.1987 , 180 , 433 .
[56] A. J. Van Bommel , J. E. Crombeen , A. Van Tooren , Surf. Sci. 1975 , 48 , 463 .
[57] Y. Zhang , J. Small , W. Pontius , P. Kim , Appl. Phys. Lett. 2005 , 86 ,073104 .
[58] D. D. L. Chung , J. Mater. Sci. 1987 , 22 , 4190 .
[59] X. Lu , M. Yu , H. Huang , R. Ruoff , Nanotechnology 1999 , 10 , 269 .
[60] X. Du , I. Skachko , A. Barker , E. Y. Andrei , Nat. Nanotechnol. 2008 , 3 , 491 .
[61] S. V. Morozov , K. S. Novoselov , M. I. Katsnelson , F. Schedin , D. C. Elias , J. A. Jaszczak , A. K. Geim , Phys. Rev. Lett. 2008 , 100 , 016602.
[62] E. V. Castro , H. Ochoa , M. I. Katsnelson , R. V. Gorbachev , D. C. Elias , K. S. Novoselov , A. K. Geim , Phys. Rev. Lett. 2008 , 100 , 016602.
[63] A. A. Balandin , S. Ghosh , W. Bao , I. Calizo , D. Teweldebrhan , F. Miao , C. N. Lau , Nano Lett. 2008 , 8 , 902.
[64] C. Lee , X. Wei , J. W. Kysar , J. Hone , Science 2008 , 321 , 385.
[65] S. Berciaud , S. Ryu , L. E. Brus , T. F. Heinz , Nano Lett. 2009 , 9 , 346.
[66] C. Soldano , A. Mahmood , E. Dujardin , Carbon 2010 , 48 , 2127.
[67] X. L. Li , G. Y. Zhang , X. D. Bai , X. M. Sun , X. R. Wang , E. G. Wang , H. J. Dai , Nat. Nanotechnol. 2008 , 3 , 538 .
[68] Y. Hernandez , V. Nicolosi , M. Lotya , F. M. Blighe , Z. Sun , S. De , I. T. McGovern , B. Holland , M. Byrne , Y. K. Gun'ko , J. J. Boland , P. Niraj , G. Duesberg , S. Krishnamurthy , R. Goodhue , J. Hutchison , V. Scardaci , A. C. Ferrari , J. N. Coleman , Nat. Nanotechnol. 2008 , 3 , 563
[69]U. Khan , A. O'Neill , M. Lotya , S. De , J. N. Coleman , Small 2010 , 6 , 864 .
[70] C. Valles , C. Drummond , H. Saadaoui , C. A. Furtado , M. He , O. Roubeau , L. Ortolani ,
[71] M. Monthioux , A. Penicaud , J. Am. Chem. Soc. 2008 , 130 , 15802 .
[72] J. S. Moon , D. Curtis , M. Hu , D. Wong , C. McGuire , P. M. Campbell , G. Jernigan , J. L. Tedesco , B. VanMil , R. Myers-Ward , C. J. Eddy , D. K. Gaskill , IEEE Electron. Device Lett. 2009 , 30 , 650 .
[73] O. C. Compton , S. T. Nguyen , Small 2010 , 6 , 711 .
[74] Y. Si , E. T. Samulski , Nano Lett. 2008 , 8 , 1679 .
[75] D. R. Dreyer , S. Park , C. W. Bielawski , R. S. Ruoff , Chem. Soc. Rev. 2010 , 39 , 228 .
[76] S. Park , J. An , I. Jung , R. D. Piner , S. J. An , X. Li , A. Velamakanni , R. S. Ruoff , Nano Lett. 2009 , 9 , 1593 . M. A. Rafi ee , J. Rafi ee , Z. Wang , H. Song , Z.-Z. Yu , N. Koratkar , ACS Nano 2009 , 3 , 3884 .
[76] Y. Shao , J. Wang , M. Engelhard , C. Wang , Y. Lin , J. Mater. Chem. 2010 , 20 , 743 .
[77] L. J. Cote , R. Cruz-Silva , J. Huang , J. Am. Chem. Soc. 2009 , 131 , 1 1027 .
[78] V. Strong , S. Dubin , M. F. El-Kady , A. Lech , Y. Wang , B. H. Weiller , R. B. Kaner , ACS Nano 2012 , 6 , 1395 .
[79] Y. Dedkov , A. Shikin , V. Adamchuk , S. Molodtsov , C. Laubschat , A. Bauer , G. Kaindl , Phys. Rev. B 2001 , 64 , 035405
[80] P. W. Sutter , J.-I. Flege , E. A. Sutter , Nat. Mater. 2008 , 7 , 406 .
[81] T. A. Land , T. Michely , R. J. Behm , J. C. Hemminger , G. Comsa , Surf. Sci. 1992 , 264 , 261 .
[82] Y. S. Dedkov , M. Fonin , C. Laubschat , Appl. Phys. Lett. 2008 , 92 , 052506 .
[83] A. T. N'Diaye , J. Coraux , T. N. Plasa , C. Busse , T. Michely , New J. Phys. 2008 , 10 , 043033 .
[84] Y. Wang , C. Miao , B.-c. Huang , J. Zhu , W. Liu , Y. Park , Y.-h. Xie , J. C. S. Woo , IEEE Trans. Electron Devices 2010 , 57 , 3472 .
[85] W. Cai , R. D. Piner , Y. Zhu , X. Li , Z. Tan , H. C. Floresca , C. Yang , L. Lu , M. J. Kim , R. S. Ruoff , Nano Res. 2009 , 2 , 851 .
W. Liu , C.-H. Chung , C.-Q. Miao , Y.-J. Wang , B.-Y. Li , L.-Y. Ruan , K. Patel , Y.-J. Park , J. Woo , Y.-H.

Xie , Thin Solid Films 2010 , 518 , S128 .

[86] A. Reina , X. Jia , J. Ho , D. Nezich , H. Son , V. Bulovic , M. S. Dresselhaus , J. Kong , Nano Lett. 2009 , 9 , 30 .

[87] G. Lopez , E. Mittemeijer , Scr. Mater. 2004 , 51 , 1 .

[88] G. L. Selman , P. J. Ellison , A. s. Darling , Platinum Metals Rev. 1970 , 14 , 14 .

[89] S. Bhaviripudi , X. Jia , M. S. Dresselhaus , J. Kong , Nano Lett. 2010 , 10 , 4128 .

[90] J. Wu , W. Pisula , K. Muellen , Chem. Rev. 2007 , 107 , 718 .

[91] X. Yang , X. Dou , A. Rouhanipour , L. Zhi , H. J. Rader , K. Müllen , J. Am. Chem. Soc. 2008 , 130 , 4216 .

[92] J. Cai , P. Ruffi eux , R. Jaafar , M. Bieri , T. Braun , S. Blankenburg , M. Muoth , A. P. Seitsonen , M. Saleh , X. Feng , K. Muellen , R. Fasel , Nature 2010 , 466 , 470 .

[93] X. Yan , X. Cui , L.-s. Li , J. Am. Chem. Soc. 2010 , 132 , 5944 .

[94] X. Yan , X. Cui , B. Li , L.-s. Li , Nano Lett. 2010 , 10 , 1869 .

[95] Kusmartsev, F. V.; Wu, W. M.; Pierpoint, M. P.; Yung, K. C. . "Application of Graphene within Optoelectronic Devices and Transistors", 2014. arXiv:1406.0809 [cond-mat.mtrl-sci].

[97] Meyer, J.; Geim, A. K.; Katsnelson, M. I.; Novoselov, K. S.; Booth, T. J.; Roth, S. "The structure of suspended graphene sheets". Nature 446 (7131): 60–63, 2007. arXiv:cond-mat/0701379.Bibcode:2007Natur.446...60M. doi:10.1038/nature05545. PMID 17330039.

[98] Neto, A Castro; Peres, N. M. R.; Novoselov, K. S.; Geim, A. K.; Geim, A. K.. "The electronic properties of graphene" (PDF). Rev Mod Phys 81: 109, 2009.

[99] Charlier, J.-C.; Eklund, P.C.; Zhu, J.; Ferrari, A.C. "Electron and Phonon Properties of Graphene: Their Relationship with Carbon Nanotubes". In Jorio, A.; Dresselhaus and, G.; Dresselhaus, M.S. Carbon Nanotubes: Advanced Topics in the Synthesis, Structure, Properties and Applications (Berlin/Heidelberg: Springer-Verlag), 2008.

[100] Semenoff, G. W. "Condensed-Matter Simulation of a Three-Dimensional Anomaly".Physical Review Letters 53 (26): 2449, 1984.

[101] Avouris, P.; Chen, Z.; Perebeinos, V. "Carbon-based electronics". Nature Nanotechnology2 (10):605-15, 2007.

[102] Semenoff, G. W. "Condensed-Matter Simulation of a Three-Dimensional Anomaly".Physical Review Letters 53 (26): 2449, 1984.

[103] Lamas, C.A.; Cabra, D.C.; Grandi, N. "Generalized Pomeranchuk instabilities in graphene".Physical Review B 80 (7): 75108, 2009.

[104] Lamas, C.A.; Cabra, D.C.; Grandi, N. "Generalized Pomeranchuk instabilities in graphene".Physical Review B 80 (7): 75108, 2009.

[105] Geim, A. K.; Novoselov, K. S. "The rise of graphene". Nature Materials 6 (3): 183–91, 2007.

[106] Novoselov, K. S.; Geim, A. K.; Morozov, S. V.; Jiang, D.; Katsnelson, M. I.; Grigorieva, I. V.; Dubonos, S. V.; Firsov, A. A. "Two-dimensional gas of massless Dirac fermions in graphene".Nature 438 (7065): 197–200, 2005.

[107] Morozov, S.V.; Novoselov, K.; Katsnelson, M.; Schedin, F.; Elias, D.; Jaszczak, J.; Geim, A. "Giant Intrinsic Carrier Mobilities in Graphene and Its Bilayer". Physical Review Letters 100 (1): 016602, 2008.

[109] Chen, J. H.; Jang, Chaun; Xiao, Shudong; Ishigami, Masa; Fuhrer, Michael S. "Intrinsic and Extrinsic Performance Limits of Graphene Devices on SiO2". Nature Nanotechnology 3 (4): 206–9, 2008.

[110] Akturk, A.; Goldsman, N. "Electron transport and full-band electron–phonon interactions in graphene". Journal of Applied Physics 103 (5): 053702, 2008.

[111] Kusmartsev, F. V.; Wu, W. M.; Pierpoint, M. P.; Yung, K. C. "Application of Graphene within Optoelectronic Devices and Transistors", 2014.

[112] Physicists Show Electrons Can Travel More Than 100 Times Faster in Graphene :: University Communications Newsdesk, University of Maryland. Newsdesk.umd.edu (2008-0324).

[113] Jens Baringhaus et al., Exceptional ballistic transport in epitaxial graphene nanoribbons, Nature, 2014, DOI: 10.1038/nature12952

[114] Baringhaus, J.; Ruan, M.; Edler, F.; Tejeda, A.; Sicot, M.; Taleb-Ibrahimi, A.; Li, A. P.; Jiang, Z.; Conrad, E. H.; Berger, C.; Tegenkamp, C.; De Heer, W. A. "Exceptional ballistic transport in epitaxial graphene nanoribbons". Nature 506 (7488): 349, 2014.

[115] Chen, J. H.; Jang, C.; Adam, S.; Fuhrer, M. S.; Williams, E. D.; Ishigami, M. "Charged Impurity Scattering in Graphene". Nature Physics 4 (5): 377–381, 2008.

[116] A. J. Frenzel, C. H. Lui, Y. C. Shin, J. Kong, N. Gedik, Semiconducting-to-Metallic Photoconductivity Crossover and Temperature-DependentDrude Weight in Graphene, Physical Review Letters, 2014, DOI: 10.1103/PhysRevLett.113.056602

[117] Schedin, F.; Geim, A. K.; Morozov, S. V.; Hill, E. W.; Blake, P.; Katsnelson, M. I.; Novoselov, K. S. "Detection of individual gas molecules adsorbed on graphene". Nature Materials 6 (9): 652–655, 2007.

[118] Adam, S.; Hwang, E. H.; Galitski, V. M.; Das Sarma, S. "A self-consistent theory for graphene transport". Proc. Nat. Acad. Sci. USA 104 (47): 18392–7, 2007.

[119] Steinberg, Hadar; Barak, Gilad; Yacoby, Amir; et al. "Charge fractionalization in quantum wires (Letter)". Nature Physics 4 (2): 116–119, 2008.

[120] Trisetyarso, Agung. "Dirac four-potential tunings-based quantum transistor utilizing the Lorentz force". Quantum Information & Computation 12 (11–12): 989, 2012.

[121] Chen, Shanshan; Wu, Qingzhi; Mishra, Columbia; Kang, Junyong; Zhang, Hengji; Cho, Kyeongjae; Cai, Weiwei; Balandin, Alexander A.; Ruoff, Rodney S. "Thermal conductivity of isotopically modified graphene". Nature Materials (2012-01-10) 11 (3): 203, 2012.

[122] Y.-W. Son, M. L. Cohen, S. G. Louie, “Energy gaps in graphene nanoribbons”, Phys. Rev. Lett. Vol. 97, n. 21, 216803-1-4, 2006.

[123] G. Iannaccone, G. Fiori, M. Macucci, P. Michetti, M. Cheli, A. Betti, P. Marconcini, "Perspectives of graphene nanoelectronics: probing technological options with modeling", IEDM 2009, 7-9 December, Baltimore, USA.

[124] E. McCann, V. I. Fal’ko, “Landau-level degeneracy and quantum Hall effect in a graphite layer”, Phys. Rev. Lett. Vol. 96, n. 8, 086805-1-4, 2006.

[125] E.V. Castro, K. S. Novoselov, V. Morozov, N.M.R. Peres, J.M.B. Lopes dos Santos, J. Nilsson, F. Guinea, A. K. Geim, and A. H. Castro Neto, “Biased bilayer graphene: Semiconductor with a gap tunable by the electric field effect”, Phys. Rev. Lett., Vol. 99, p. 216902, 2007.

[126] T. Ohta et al., “Controlling the electronic structure of bilayer graphene”, Science, Vol. 313, n. 5789, pp. 951-954, 2008.

[127] Y. Zhang, T.T. Tang, C. Girit, Z. Hao, M. C. Martin, A. Zettl, M. F. Crommie, Y. R. Shen, F. Wang, "Direct observation of a widely tunable bandgap in bilayer graphene", Nature,Vol. 459, p. 820-823, 2009.

[128] S. Y. Zhou et al., “Substrate-induced bandgap opening in epitaxial graphene”, Nat. Mat., Vol. 6, n. 10, p. 770, 2007.

[129] M. Cheli, P. Michetti, G. Iannaccone, “Physical Insights on Nanoscale FETs based on epitaxial graphene on SiC”, Proc. ESSDERC 2009, 193-196, 2009.

[130] T. J. Echtermeyer, M. C. Lemme, M. Baus, B. N. Szafranek, A. K. Geim, H. Kurz, “Nonvolatile Switching in Graphene Field-Effect Devices”, IEEE EDL, Vo. 29, pp. 952-954, 2009.

[131] T. J. Echtermeyer, M. C. Lemme, M. Baus, B. N. Szafranek, A. K. Geim, H. Kurz,“Nonvolatile Switching in Graphene Field-Effect Devices”, IEEE EDL, Vo. 29, pp. 952-954, 2009.

[132] Fodor, J. K. Simulations involving carbon nanotubes and nanoribbons. Gainesville, Fla.: University of Florida, 2007. Nihar Mohanty, David Moore, Zhiping Xu, T. S. Sreeprasad, Ashvin Nagaraja, Alfredo A. Rodriguez and Vikas Berry. "Nanotomy Based Production of Transferrable and Dispersible Graphene-Nanostructures of Controlled Shape and Size". Nature Communications 3 (5): 844, 2012.
[133] Brumfiel, G. "Nanotubes cut to ribbons New techniques open up carbon tubes to create ribbons", 2009.
[134] Kosynkin, Dmitry V.; Higginbotham, Amanda L.; Sinitskii, Alexander; Lomeda, Jay R.; Dimiev, Ayrat; Price, B. Katherine; Tour, James M. "Longitudinal unzipping of carbon nanotubes to form graphene nanoribbons". Nature 458 (7240): 872-6, 2009.
[135] Liying Jiao, Li Zhang, Xinran Wang, Georgi Diankov & Hongjie Dai. "Narrow graphene nanoribbons from carbon nanotubes". Nature 458 (7240): 877–80, 2009.
[136] "Writing Graphene Circuitry With Ion 'Pens'". ScienceDaily. Mar 27, 2012.
[137] "AIP's Physics News Highlights March 27, 2012". American Institute of Physics (AIP). 2012-03-28.
[138] S. Tongay, M. Lemaitre, J. Fridmann, A. F. Hebard, B. P. Gila, and B. R. Appleton. "Drawing graphene nanoribbons on SiC by ion implantation".Appl. Phys. Lett. 100 (073501), 2012.
[139] Barone, V., Hod, O., and Scuseria, G. E. "Electronic Structure and Stability of Semiconducting Graphene Nanoribbons". Nano Letters 6 (12): 2748–54, 2006.
[140] Han., M.Y., Özyilmaz, B., Zhang, Y., and Kim, P. "Energy Band-Gap Engineering of Graphene Nanoribbons". Physical Review Letters 98 (20), 2007.
[141]Tapasztó, Levente; Dobrik, Gergely; Lambin, Philippe; Biró, László P. "Tailoring the atomic structure of graphene nanoribbons by scanning tunnelling microscope lithography". Nature Nanotechnology 3 (7): 397–401, 2008.
[141] Son Y.-W., Cohen M. L., and Louie S. G. "Energy Gaps in Graphene Nanoribbons". Physical Review Letters 97 (21), 2006.
[142] L. F. Huang, G. R. Zhang, X. H. Zheng, P. L. Gong, T. F. Cao, and Z. Zeng. "Understanding and tuning the quantum-confinement effect and edge magnetism in zigzag graphene nanoribbon". J. Phys.: Condens. Matter 25 (5): 055304, 2013.
[143] Fiori G., Iannaccone G. "Simulation of Graphene Nanoribbon Field-Effect Transistors". IEEE Electron Device Letters 28 (8): 760, 2007.
[144] Gianluca Fiori; Giuseppe Iannaccone, "NanoTCAD ViDES," https://nanohub.org/resources/vides, 2009. (DOI: 10.4231/D3RJ48T8X).
[145] Wang, Z. F., Shi, Q. W., Li, Q., Wang, X., Hou, J. G., Zheng, H., Yao, Y., Chen, J. "Z-shaped graphene nanoribbon quantum dot device". Applied Physics Letters 91 (5): 053109, 2007.
[146] Bullis, Kevin. "Graphene Transistors". Technology Review (Cambridge: MIT Technology Review, Inc), 2008-01-28.
[148] Bullis,Kevin. "TR10: Graphene Transistors". Technology Review(Cambridge: MIT Technology Review, Inc), 2008-02-25.
[149] Wang, Xinran; Ouyang, Yijian; Li, Xiaolin; Wang, Hailiang; Guo, Jing; Dai, Hongjie. "Room-Temperature All-Semiconducting Sub-10-nm Graphene Nanoribbon Field-Effect Transistors". *Physical Review Letters* 100 (20), 2008. arXiv:0803.3464
[150]Jing; Dai, Hongjie. "Room-Temperature All-Semiconducting Sub-10-nm Graphene Nanoribbon Field-Effect Transistors". Physical Review Letters 100 (20), 2008.
[150] Ballon, M. S. Carbon nanoribbons hold out possibility of smaller, speedier computer chips. Stanford Report, 2008-05-28.
[151] Schwierz F. Graphene transistors. Nat. Nanotechnol. 5, 487–496, 2010.

[152] "The Nobel Prize in Physics 2010 - Advanced Information". Nobelprize.org.Nobel Media AB 2014. Web. 22 Aug 2014. http://www.nobelprize.org/nobel_prizes/physics/laureates/2010/advanced.html
Gianluca Fiori; Giuseppe Iannaccone, "NanoTCAD ViDES,"

[153] https://nanohub.org/resources/vides, 2009. (DOI: 10.4231/D3RJ48T8X).

[154] G. Fiori, G. Iannaccone, "Simulation of Graphene Nanoribbon Field-Effect Transistors", IEEE, Electron Device Letters, Vol. 28, Issue 8, pp. 760 - 762, 2007.

[155] G. Fiori, G. Iannaccone, G. Klimeck, "A Three-Dimensional Simulation Study of the Performance of Carbon Nanotube Field-Effect Transistors With Doped Reservoirs and Realistic Geometry", IEEE Transaction on Electron Devices, Vol. 53, Issue 8, pp. 1782-1788, 2006. doi: 10.1109/TED.2006.878018

[156] S. Datta, "Nanoscale device modeling: Green's function method," Superlattices Microstruct., vol. 28, no. 4, pp. 253–277, Jul. 2000.

[157] J. Guo et al., "Performance analysis and design optimization of near ballistic carbon nanotube field-effect transistors," in IEDM Tech. Dig., 2004, pp. 703–706

[158] Y.W. Son, M.L. Cohen, and S.G. Louie, "Energy gaps in graphene nanoribbons", Phys. Rev. Lett., Vol. 97, pp.216803, 2006.

[159] R. Saito, G. Dresselhaus, and M. S. Dresselhaus, Physical Properties of Carbon Nanotubes. London, U.K.: Imperial College Press, 2003, pp. 35–58.

[160] Xie, Huaqing; Chen, Lifei; Yu, Wei; Wang, Bingqian, "Temperature dependent thermal conductivity of a free-standing graphene nanoribbon," Applied Physics Letters , vol.102, no.11, pp.111911,111911-4, Mar 2013.

[161] J. G. Son, M. Son, K. J. Moon, B. H. Lee, J. M. Myoung, M. S. Strano, et al.,"Sub-10 nm Graphene Nanoribbon Array Field-Effect Transistors Fabricated by Block Copolymer Lithography," Advanced Materials, vol. 25, pp. 4723-4728, 2013.

[162] S. Mudanai, Y Y Fang, Q Quyang, "Modeling of direct tunneling current through gate dielectric stacks", IEEE Trans. Electron Dev, vol. 47, Number. 10, pp. 1851–1857, 2000.

[163] Rasmita Sahoo et al., "Carbon Nanotube Field Effect Transistor: Basic Characterization and Effect of High Dielectric Material" International Journal of Recent Trends in Engineering, Vol 2, No. 7, November 2009.

[164] A. Kawamoto., J. Jameson, K. Cho, and R. Dutton, "Challenges for Atomic Scale Modeling in Alternative Gate Stack Engineering," IEEE Trans. Electron Dev, vol. 47, pp. 1787-1794, October 2000.

[165] Cheng B, Cao M, Rao R, et al, "The impact of high-k gate dielectrics and metal gate electrodes on sub-100 nm MOSFETs," IEEE Trans. Electron Dev, vol. 46, 1537-1544, July 1999.

[166] Youngki Yoon; Yijian Ouyang; Guo, Jing, "Scaling Behaviors of Graphene Nanoribbon FETs," Device Research Conference, 2007 65th Annual , vol., no., pp.271,272, 18-20 June 2007 doi: 10.1109/DRC.2007.4373750.

[167] Obradovic, B.; Kotlyar, R.; Heinz, F.; Matagne, P.; Rakshit, T.; Giles, M.D.; Stettler, M.A; Nikonov, D.E., "Analysis of graphene nanoribbons as a channel material for field-effect transistors," Applied Physics Letters , vol.88, no.14, pp.142102,142102-3, Apr 2006.

[168] Chen, Z. et. al. "IDDQ Testing for Deep-Submicron ICs: Challenges and Solutions",IEEE Design and Test of Computers.pp: 24-33, 2002.

[169] Sai-Kong Chin; Dawei Seah; Kai-Tak Lam; Samudra, G.S.; Liang, Gengchiau, "Device Physics and Characteristics of Graphene Nanoribbon Tunneling FETs," Electron Devices, IEEE Transactions on , vol.57, no.11, pp.3144,3152, Nov. 2010.

[170] Guo, Jing; Datta, Supriyo; Lundstrom, Mark, "A numerical study of scaling issues for Schottky-barrier carbon nanotube transistors," Electron Devices, IEEE Transactions on , vol.51, no.2,

pp.172,177, Feb. 2004.

[171] Nakada K., Fujita M., Dresselhaus G. and Dresselhaus M.S. (1996). "Edge state in graphene ribbons: Nanometer size effect and edge shape dependence". Physical Review B 54 (24): 17954.

R. Lake, G. Klimeck, R. C. Bowen, and D. Jovanovic, “Single and Multiband modeling of

[172] quantum electron transport through layered semiconductors devices”, J. Appl. Phys., Vol. 81, pp.7845-7869, Feb. 1997.

[173] A. Svizhenko, M. P. Anantram, T. R. Govindam, and B. Biegel, “Two dimensional quantum mechanical modeling of nanotransistors”, J. Appl.Phys., Vol. 91, pp. 2343-2354, Nov. 2001.

[174] J. Guo, S. Datta, M. Lundstrom, and M. P. Anantram, Multi-scale modelingof carbon nanotube transistors, Int. J. Multiscale Comput. Eng., Vol. 2, pp.257260, 2004.

[175] A. Trellakis, A. T. Galick, A. Pacelli, and U. Ravaioli, “Iteration scheme for the solution of the two-dimensional Schrdinger-Poisson equations in quantum structures”, J. Appl. Phys, Vol. 81, p. 7880-7884, 1997.

24: Weiss, N. O., Zhou, H., Liao, L., Liu, Y., Jiang, S., Huang, Y. and Duan, X. 2012. *Adv. Mat.*, 5782–5825.

[176] Youngki Yoon; Fiori, G.; Seokmin Hong; Iannaccone, G.; Guo, Jing, "Performance Comparison of Graphene Nanoribbon FETs With Schottky Contacts and Doped Reservoirs," *Electron Devices, IEEE Transactions on* , vol.55, no.9, pp.2314,2323, Sept. 2008

Appendix A

Numerical Implementation

The Green's function is computed by means of the Recursive Green's Function (RGF) technique [174, 175]. Particular attention must be put in the definition of each self-energy matrix, which can be interpreted as a boundary condition of the Schrödinger equation. In particular, in our simulation we have considered a self-energy for semi-infinite leads as boundary conditions, which enables to consider the CNT/GNR as connected to infinitely long CNTs/GNRs at its ends.

In addition, contacts are considered for both CNT and GNR following a phenomenological approach described in [176].

From a numerical point of view, the code is based on the Newton-Raphson (NR) method with a predictor/corrector scheme [177]. In Fig. 3.1 we sketched a flow-chart of the whole code. In particular, the Schrödinger /NEGF equations are solved at the beginning of each NR cycle, starting from an initial potential $\tilde{}$ and the charge density in the CNT /GNR and SNWT is kept constant until the NR cycle converges (i.e. the correction on the potential is smaller than a predetermined value). The algorithm is then repeated cyclically until the norm of the difference between the potential computed at the end of two subsequent NR cycles is smaller than a predetermined value.

Some convergence problems however may be encountered using this iterative scheme. Indeed, since the electron density is independent of the potential within a NR cycle, the Jacobian is null for points of the domain including carbon atoms/SNWT region, losing control over the correction of the potential. We have used a suitable expression for the charge predictor, in order to give an approximate expression for the Jacobian at each step of the NR cycle. To this purpose, we have used an exponential function for the predictor In particular, if *n* is the electron density the electron density n_i at the *i-th* step of the NR cycle can be expressed as

$$n_i = n\, exp\left(\frac{\Phi_i - \tilde{\Phi}}{V_T}\right) \qquad (5.1)$$

Where $\tilde{\Phi}$ and Φ_i are the electrostatic potentials computed at the first and i_{th} step of the NR cycle, respectively, and V_T is the thermal voltage. Same considerations follow for the hole concentration.

Since the electron density n is extremely sensitive to small changes of the electrostatic potential between two NR cycles, the exponential function acts in the overall procedure as a dumping factor for charge variations. In this way, convergence has been improved in the subthreshold regime and in the strong inversion regime. Convergence is still difficult in regions of the device where the charge is not compensated by fixed charge, where the right-hand term of the Poisson equation is considerably large.

An under-relaxation of the potential and of the charge can also be performed in order to help convergence. In particular, three different under-relaxations can be performed inside ViDES :

• Relaxation on the potential at each NR cycle

$$\Phi_i^{new} = \Phi_i^{new} + \varepsilon(\Phi_i^{old} - \Phi_i^{new}) \qquad (5.2)$$

• Relaxation on the potential at the end of each NR cycle

$$\Phi_f = \Phi_f + \varepsilon(\widetilde{\Phi} - \Phi_f) \qquad (5.3)$$

• Relaxation of the charge density ρNEGF computed by the NEGF modules

$$\rho_{NEGF}^{new} = \rho_{NEGF}^{new} + \varepsilon(\rho_{NEGF}^{old} - \rho_{NEGF}^{new}) \qquad (5.4)$$

Appendix B

B.1 Pyhthon script for simulating transfer characteristics of CNT SBFET

```
from NanoTCAD_ViDES import *

#  I define the nanotube
CNT=nanotube(13,15);

#  I create the grid
x=nonuniformgrid(array([-2,0.3,0,0.2,2,0.3]))
y=nonuniformgrid(array([-2,0.3,0,0.2,2,0.3]));

grid=grid3D(x,y,CNT.z,CNT.x,CNT.y,CNT.z);

#I define the contacts
CNT.contact='Schottky'

# Now I define the gate regions
top_gate=gate("hex",grid.xmax,grid.xmax,grid.ymin,grid.ymax,grid.zmi n,grid.zmax)
bottom_gate=gate("hex",grid.xmin,grid.xmin,grid.ymin,grid.ymax,grid. zmin,grid.zmax)

# I take care of the solid
SiO2=region ("hex",-2, 2,-2, 2, grid.gridz [0], grid.gridz [grid.nz-1]);
SiO2.eps=3.9;


#  I create the interface
p=interface3D(grid,top_gate,bottom_gate,SiO2);

#  I work in the mode space, using 2 modes
p.modespace="yes"
CNT.Nmodes=2;

#  Vds = 0.5 V
CNT.mu2=-0.5;

#  I start the Vgs sweep. In particular 0<=Vgs<=1.25 V, with
#  with 0.25V as voltage step
Vgmin=0.0;
Vgmax=1.25;
Vgstep=0.25;

#I create the vectors in which I store the data vg=zeros (20);
current=zeros(20);
counter=0;
Vgs=Vgmin;
```

```
while (Vgs<=Vgmax):
    # I set the Fermi level of the top and bottom gate top_gate.Ef=-Vgs;
    set_gate (p, top_gate);
    bottom_gate.Ef=-Vgs; set_gate
    (p,bottom_gate);

    #If the first voltage, then I computes the initial solution if (Vgs==Vgmin):
        # I compute the initial solution
        p.normpoisson=1e-3;

        solve_init (grid, p, CNT);

    p.normpoisson=1e-1;
    p.normd=5e-2;
    solve_self_consistent (grid, p, CNT);
    vg[counter]=Vgs; current[counter]=CNT.current();
    counter=counter+1; Vgs=Vgs+Vgstep;


tempo=[vg,current]
savetxt ("transfer1.out",transpose(tempo));
```

B.2 Pyhthon script for simulating transfer characteristics of GNR SBFET

```
from NanoTCAD_ViDES import *

#  The width of the nanoribbon is 1.37 nm, and it is 15 nm long GNR=nanoribbon(6,15);

#  I create the grid
xg=nonuniformgrid(array([-2,0.3,0,0.2,2,0.3])) yg=nonuniformgrid(array([-
1,0.3,0,0.2,1.37,0.2,2.37,0.3])); grid=grid3D(xg,yg,GNR.z,GNR.x,GNR.y,GNR.z);

#  I define Schottky contacts
GNR.contact='Schottky'

#  Now I define the gate regions
top_gate=gate("hex",grid.xmax,grid.xmax,grid.ymin,grid.ymax,grid.zmi n,grid.zmax)
bottom_gate=gate("hex",grid.xmin,grid.xmin,grid.ymin,grid.ymax,grid. zmin,grid.zmax)
```

```
# I take care of the solid
SiO2=region ("hex",-2, 2,-2, 2, grid.zmin, grid.zmax);
SiO2.eps=3.9;


#I create the interface
p=interface3D (grid, top_gate, bottom_gate, SiO2);



#  Vds = 0.5 V
GNR.mu2=-0.5;

#  I start the Vgs sweep. In particular 0<=Vgs<=1.25 V, with
#  with 0.25V as voltage step
Vgmin=0.0;
Vgmax=1.25;
Vgstep=0.25;

#I create the vectors in which I store the data
vg=zeros(20);
current=zeros(20);

counter=0;
Vgs=Vgmin;
while (Vgs<=Vgmax):
        # I set the Fermi level of the top and bottom gate top_gate.Ef=-Vgs;
        set_gate(p,top_gate); bottom_gate.Ef=-
        Vgs; set_gate(p,bottom_gate);

        #If the first voltage, then I compute the initial solution if (Vgs==Vgmin):
                # I compute the initial solution p.normpoisson=1e-3;

                solve_init(grid,p,GNR);

        p.normpoisson=1e-1; p.normd=5e-
        2;
        solve_self_consistent(grid,p,GNR); vg[counter]=Vgs;
        current[counter]=GNR.current(); counter=counter+1;
        Vgs=Vgs+Vgstep;


tempo=[vg,current]
savetxt("transfer2.out",transpose(tempo));
```

B.3 Pyhthon script for simulating output characteristics of CNT SBFET

```
from NanoTCAD_ViDES import *

#  I define the nanotube
CNT=nanotube(13,15);

#  I create the grid
x=nonuniformgrid(array([-2,0.3,0,0.2,2,0.3]));
y=nonuniformgrid(array([-2,0.3,0,0.2,2,0.3]));
grid=grid3D(x,y,CNT.z,CNT.x,CNT.y,CNT.z);

#I define the contacts
CNT.contact='Schottky'

# Now I define the gate regions top_gate=gate("hex",2,2,-2,2,grid.gridz[0],grid.gridz[grid.nz-
1]) bottom_gate=gate("hex",-2,-2.5,-2,2,grid.gridz[0],grid.gridz[grid.nz-1])

# I take care of the solid
SiO2=region("hex",-2,2,-2,2,grid.gridz[0],grid.gridz[grid.nz-1]);
SiO2.eps=3.9;


#  I create the interface
p=interface3D(grid,top_gate,bottom_gate,SiO2);


# I work in the mode space, using 2 modes
p.modespace="yes"
CNT.Nmodes=2;


#  I set set Vgs= 0.5V
top_gate.Ef=-0.5;
set_gate(p,top_gate);
bottom_gate.Ef=-0.5;
set_gate(p,bottom_gate);

p.normpoisson=1e-3;
solve_init(grid,p,CNT);

#  I start the Vds sweep. In particular 0.05<=Vds<=0.55 V, with
#  with 0.1V as voltage step
Vdsmin=0.05;
Vdsmax=0.55;
Vdstep=0.1;

Np=int(abs(Vdsmin-Vdsmax)/Vdstep)+1; vg=zeros(Np);
current=zeros(Np);
```

```
p.underel=0.1;

counter=0;
Vds=Vdsmin;
while (Vds<=Vdsmax):

    CNT.mu2=-Vds;
    p.normpoisson=1e-1; p.normd=5e-
    3;
    solve_self_consistent(grid,p,CNT); vg[counter]=Vds;
    current[counter]=CNT.current();
    # I save the output files if (rank==0):
        string="./datiout/Phi%s.out" %Vds; savetxt(string,p.Phi);
        string="./datiout/ncar%s.out" %Vds;
        savetxt(string,p.free_charge); a=[CNT.E,CNT.T];
        string="./datiout/T%s.out" %Vds;
        savetxt(string,transpose(a));
        string="./datiout/jayn%s.out" %Vds;
        fp=open(string,"w");
        string2="%s" %current[counter]; fp.write(string2);
        fp.close();
    counter=counter+1;
    Vds=Vds+Vdstep;


tempo=[vg,current]
savetxt("idvd1.out",transpose(tempo));
```

B.4 Pyhthon script for simulating output characteristics of GNR SBFET

```
from NanoTCAD_ViDES import *

#  The width of the nanoribbon is 1.37 nm, and it is 15 nm long GNR=nanoribbon(6,15);

#  I create the grid
xg=nonuniformgrid(array([-2,0.3,0,0.2,2,0.3])) yg=nonuniformgrid(array([-
1,0.3,0,0.2,1.37,0.2,2.37,0.3])); grid=grid3D(xg,yg,GNR.z,GNR.x,GNR.y,GNR.z);

# I define Schottky contacts
GNR.contact='Schottky'

#  Now I define the gate regions
top_gate=gate("hex",grid.xmax,grid.xmax,grid.ymin,grid.ymax,grid.zmin, grid.zmax)
bottom_gate=gate("hex",grid.xmin,grid.xmin,grid.ymin,grid.ymax,grid.zm in,grid.zmax)

# I take care of the solid SiO2=region("hex",-2,2,-2,2,grid.zmin,grid.zmax);
SiO2.eps=3.9;
```

```
#  I create the interface p=interface3D(grid,top_gate,bottom_gate,SiO2);


#  I set Vgs= 0.5V
top_gate.Ef=-0.5; set_gate(p,top_gate);
bottom_gate.Ef=-0.5;
set_gate(p,bottom_gate);

p.normpoisson=1e-3;
solve_init(grid,p,GNR);


#  I start the Vds sweep. In particular 0.05<=Vds<=0.55 V, with
#  with 0.1V as voltage step

Vdsmin=0.05;
Vdsmax=0.55;
Vdstep=0.1;

Np=int(abs(Vdsmin-Vdsmax)/Vdstep)+1;
vg=zeros(Np);
current=zeros(Np);
p.underel=0.1;

counter=0;
Vds=Vdsmin;
while (Vds<=Vdsmax):

        GNR.mu2=-Vds;
        p.normpoisson=1e-1;
        p.normd=5e-3;
        solve_self_consistent(grid,p,GNR); vg[counter]=Vds;
        current[counter]=GNR.current();
        # I save the output files if (rank==0):
                string="./datiout/Phi%s.out" %Vds; savetxt(string,p.Phi);
                string="./datiout/ncar%s.out" %Vds;
                savetxt(string,p.free_charge); a=[GNR.E,GNR.T];
                string="./datiout/T%s.out" %Vds;
                savetxt(string,transpose(a)); string="./datiout/jayn%s.out"
                %Vds; fp=open(string,"w");
                string2="%s" %current[counter]; fp.write(string2);
                fp.close();
        counter=counter+1;
        Vds=Vds+Vdstep;


tempo=[vg,current]
savetxt("idvds2.out",transpose(tempo));
```

NanoTCAD ViDES main python script

```
#
=================================================================
===============
#    Copyright (c) 2010-2012, G. Fiori, G. Iannaccone, University of Pisa
#
#    This file is released under the BSD license.
#    See the file "license.txt" for information on usage and
#    redistribution of this file, and for a DISCLAIMER OF ALL WARRANTIES.
#
=================================================================
===============

from numpy import *
from NanoTCAD_ViDESmod import * from
section import *
import sys import
types

writeout("\n")
writeout("-----------------------------------------------------------
-------\n")
writeout("                                        NanoTCAD ViDES ")
writeout("                                    Version 1.4 (rel-1-4)")
writeout("                                   Last Modified 29 Aug 2013")
writeout("                                    Copyright (C) 2004-2013                \n")
writeout("-----------------------------------------------------------
-------\n")
writeout("\n")

NEmax=5e3;
DIGIT_PRECISION=20;
max_number_of_cores_on_a_server=8;

#I check if mpi4py is installed on the machine or not try:
        from mpi4py import MPI
        mpi4py_loaded = True
        sizeMPI = MPI.COMM_WORLD.Get_size() except
ImportError:
        mpi4py_loaded = False


#I check if pylab is installed on the machine or not try:
        if (mpi4py_loaded):
                if (sizeMPI<=max_number_of_cores_on_a_server): from pylab
                        import *
```

```
                pylab_loaded = True
        else:
                from pylab import *
                pylab_loaded = True
#except ImportError: except
Exception:
        pylab_loaded = False
        writeout("pylab not installed on this machine or not set up correctly DISPLAY
variable")

#definition of constants
kboltz=1.3807e-23 hbar=1.05459e-34
m0=9.1095e-31 q=1.60219e-19
eps0=8.85e-12

#Slater-Costner parameter for sp3d5s* tight-binding Hamiltonian in Si thop_Si=array([-1.95933,-
4.24135,-1.52230,3.02562,3.15565,-2.28485,-0.80993,4.10364,-1.51801,-1.35554,2.38479,-
1.68136,2.58880,-1.81400]); onsite_Si=array([-
2.15168,4.22925,4.22925,4.22925,13.78950,13.78950,13.78950,13.78950,13
.78950,19.11650]);

def MPIze(channel):
        if (mpi4py_loaded): del
                channel.E;
                channel.E=zeros(NEmax);
                Eupper_save=channel.Eupper;
                Elower_save=channel.Elower;
                vt=kboltz*channel.Temp/q;
                sizeMPI = MPI.COMM_WORLD.Get_size() if
                (mpi4py_loaded):
                        rank = MPI.COMM_WORLD.Get_rank()
                        channel.rank=rank;
                #  I compute the maximum and the minimum
                #  of the energy interval
                if ((channel.Eupper>900)&(channel.Elower<-900)):
                        Eupper=max(max(channel.mu1,max(-
channel.Phi)),channel.mu2)+0.5*channel.gap()+10*vt;
                        Elower=min(min(channel.mu1,min(-
channel.Phi)),channel.mu2)-0.5*channel.gap()-10*vt; else:
                        Eupper=channel.Eupper;
                        Elower=channel.Elower;
#               string="Eupper and Elower %s %s " %(Eupper,Elower)
#               if (rank==0): writeout(string)
                E=arange(Elower,Eupper,channel.dE);
                arraydim=size(E)/sizeMPI;

excess=size(E)-sizeMPI*arraydim if (rank<excess):
        channel.Elower=E[rank*(arraydim+1)];
```

```
                channel.Eupper=E[(rank+1)*(arraydim+1)-1]; else:
                channel.Elower=E[(rank-
excess)*arraydim+excess*(arraydim+1)];
                if (rank==(sizeMPI-1)):
                    channel.Eupper=E[size(E)-1];
                else: channel.Eupper=E[(rank-excess+1)*arraydim-
1+excess*(arraydim+1)];

#           string="Inizio rank %s %s %s"
%(rank,channel.Elower,channel.Eupper)
#            writeout(string)
            channel.charge_T();
            #writeout("Finito rank "),rank,channel.Elower,channel.Eupper;

            # I send the charge and the transmission coefficient if (rank!=0):
                temp=array(channel.charge);
                MPI.COMM_WORLD.Send([temp, MPI.DOUBLE],dest=0,tag=11); del temp;

                NPE=zeros(1,int);
                NPE[0]=int(ceil((channel.Eupper-
channel.Elower)/channel.dE))+1;
                #size(arange(channel.Elower,channel.Eupper,channel.dE)); #int((channel.Eupper-
                channel.Elower)/channel.dE); #size(nonzero(channel.E));
                temp=array(channel.T[:NPE[0]]); temp2=array(channel.E[:NPE[0]]);
#                 NPE[0]=size(temp);
                MPI.COMM_WORLD.Send([NPE, MPI.INT],dest=0,tag=10);
                MPI.COMM_WORLD.Send([temp, MPI.DOUBLE],dest=0,tag=12);
                MPI.COMM_WORLD.Send([temp2, MPI.DOUBLE],dest=0,tag=14);
                #writeout("Spedito rank "),rank
                del temp; del
                temp2;
            else:
                channel.charge=array(channel.charge);
                NNEE=int(ceil((channel.Eupper-
channel.Elower)/channel.dE))+1;
#size(arange(channel.Elower,channel.Eupper,channel.dE));
#                 NNEE=((channel.Eupper-channel.Elower)/channel.dE);
#                 size(nonzero(channel.E));
                channel.T=array(channel.T[:NNEE]);
                channel.E=array(channel.E[:NNEE]);
                for i in range(1,sizeMPI):
                    temp=empty(size(channel.charge),dtype=double);
                    MPI.COMM_WORLD.Recv([temp,
MPI.DOUBLE],source=i,tag=11);
                    channel.charge=channel.charge+temp; del temp;
```

```
                        NPE=empty(1,int);
                        MPI.COMM_WORLD.Recv([NPE, MPI.INT],source=i,tag=10);
                        temp=empty(NPE[0],dtype=double); MPI.COMM_WORLD.Recv([temp,
MPI.DOUBLE],source=i,tag=12);
                        temp2=empty(NPE[0],dtype=double);
                        MPI.COMM_WORLD.Recv([temp2,
MPI.DOUBLE],source=i,tag=14);
                        channel.T=concatenate((channel.T,temp));
                        channel.E=concatenate((channel.E,temp2)); del temp;
                        del temp2; #writeout("Preso rank "),i

            channel.charge = MPI.COMM_WORLD.bcast(channel.charge, root=0)
            channel.T = MPI.COMM_WORLD.bcast(channel.T, root=0)
            channel.E = MPI.COMM_WORLD.bcast(channel.E, root=0)
            channel.Eupper=Eupper_save;
            channel.Elower=Elower_save;
#             MPI.Finalize();
      else:
            writeout("**********************************")
            writeout("MPI not installed on this machine")
            writeout("**********************************")
      return;

def MPIze_kt(channel): if
      (mpi4py_loaded):

            kmin_save=channel.kmin;
            kmax_save=channel.kmax;
            vt=kboltz*channel.Temp/q;
            sizeMPI = MPI.COMM_WORLD.Get_size() if
            (mpi4py_loaded):
                  rank = MPI.COMM_WORLD.Get_rank()
                  channel.rank=rank;
            #  I compute the maximum and the minimum
            #  of the wave-vector kt
            kt_max=channel.kmax;
            kt_min=channel.kmin;
            if (rank==0): writeout("kt_max, kt_min"),kt_max,kt_min
            k=arange(kt_min,kt_max,channel.dk); arraydim=size(k)/sizeMPI;
            channel.kmin=k[rank*arraydim];

            if (rank==(sizeMPI-1)):
                  channel.kmax=k[size(k)-1];
            else: channel.kmax=k[(rank+1)*arraydim-1];

            channel.charge_T();

            NE=size(channel.E);
```

```
            # I send the charge and the transmission coefficient if (rank!=0):
                temp=array(channel.charge); MPI.COMM_WORLD.Send([temp,
                MPI.DOUBLE],dest=0,tag=11); del temp;


                temp=array(channel.T);
                MPI.COMM_WORLD.Send([temp, MPI.DOUBLE],dest=0,tag=12); del temp;
            else:
                channel.charge=array(channel.charge);
                channel.T=array(channel.T); for i in
                range(1,sizeMPI):
                    temp=empty(size(channel.charge),dtype=double);
                    MPI.COMM_WORLD.Recv([temp,
MPI.DOUBLE],source=i,tag=11);
                    channel.charge=channel.charge+temp; del temp;
                    temp=empty(NE,dtype=double);
                    MPI.COMM_WORLD.Recv([temp,
MPI.DOUBLE],source=i,tag=12);
                    channel.T=channel.T+temp; del temp;

            channel.charge = MPI.COMM_WORLD.bcast(channel.charge, root=0) channel.T =
            MPI.COMM_WORLD.bcast(channel.T, root=0) channel.kmin=kmin_save;
            channel.kmax=kmax_save;
#             MPI.Finalize();

        else:
            writeout("*********************************")
            writeout("MPI not installed on this machine")
            writeout("*********************************")
        return;

def set_gate(interface,gate):
        interface.boundary_conditions[gate.index]=gate.Ef;

def solve_init(grid,interface,channel):

        #  I get the rank if
        (mpi4py_loaded):
            channel.rank = MPI.COMM_WORLD.Get_rank()
        #  I set the rank
        if (mpi4py_loaded):
            rank = MPI.COMM_WORLD.Get_rank()
            interface.rank=rank;
        else:
            interface.rank=0;
```

```
        #  I first give an estimation of the density of states
        #  when computing the flat band potential in the regions
        #  where the fixed_charge is not equal to zero, assuming
        #  full ionization

        #  I save the temperature, mu1, mu2, the potential, n, Nc, Eupper, Elower
#         temp_save=channel.Temp;
        mu1_save=channel.mu1;
        mu2_save=channel.mu2;
        Nc_save=channel.Nc;
        Eupper_save=channel.Eupper;
        Elower_save=channel.Elower;
        boundary_conditions_save=copy(interface.boundary_conditions);
        normpoisson_save=interface.normpoisson;

        interface.normpoisson=1e-3;
        # I impose a low-temperature, so to compute the LDOS, instead of
the
        # LDOS multiplied by the Fermi-Dirac
        name=grid.__class__.__name__;
        name_channel=channel.__class__.__name__; if
        (name=="grid3D"):
                if (name_channel=="multilayer_graphene"): channel.Nc=8;
                        x_save=channel.x y_save=channel.y
                        z_save=channel.z
                        channel.atoms_coordinates();
                else:
                        channel.Nc=6;
                channel.Phi=zeros(channel.n*channel.Nc);
                channel.mu1=0;
                channel.mu2=0;
                vt=kboltz*channel.Temp/q;
                channel.Eupper=channel.gap()+10*vt;
                channel.Elower=0;
                #  I compute the NEGF
                #         if (interface.modespace=="yes"):
                #                 channel.mode_charge_T();
                #         else:
                #                 if (interface.MPI=="yes"):
                #                         MPIze(channel);
                #                 else:
                channel.charge_T();

        #
N1D=abs(sum(channel.charge))/(6*channel.Nc)/(3*channel.acc)*1e9;
                Ec=channel.gap()*0.5;

N1D=sum(abs(channel.charge))/(6*channel.n)/(4*channel.acc)*1e9*exp(Ec/
vt);
```

```
#       return N1D

            # I compute the mean z: if atoms have a z-coordinate > zmean => I impose the
electrochemical potential mu2
            # if atoms have a z-coordinate < zmean => I impose the electrochemical
potential mu1
            zmean=(grid.zmin+grid.zmax)*0.5;
            indexS=nonzero((abs(interface.fixed_charge)>1e-
20)&(grid.z3D<zmean)); indexD=nonzero((abs(interface.fixed_charge)>1e-
20)&(grid.z3D>=zmean));
            potential=zeros(grid.Np);

argoS=(abs(interface.fixed_charge[indexS])*grid.surf[indexS,5]/N1D);

argoD=(abs(interface.fixed_charge[indexD])*grid.surf[indexD,5]/N1D);

                    potential[indexS]=(vt*(log(exp(argoS)-
            1))+Ec)*sign(interface.fixed_charge[indexS])+mu1_save;
                    potential[indexD]=(vt*(log(exp(argoD)-
            1))+Ec)*sign(interface.fixed_charge[indexD])+mu2_save;

            interface.boundary_conditions[indexS]=potential[indexS];
            interface.boundary_conditions[indexD]=potential[indexD];



            solve_Poisson(grid,interface); elif
      (name=="grid2D"):
            channel.Nc=8;
            channel.Phi=zeros(channel.n*channel.Nc);
            channel.mu1=0;
            channel.mu2=0;
            vt=kboltz*channel.Temp/q;
            channel.Eupper=channel.gap()+10*vt;
            channel.Elower=0;
            #  I compute the NEGF
            #       if (interface.modespace=="yes"):
            #             channel.mode_charge_T();
            #       else:
            #if (interface.MPI_kt=="yes"):
            # MPIze_kt(channel); #else:
            channel.charge_T();

            Ec=channel.gap()*0.5;

N1D=sum(abs(channel.charge))/(8*channel.n)/(8*channel.acc)*1e9*exp(Ec/
vt);

            # I compute the mean z: if atoms have a z-coordinate > zmean => I impose the
electrochemical potential mu2
```

```
        # if atoms have a z-coordinate < zmean => I impose the electrochemical
potential mu1
        ymean=(grid.ymin+grid.ymax)*0.5;
        indexS=nonzero((abs(interface.fixed_charge)>1e-
20)&(grid.y2D<ymean)); indexD=nonzero((abs(interface.fixed_charge)>1e-
20)&(grid.y2D>=ymean));
        potential=zeros(grid.Np);
        argoS=(abs(interface.fixed_charge[indexS])/N1D);
        argoD=(abs(interface.fixed_charge[indexD])/N1D);

                potential[indexS]=(vt*(log(exp(argoS)-
            1))+Ec)*sign(interface.fixed_charge[indexS])+mu1_save;
                potential[indexD]=(vt*(log(exp(argoD)-
            1))+Ec)*sign(interface.fixed_charge[indexD])+mu2_save;

#           potential[indexS]=Ec;
#           potential[indexD]=Ec;

        interface.boundary_conditions[indexS]=potential[indexS];
        interface.boundary_conditions[indexD]=potential[indexD];

        solve_Poisson(grid,interface);

    #going back to the old values
    channel.Nc=Nc_save
    channel.mu2=mu2_save;
    channel.mu1=mu1_save;
    channel.Eupper=Eupper_save;
    channel.Elower=Elower_save;
    interface.boundary_conditions=boundary_conditions_save;
    interface.normpoisson=normpoisson_save;
    if (name_channel=="multilayer_graphene"):
        channel.x=x_save
        channel.y=y_save
        channel.z=z_save
        del  x_save,y_save,z_save   #deleting
    the save variables del
mu1_save,mu2_save,Nc_save,Eupper_save,Elower_save,boundary_conditions_ save;

    return;


def solve_self_consistent(grid,interface,channel): normad=1e30;
# Phiold=1.0*interface.Phi;
    interface.Phiold=interface.Phi.copy(); counter=1;


    if (mpi4py_loaded):
        rank = MPI.COMM_WORLD.Get_rank() else:
        rank=0;
```

```
        while (normad>interface.normd):
                #  I pass the potential in correspondence of the
                # atoms of the material for which I compute the NEGF
                channel.Phi=interface.Phi[grid.swap]
                #  I compute the NEGF

#                 channel.Phi=zeros(size(grid.swap));
#                 savetxt("Phi.before",interface.Phi[grid.swap]);

                if (interface.modespace=="yes"):
                        channel.mode_charge_T();
                else:
                        if (interface.MPI=="yes"):
                                MPIze(channel);
                        elif (interface.MPI_kt=="yes"):
                                MPIze_kt(channel);
                        else: channel.charge_T();

#                 savetxt("Phi.temp2",interface.Phi);

#                 a=[channel.E,channel.T];
#                 savetxt("T.temp",transpose(a));

                if (rank==0):
                        writeout("-----------------------------------------")
                        string="                        CURRENT = %s A/m"
%(channel.current());
                        writeout(string);
                        writeout("-----------------------------------------")

                #  I pass back the free_charge term to
                #  the 3D domain
                interface.free_charge[grid.swap]=channel.charge

                if (rank==0): savetxt("ncar.ini",interface.free_charge);
                        savetxt("Phi.ini",interface.Phi);

                # I solve Poisson
                solve_Poisson(grid,interface);
#                 normad=sqrt(sum((interface.Phiold-interface.Phi)**2));
#                 Phiold=zeros(grid.Np);
                normad=max(abs(interface.Phiold-interface.Phi))

interface.Phi=interface.Phi+(interface.underel)*(interface.Phiold-interface.Phi)
```

```
            del interface.Phiold;
#             del Phiold;
#             Phiold=1.0*interface.Phi;
            interface.Phiold=interface.Phi.copy();

            if (rank==0): print()
            string="Iteration # %s; ||Phi-Phiold||2 = %s" %(counter,normad)
            if (rank==0): writeout(string) if (rank==0):
            print() counter=counter+1;
            if (counter>600): return;



def                     solve_Poisson(grid,interface):
    name=grid.__class__.__name__;               if
    (name=="grid3D"):
        solvePoisson(grid,interface); elif
    (name=="grid2D"):
        solvePoisson2D(grid,interface); elif
    (name=="grid1D"):
        solvePoisson1D(grid,interface);
    interface.Phi=array(interface.Phi)
    return;

def nonuniformgrid(argu):
    #This is a wrapper for the nonuniformgridmod function
    #so to convert both the argument and the output to numpy arrays #I convert the argument in
    an array
    argarr=array(argu);
    out=nonuniformgridmod(argarr);
    # I return a pyarray
    outarr=array(out); return outarr;

#Fermi-Dirac Function def
Fermi(x):
    return 1/(1+exp(x));

def delete_class(class_obj):
    del_class(class_obj); del class_obj;
    return;

# This is the class for the nanotube class nanotube:
    acc=0.144;
    def __init__(self,n,L): self.Nc=int(4*(floor((floor(L/nanotube.acc)-1)/3))+2);
        self.n=n;
```

```
            self.Phi=zeros(n*self.Nc);
            self.Eupper=1000.0;
            self.Elower=-1000.0; self.dE=1e-
            3; self.thop=-2.7; self.eta=1e-5;
            self.mu1=0; self.mu2=0;
            self.Temp=300;
            self.contact="doped";
            self.E=zeros(NEmax);
            self.T=zeros(NEmax);
            self.charge=zeros(self.n*self.Nc);
            self.Nmodes=n;
            self.x=zeros(n*self.Nc);
            self.y=zeros(n*self.Nc);
            self.z=zeros(n*self.Nc);
            self.L=int(self.Nc/2+((self.Nc-1)-
self.Nc*0.5)*0.5)*nanotube.acc;
            self.atoms_coordinates(); self.rank=0;
      def gap(self):
            return abs(2*self.acc*self.thop*pi/(self.n*sqrt(3)*self.acc)); def atoms_coordinates(self):
            CNT_atoms_coordinates(self);
            self.x=array(self.x); self.y=array(self.y);
            self.z=array(self.z); return;
      def charge_T(self): CNT_charge_T(self);
            self.E=array(self.E); self.T=array(self.T);
            self.charge=array(self.charge); return;
      def mode_charge_T(self):
            CNTmode_charge_T(self);
            self.E=array(self.E); self.T=array(self.T);
            self.charge=array(self.charge); return
      def current(self): vt=kboltz*self.Temp/q;
            E=self.E;
            T=self.T; arg=2*q*q/(2*pi*hbar)*T*(Fermi((E-self.mu1)/vt)-Fermi((E-
self.mu2)/vt))*self.dE; return
            sum(arg);


# This is the class for the nanoribbon class GNRphonon:


      def __init__(self,dimer):
            self.N=1000; # number of points qx (longitudinal direction) while (((((self.N)-
            1)%(dimer/2))!=0) | (((self.N)%2)==0)):
                  (self.N)+=1;
            self.dimer=dimer; # numero dimer lines self.rank=0;
            self.phi=0.0; # channel potential (midgap) self.numberAC=2; # number of AC modes
            of different simmetry
considered (=2: LA+TA, =1: only LA) self.Ecutoff=1.0; #
            cutoff energy
            self.delta=2; # integer: it specifies the sampling along the kx direction
```

```
        self.deltak=0;
        self.kyE=zeros(dimer); # transverse electron wavevector self.qy=zeros(dimer); #
        transverse phonon wavevector self.kx=zeros(self.N); # longitudinal electron
        wavevector self.qx=zeros(self.N); # longitudinal phonon wavevector self.qx0=0.0; #
        fixed value for qx (computation of graphene
branches)
        self.qy0=0.0; # fixed value for qy (computation of graphene branches)
        self.kxup=0; # maximum value for kx (computation of rates) self.kxdown=0; #
        minimum value for kx (computation of rates) self.dim1=self.N;
        self.dim2=dimer;
        self.dim3=6;
        self.mmin=0;
        self.mmax=dimer-1;
        self.kxmin=0;
        self.kxmax=0;
        self.Phi_r1=39.87*10.0;  # first neighbors
        self.Phi_ti1=17.28*10.0;
        self.Phi_to1=9.89*10.0;
        self.Phi_r2=7.29*10.0;   # second neighbors
        self.Phi_ti2=-4.61*10.0; self.Phi_to2=-0.82*10.0;
        self.Phi_r3=-2.64*10.0; # third neighbors
        self.Phi_ti3=3.31*10.0; self.Phi_to3=0.58*10.0;
        self.Phi_r4=0.10*10.0; # fourth neighbors
        self.Phi_ti4=0.79*10.0; self.Phi_to4=-0.52*10.0;

        self.energyE=zeros((self.dim1,(2*self.dim2))) # GNR electron
curves
        self.energyP2D=zeros((self.dim1,(self.dim2*self.dim3))) # GNR phonon subbranches
        self.minAC=zeros((self.dim2,3));# minimum of the acoustic subbranches
        self.Egraphene=zeros(self.dim3); # graphene
        self.rateAA=zeros((self.dim1,self.dim2));
        self.rateAE=zeros((self.dim1,self.dim2));
        self.rateOA=zeros((self.dim1,self.dim2));


        self.rateOE=zeros((self.dim1,self.dim2)); self.Dac=4.5*(1.60219e-19); # deformation
        potential value (eV) self.temp=300; # temperature (K)
        self.thop=2.7; # hopping parameter (eV) self.aCC=0.144e-9;
        # lattice constant (m)
    def electron_GNR(self): electron_GNR(self);
        self.kx=array(self.kx); self.kyE=array(self.kyE);
        self.energyE=array(self.energyE); return;
    def phonon_GNR(self):
        phonon_GNR(self);
        self.qx=array(self.qx);
        self.qy=array(self.qy);
        self.energyP2D=array(self.energyP2D);
        return;
    def phonon_graphene(self): phonon_graphene(self);
        self.Egraphene=array(self.Egraphene); return;
```

```
        def rateACABS(self): rateACABS(self);
                self.rateAA=array(self.rateAA); return;
        def rateACEM(self): rateACEM(self);
                self.rateAE=array(self.rateAE); return;

        def rateOPTABS(self): rateOPTABS(self);
                self.rateOA=array(self.rateOA); return;
        def rateOPTEM(self): rateOPTEM(self);
                self.rateOE=array(self.rateOE); return;

# This is the class for the nanoribbon class nanoribbon:
        acc=0.144;
        def __init__(self,n,L): self.Nc=int(4*(int((int(L/nanoribbon.acc)-1)/3))+2);
                self.n=n;
                self.Phi=zeros(n*self.Nc);
                self.Eupper=1000.0;
                self.Elower=-1000.0;
                self.dE=1e-3; self.thop=-2.7;
                self.eta=1e-5; self.mu1=0;
                self.mu2=0;
                self.Temp=300;
                self.contact="doped";
                self.E=zeros(NEmax);
                self.T=zeros(NEmax);
                self.charge=zeros(self.n*self.Nc);
                self.defects="no";
                self.roughness="no";
                self.rank=0; self.atoms_coordinates();
        def atoms_coordinates(self):
                GNR_atoms_coordinates(self);
                self.x=array(self.x); self.y=array(self.y);
                self.z=array(self.z); return;
        def gap(self):
                return GNRgap(self); def
        charge_T(self):
                GNR_charge_T(self); self.E=array(self.E);
                self.T=array(self.T);
                self.charge=array(self.charge); return;
        def current(self): vt=kboltz*self.Temp/q;
                E=array(self.E); T=array(self.T);
                arg=2*q*q/(2*pi*hbar)*T*(Fermi((E-self.mu1)/vt)-Fermi((E-
self.mu2)/vt))*self.dE
                return sum(arg);

# This is the class for the graphene class graphene:
        acc=0.144;
        n=1;
        def __init__(self,L): self.Nc=int(4*(floor((floor(L/graphene.acc)-1)/3)));
                self.Phi=zeros(self.Nc);
```

```
        self.Ei=zeros(self.Nc);
        self.Eupper=1000.0; self.Elower=-1000.0;
        self.delta=sqrt(3)*graphene.acc;
        self.kmax=pi/self.delta; self.kmin=0;
        self.dk=0.1; self.dE=1e-3;
        self.thop=-2.7; self.eta=1e-8;
        self.mu1=0.0; self.mu2=0.0;
        self.Temp=300;
        self.E=zeros(NEmax);
        self.T=zeros(NEmax);
        self.charge=zeros(self.Nc);
        self.rank=0; self.atoms_coordinates();
        self.gap(); self.T2D="no"

def atoms_coordinates(self):
        GNR_atoms_coordinates(self);
        self.y=array(self.z);
        self.x=zeros(size(self.y)); del self.z;
        return; def
gap(self):
        return 0;
def charge_T(self):
        # Number of slices and atoms
        slices=self.Nc;
        atoms=1;
        # I define the vector of the k-wave vector
        kvect=arange(self.kmin,self.kmax,self.dk)
        # I start defining the Hamiltonian for the graphene flake
        h=zeros((2*slices,3),dtype=complex);
        h[0][0]=1;
        for i in range(1,slices+1): h[i][0]=i
                h[i][1]=i

        kk=1;
        for ii in range(slices+1,2*slices): if ((ii%2)==1):
                        h[ii][0]=kk;
                        h[ii][1]=kk+1;
                        h[ii][2]=self.thop;
                kk=kk+1;

        # I then compute the charge and the T for each energy and k and perform the integral
        i=0;
        k=self.kmin;
        H = Hamiltonian(atoms, slices) if
        (self.T2D=="yes"):
                EE=arange(self.Elower,self.Eupper,self.dE);
                kvect=arange(self.kmin,self.kmax+self.dk,self.dk);
                X,Y=meshgrid(EE,kvect);
                Z=zeros((size(EE),size(kvect))) while
```

```
(k<=(self.kmax+self.dk*0.5)):
        if (self.rank==0): writeout("----------------------------------")
        string=" kx range: [%s,%s] " %(self.kmin,self.kmax); if (self.rank==0):
        writeout(string)
        string="            iteration %s " %i;
        if (self.rank==0): writeout(string);

        if (self.rank==0): writeout("----------------------------------")
        flaggo=0;
        kk=1;
        # I fill the Hamiltonian for the actual wavevector k in the cycle
        for ii in range(slices+1,2*slices): if ((ii%2)==0):
                h[ii][0]=kk;
                h[ii][1]=kk+1;
                if ((flaggo%2)==0):

h[ii][2]=self.thop+self.thop*exp(k*self.delta*1j);
                else: h[ii][2]=self.thop+self.thop*exp(-
k*self.delta*1j);
                flaggo=flaggo+1;
            kk=kk+1;

        H.Eupper = self.Eupper;
        H.Elower = self.Elower;
        H.rank=self.rank;
        H.H = h
        H.dE=self.dE;
        H.Phi=self.Phi;
        H.Ei=-self.Phi;
        H.eta=self.eta;
        H.mu1=self.mu1;
        H.mu2=self.mu2;
        H.Egap=self.gap();

        #  I then compute T and the charge for the actual kx H.charge_T()

        #  I sum up all the contribution
        if (i==0): self.E=H.E;
            # the factor 2 is because I integrate over kx>0
            self.T=H.T*(2*self.dk/(2*pi));
            self.charge=H.charge*(2*self.dk/(2*pi));
        else:
            # the factor 2 is because I integrate over kx>0
            self.T=self.T+H.T*(2*self.dk/(2*pi));
            self.charge=self.charge+H.charge*(2*self.dk/(2*pi));

        if (self.T2D=="yes"):
            Z[:,i]=H.T[:size(EE)];
        k=k+self.dk
        i=i+1;
```

```
        if (self.T2D=="yes"):

                plt.imshow(Z, interpolation='bilinear', cmap=cm.gray, origin='lower',
extent=[self.kmin,self.kmax,self.Elower,self.Eupper])
                show()

        del H; self.E=array(self.E);
        self.T=array(self.T)*1e9;
        self.charge=array(self.charge)*1e9; del kvect,h;
        return;

    def current(self): vt=kboltz*self.Temp/q;
        E=array(self.E); T=array(self.T);
        arg=2*q*q/(2*pi*hbar)*T*(Fermi((E-self.mu1)/vt)-Fermi((E-
self.mu2)/vt))*self.dE
        return sum(arg);

# This is the class for the graphene bilayer class
bilayer_graphene:
    acc=0.144;
    acc_p=0.35; n=2;
    def __init__(self,L): self.Nc=int(4*(floor((floor(L/bilayer_graphene.acc)-1)/3))); self.n=2;
        self.Phi=zeros(bilayer_graphene.n*self.Nc);
        self.Ei=zeros(bilayer_graphene.n*self.Nc); self.Eupper=1000.0;
        self.Elower=-1000.0;
        self.delta=sqrt(3)*bilayer_graphene.acc;
        self.kmax=pi/self.delta;
        self.kmin=0;
        self.dk=0.1; self.dE=1e-3;
        self.thop=-2.7; self.tp=-0.35;
        self.eta=1e-8; self.mu1=0.0;
        self.mu2=0.0; self.Temp=300;
        self.E=zeros(NEmax);
        self.T=zeros(NEmax);
        self.charge=zeros(bilayer_graphene.n*self.Nc); self.rank=0;
        self.atoms_coordinates(); self.gap();
        self.T2D="no"

    def atoms_coordinates(self): n_save=self.n;

    self.n=1; GNR_atoms_coordinates(self);
    ydown=array(self.z); yup=ydown-self.acc*0.5;
    NN=size(ydown);
    kkk=0;
    self.y=zeros(2*NN); for i in
    range(0,NN):
        self.y[kkk]=ydown[i];
        self.y[kkk+1]=yup[i];
        kkk=kkk+2;
```

```
self.x=zeros(size(self.y)); i=linspace(0,size(self.y)-1,size(self.y))
i_even=nonzero((i%2)==0); i_odd=nonzero((i%2)==1);
self.x[i_even]=0; self.x[i_odd]=bilayer_graphene.acc_p; del
self.z,i,i_even,i_odd; self.n=n_save;


return; def gap(self):
#  This is an rough exstimation of
#  the Energy gap: for sure this is
#  the largest attainable value, within
#  the pz tight-binding model
return abs(self.tp); def charge_T(self):
#  Number of slices and atoms slices=self.Nc;
atoms=self.n;
# I define the vector of the k-wave vector
kvect=arange(self.kmin,self.kmax,self.dk)
#  I start defining the Hamiltonian for the bilayer graphene h=zeros((4*slices+2*(slices/4)-
2,3),dtype=complex); h[0][0]=1;
for i in range(1,2*slices+1): h[i][0]=i
        h[i][1]=i
        h[i][2]=0.0;

#  I then compute the charge and the T for each energy
#  and k and perform the integral
i=0;
k=self.kmin;
H = Hamiltonian(atoms, slices) if
(self.T2D=="yes"):
        EE=arange(self.Elower,self.Eupper,self.dE);
        kvect=arange(self.kmin,self.kmax+self.dk,self.dk);
        X,Y=meshgrid(EE,kvect);
        Z=zeros((size(EE),size(kvect))) while
(k<=(self.kmax+self.dk*0.5)):


                if (self.rank==0): writeout("----------------------------------")
                string=" kx range: [%s,%s] " %(self.kmin,self.kmax); if (self.rank==0):
                writeout(string);
                string="            k: %s " %k;
                if (self.rank==0): writeout(string);
                if (self.rank==0): writeout("----------------------------------")

                # ------------------------------------------------
                #  BEGINNING OF THE HAMILTONIAN DEFINITION
                #  FOR THE GRAPHENE BILAYER
                # ------------------------------------------------

                # I work on the bottom graphene layer kk=1;
                flaggo=0;
                for ii in range(2*slices+1,3*slices): if ((ii%2)==1):
```

```
                        h[ii][0]=kk;
                        h[ii][1]=kk+2;
                        h[ii][2]=self.thop;
                        kk=kk+2;
                else:
                        h[ii][0]=kk;
                        h[ii][1]=kk+2;
                        if ((flaggo%2)==0):

h[ii][2]=self.thop+self.thop*exp(k*self.delta*1j);
                        else: h[ii][2]=self.thop+self.thop*exp(-
k*self.delta*1j);
                        kk=kk+2;
                        flaggo=flaggo+1;

        # I work on the top graphene layer kk=2;
        flaggo=1;
        for ii in range(3*slices,4*slices-1): if ((ii%2)==0):
                        h[ii][0]=kk;
                        h[ii][1]=kk+2;
                        h[ii][2]=self.thop;
                        kk=kk+2;
                else:
                        h[ii][0]=kk;
                        h[ii][1]=kk+2;
                        if ((flaggo%2)==0):

h[ii][2]=self.thop+self.thop*exp(k*self.delta*1j);
                        else:


                                h[ii][2]=self.thop+self.thop*exp(-
k*self.delta*1j);
                        kk=kk+2;
                        flaggo=flaggo+1;


        #  I now work on the perpendicular hopping parameter kk=3;
        for ii in range(4*slices-1,4*slices+int(slices/2)-2): h[ii][0]=kk;
                h[ii][1]=kk+3;
                h[ii][2]=self.tp;
                kk=kk+4;

        #  ------------------------------------------------
        #                  END OF THE HAMILTONIAN
        #  ------------------------------------------------

        H.Eupper = self.Eupper; H.Elower =
        self.Elower; H.H = h
        H.rank=self.rank; H.dE=self.dE;
        H.Phi=self.Phi;
```

```
                ind_even=arange(0,size(H.Phi),2);
                ind_odd=ind_even+1; H.Ei[ind_even]=-
(self.Phi[ind_even]+self.Phi[ind_odd])*0.5; H.Ei[ind_odd]=-
                (self.Phi[ind_even]+self.Phi[ind_odd])*0.5; H.Ei_flag="no"

                H.eta=self.eta;
                H.mu1=self.mu1;
                H.mu2=self.mu2;
                H.Egap=self.gap();

#                 return H.H

                #  I then compute T and the charge for the actual kx H.charge_T()

                #  I sum up all the contribution
                if (i==0): self.E=H.E;
                        # the factor 2 is because I integrate over kx>0
                        self.T=H.T*(2*self.dk/(2*pi));
                        self.charge=H.charge*(2*self.dk/(2*pi));
# self.charge=H.charge; else:

                        # The spin is taken into account in the integral for
the current
                        # the factor 2 is because I integrate over kx>0
                        self.T=self.T+H.T*(2*self.dk/(2*pi));


                        #  2 because I take into account
                        #  that I integrate over kx>0
                        self.charge=self.charge+H.charge*(2*self.dk/(2*pi));

                if (self.T2D=="yes"):
                        Z[:,i]=H.T[:size(EE)];
                k=k+self.dk
                i=i+1;

        if (self.T2D=="yes"):
                plt.imshow(Z, interpolation='bilinear', cmap=cm.gray, origin='lower',
extent=[self.kmin,self.kmax,self.Elower,self.Eupper])
                show()

        del H; self.E=array(self.E);
        self.T=array(self.T)*1e9;
        self.charge=array(self.charge)*1e9;
# self.charge=array(self.charge); del kvect,h;
        return;

    def current(self): vt=kboltz*self.Temp/q;
        E=array(self.E); T=array(self.T);
        arg=2*q*q/(2*pi*hbar)*T*(Fermi((E-self.mu1)/vt)-Fermi((E-
```

```
self.mu2)/vt))*self.dE
            return sum(arg);


# This is the class for the general Hamiltonian class Hamiltonian:
    def __init__(self, n, Nc): self.Nc=Nc;
            self.n=n;
            self.x=zeros(n*self.Nc);
            self.y=zeros(n*self.Nc);
            self.z=zeros(n*self.Nc);
            self.Phi=zeros(n*self.Nc);
            self.Ei=zeros(n*self.Nc);
            self.Eupper=1000.0;
            self.Elower=-1000.0;
            self.dE=0.001; self.eta=1e-8;
            self.mu1=0; self.mu2=0;
            self.Temp=300;
            self.E=zeros(NEmax);
            self.T=zeros(NEmax);
            self.charge=zeros(n*self.Nc);
            self.Egap=0;
            self.rank=0;
            # if this flag is set to "yes" then Ei=-Phi self.Ei_flag="yes"
#  The +1 will be then replaced by the number of orbitals per atoms in the nearest neighbourgh approximation
#       self.H=zeros((((Nc*n)*(Nc*n+1)/2),2+100+10));
    def current(self): vt=kboltz*self.Temp/q;
            E=array(self.E); T=array(self.T);
            arg=2*q*q/(2*pi*hbar)*T*(Fermi((E-self.mu1)/vt)-Fermi((E-
self.mu2)/vt))*self.dE
            return sum(arg); def
    charge_T(self):
            if (self.Ei_flag=="yes"): self.Ei=-
                self.Phi;
            H_charge_T(self); self.E=array(self.E);
            self.T=array(self.T);
            self.charge=array(self.charge);
    def gap(self): return 0.5;
#  This is the class for the zincblend structures
#  This is the class for the zincblend structures class Zincblend:
    def __init__(self, material, sqci, tilt, edge, zmax): self.material = material
            if self.material == 'Si':
                self.aux   =   [-2.15168,    4.22925,
                                19.11650,
                                13.78950,          -
                                1.95933,           -
                                4.24135,           -
                                1.52230,
                                3.02562,
```

```
                                        3.15565,        -
                                        2.28485,        -
                                        0.80993,
                                        4.10364,        -
                                        1.51801,        -
                                        1.35554,
                                        2.38479,        -
                                        1.68136,
                                        2.58880,        -
                                        1.81400,
                                        ]
                    self.skparameters = array(self.aux, dtype=float) self.a0 = 5.431
                    self.flag = 0


          if self.material == 'Ge': self.aux = [-1.95617,
5.30970, 19.29600, 13.58060, -1.39456, -3.56680, -
     2.01830, 2.73135, 2.68638, -2.64779, -1.12312,
    4.28921, -1.73707, -2.00115, 2.10953, -1.32941,
                                        2.56261, -1.95120
                          ]
       self.skparameters = array(self.aux, dtype=float) self.a0 = 5.6575
       self.flag = 0

         if self.material == 'InAs': self.aux = [ -5.500420,
              4.151070, -0.581930, 6.971630, 19.710590,
          19.941380, 13.031690, 13.307090, -1.694350, -
 4.210450, -2.426740, -1.159870, 2.598230, 2.809360,
2.067660, 0.937340, -2.268370, -2.293090, -0.899370,
            -0.488990, 4.310640, -1.288950, -1.731410, -
                1.978420, 2.188860, 2.456020, -1.584610,
                                          2.717930, -
                                          0.505090
                                          ]
                    self.skparameters = array(self.aux, dtype=float) self.a0 = 6.0583
                    self.flag = 1

               self.sqci=sqci;
               self.tilt=tilt;
               self.edge=edge;
               self.zmax=zmax;

               layers = int(4*self.zmax/(self.a0) + 1)

               if (rank==0): writeout("prima="), layers

               if layers%4==1: layers-
                     =1
               elif layers%4==2: layers-=2
               elif layers%4==3: layers+=1
```

```
            if layers%4!=0:
                writeout("INTERRUPT AT WIRE"), material, parameters[0][i]
                writeout("NUMBER OF SLICES NOT MULTIPLE OF 4")
                quit()

            layers += 8
            self.L = (self.a0/4)*(layers-1)
            self.n_aux = int((4*self.edge/self.a0)*(4*self.edge/self.a0))
+ 10;
            #forse se ci si leva il +10 non cambia nulla (provare) self.Nc_aux =
            int((4*self.zmax/self.a0)) + 10; self.zmax=self.L

            self.atoms=zeros(1);
            self.slices=zeros(1);
            self.max=zeros(1);
            self.rank=0;
            self.deltae=20.0;
            self.ics = zeros(self.n_aux*self.Nc_aux); self.ipsilon =
            zeros(self.n_aux*self.Nc_aux); self.zeta =
            zeros(self.n_aux*self.Nc_aux); self.H_aux=zeros(
(self.Nc_aux*self.n_aux)*((self.Nc_aux*self.n_aux+1)/2)*(2+100));

self.H=zeros((((self.Nc_aux*self.n_aux)*(self.Nc_aux*self.n_aux+1)/2), 2+100));

            self.Zinc();
            self.n     =     int(self.atoms[0]);     self.Nc=
            int(self.slices[0]); self.x = self.ics;
            self.y = self.ipsilon; self.z =
            self.zeta;

            self.Phi=zeros(self.n*self.Nc);
            self.Ei=zeros(self.n*self.Nc);
            self.Eupper=1000.0;
            self.Elower=-1000.0;
            self.dE=0.001; self.eta=1e-8;
            self.mu1=0; self.mu2=0;
            self.Temp=300;
            self.E=zeros(NEmax);
            self.T=zeros(NEmax);
            self.charge=zeros(self.n*self.Nc);
            self.Egap=0; def
        gap(self):
            return 0;
        def current(self): vt=kboltz*self.Temp/q;
            E=array(self.E); T=array(self.T);
            arg=2*q*q/(2*pi*hbar)*T*(Fermi((E-self.mu1)/vt)-Fermi((E-
self.mu2)/vt))*self.dE
            return sum(arg); def
        charge_T(self):
```

```
            H_charge_T(self); self.E=array(self.E);
            self.T=array(self.T);
            self.charge=array(self.charge); return;
        def Zinc(self):

            writeout(self.skparameters)
#             quit()

            Zinc(self);
#             self.zeta = array(self.zeta);
#             ics1 = []
#             ipsilon1 = []
#             zeta1 = []
#             i = 0
#             j = 0
#             k = 0
#             temp = self.zeta[0]- self.a0
#             zeta1.append(temp)
#             aux = []
#             for ln in self.zeta:
#                 if (self.zeta[i]- self.a0) == temp:
#                     #temp = self.zeta[i]- self.a0
#                     i = i + 1
#                     j = j + 1
#                 else:
#                     zeta1.append(self.zeta[i]- self.a0)
#                     temp = self.zeta[i]- self.a0
#                     i = i + 1
#                     aux.append(j)
#                     j=1;
#
#             print aux
#             print self.zeta


#             for i in range (100): #print zeta1

#             print 'slices =', int(self.slices[0])
#             print 'atoms =', int(self.atoms[0])

#             zeta2 = []
#             for i in range (int(self.slices[0])):
#                 for j in range(int(self.atoms[0])):
#                     zeta2.append(zeta1[i])
#
#             print  'ECCOLO'  #print
            zeta2


#             self.zeta = zeta2 #print

            self.zeta H_back = []
```

```
        i   = 0
        j   = 0
        bound = int(self.max[0]/102)
        writeout(bound)

        for i in range ( bound ): row = []
                for j in range(102): row.append(self.H_aux[j + 102*i])
                H_back.append(row) #print
                row
                del row



        #print H_back[40]

        new = array(H_back, dtype=complex)

        self.H = new

#         print self.H[17]

#         quit()

        return;

def ciccione(vettore,n,Nc,z,a0): ics1 = []
        ipsilon1 = [] zeta1 = []
        i = 0 j = 0 k
        = 0
        temp = z[0]- a0 z1=[];
        z1.append(temp) aux = []
        for ln in arange(0,n*Nc): if (z[i]- a0) ==
                temp:
                        #temp = self.zeta[i]- self.a0 i = i + 1
                        j = j + 1 else:
                        z1.append(z[i]- a0) temp =
                        z[i]- a0
                        i = i + 1 aux.append(j)
                        j=1;

#       TODO: the following sum is equal to the total number of
#       atoms, really present in the simulated nanowire
#
#       Ntot_atoms=sum(aux[:Nc])
#
#
        array2 = []
        for i in range(Nc): k=0;
                if (aux[i]==n):
```

```
                for j in arange(sum(aux[:i]),sum(aux[:i])+n):
                    array2.append(vettore[j])
            else:
                for j in arange(sum(aux[:i]),sum(aux[:i])+aux[i]):
                    array2.append(vettore[j]);
                for j in arange(sum(aux[:i])+aux[i],sum(aux[:i])+n): array2.append(0)

        return array(array2, dtype=float);


class grid3D:
    def __init__(self,*args):
        # I initialize the rank if
        (mpi4py_loaded):
            rank = MPI.COMM_WORLD.Get_rank() else:
            rank=0;
        # args is a tuple and len(args) return
        # the number of arguments
        # the number of arguments can be either 3 or 6
        # if 3, the first three inputs are the grid along the
        # x,y,z axis
        # if 6, the first three inputs are the grid along the
        # x,y,z axis, while the last three inputs are the x-y-z
        # coordinates of the atoms
        if (len(args)>3): xg=around(args[0],5);
            yg=around(args[1],5);
            zg=around(args[2],5);
            xC=around(args[3],5);
            yC=around(args[4],5);
            zC=around(args[5],5);
            npC=size(xC);
        else:
            xg=around(args[0],5);
            yg=around(args[1],5);
            zg=around(args[2],5);
            npC=0;

        #I create the grid if (npC!=0):
            #find the unique values for xC,yC and zC uxC=unique(xC);
            uyC=unique(yC);
            uzC=unique(zC);

            # I find the only the additional values which are in xg and not in uxC
            # the same for the other axis
            exg=intersect1d(setxor1d(xg,uxC),xg);
            eyg=intersect1d(setxor1d(yg,uyC),yg);
            ezg=intersect1d(setxor1d(zg,uzC),zg);

        if (npC!=0): x=unique(concatenate((uxC,xg),1));
            y=unique(concatenate((uyC,yg),1));
            z=unique(concatenate((uzC,zg),1));
```

```
else:
    x=xg;
    y=yg;
    z=zg;

# I start to compute the volume associated to each grid point X,Y=meshgrid(x,y);

#Number of points
nx=size(x); ny=size(y);
nxy=nx*ny; nz=size(z);
Np=nxy*nz;
string="Number of grid points %s " %Np if (rank == 0):
writeout(string)


#########################################################################
##############
#I create the Volume elements using the sorted grid xd=avervect(x);
yd=avervect(y);
zd=avervect(z);
X,Y=meshgrid(x,y);
X,Z=meshgrid(x,z);

XD,ZD=meshgrid(xd,zd);
surfxz=XD*ZD;
YD,ZD=meshgrid(yd,zd);
surfyz=YD*ZD;
XD,YD=meshgrid(xd,yd);
surfxy=XD*YD;

#The volumes for the sorted grid are finally computed
a,b=meshgrid((XD*YD).flatten(),zd); dVes=abs((a*b).flatten());

if (rank == 0): writeout("Volumes computed")


#########################################################################
##############
# I create the dist vectors
dists=zeros((Np,6));

#  I take care of dists[:,1] i=arange(0,nx);
ip1=i+1; ip1[nx-1]=nx-1;
xdistp=x[ip1]-x[i];

dists[:,1]=meshgrid(meshgrid(xdistp,y)[0].flatten(),z)[0].flatten(); del ip1,xdistp;

# I take care of dists[:,0]
```

```
        im1=i-1;
        im1[0]=0;
        xdistm=x[i]-x[im1];

dists[:,0]=meshgrid(meshgrid(xdistm,y)[0].flatten(),z)[0].flatten(); del i,im1,xdistm;

        # I take care of dists[:,3] j=arange(0,ny);
        jp1=j+1; jp1[ny-1]=ny-1;
        ydistp=y[jp1]-y[j];

dists[:,3]=meshgrid(meshgrid(x,ydistp)[1].flatten(),z)[0].flatten(); del jp1,ydistp;

        # I take care of dists[:,2] jm1=j-1;
        jm1[0]=0; ydistm=y[j]-y[jm1];

dists[:,2]=meshgrid(meshgrid(x,ydistm)[1].flatten(),z)[0].flatten(); del j,jm1,ydistm;

        # I take care of dists[:,5] k=arange(0,nz);
        kp1=k+1; kp1[nz-1]=nz-1;
        zdistp=z[kp1]-z[k];

dists[:,5]=meshgrid(meshgrid(x,y)[1].flatten(),zdistp)[1].flatten(); del kp1,zdistp;

        # I take care of dists[:,4] km1=k-1;
        km1[0]=0; zdistm=z[k]-
        z[km1];

dists[:,4]=meshgrid(meshgrid(x,y)[1].flatten(),zdistm)[1].flatten(); del k,km1,zdistm;



##########################################################################
##############
        #Now I work on the surfaces

        surfs=zeros((Np,6));

        #surf 0 XD,YD=meshgrid(xd,yd)
        ##YD[:,0]=0;
        a,b=meshgrid(YD.flatten(),zd)
        surfs[:,0]=abs((a*b).flatten()); #surf 1
        XD,YD=meshgrid(xd,yd) ##YD[:,nx-1]=0;
        a,b=meshgrid(YD.flatten(),zd)
        surfs[:,1]=abs((a*b).flatten()); #surf 2
        XD,YD=meshgrid(xd,yd)
        ##XD[0,:]=0;
        a,b=meshgrid(XD.flatten(),zd)
        surfs[:,2]=abs((a*b).flatten()); #surf 3
        XD,YD=meshgrid(xd,yd) ##XD[ny-1,:]=0;
```

```
a,b=meshgrid(XD.flatten(),zd)
surfs[:,3]=abs((a*b).flatten()); #surf 4
XD,YD=meshgrid(xd,yd)
a,b=meshgrid((XD*YD).flatten(),z)
surfs[:,4]=abs(a.flatten()); ##surfs[0:nx*ny-
1,4]=0;
#surf 5 XD,YD=meshgrid(xd,yd)
a,b=meshgrid((XD*YD).flatten(),z)
surfs[:,5]=abs(a.flatten()); ##surfs[(nz-
1)*(nx*ny):nz*nx*ny,5]=0;

if (rank == 0): writeout("Surfaces created")



#########################################################################
##############
#Now I have to go back to the unsorted grid. #I create the sorted
and unsorted coordinates #vectors as a function of the index

#sorted positions x3Ds=meshgrid(meshgrid(x,y)[0].flatten(),z)[0].flatten();
y3Ds=meshgrid(meshgrid(x,y)[1].flatten(),z)[0].flatten();
z3Ds=meshgrid(meshgrid(x,y)[1].flatten(),z)[1].flatten();

#unsorted positions

if (npC!=0): xtemp=unique(concatenate((uxC,xg),1));
    ytemp=unique(concatenate((uyC,yg),1));
    ztemp=unique(concatenate((uzC,zg),1));

    if (rank == 0): writeout("I work on the swap array"); NpC=size(xC);


    swap=array(arange(0,NpC),int); for i in
    range(0,NpC):
        ixC=nonzero(xtemp==xC[i])[0][0];
        iyC=nonzero(ytemp==yC[i])[0][0];
        izC=nonzero(ztemp==zC[i])[0][0];
        ii=ixC+iyC*nx+izC*nx*ny;
        swap[i]=ii;



#########################################################################
##############
# I now fill the attributes of the istance of the grid class self.x3D=x3Ds;
self.y3D=y3Ds
self.z3D=z3Ds
self.dVe=dVes;
self.surf=surfs;
self.dist=dists;
```

```
        self.nx=nx;
        self.ny=ny;
        self.nz=nz;
        self.Np=Np;
        self.gridx=x;
        self.gridy=y;
        self.gridz=z; if
        (npC!=0):
            self.swap=swap;
        self.xmin=min(x);
        self.xmax=max(x);
        self.ymin=min(y);
        self.ymax=max(y);
        self.zmin=min(z);
        self.zmax=max(z);
        return;

class grid2D:
    def __init__(self,*args):

        # I initialize the rank if
        (mpi4py_loaded):
            rank = MPI.COMM_WORLD.Get_rank() else:
            rank=0;

        #  args is a tuple and len(args) return
        #  the number of arguments
        #  the number of arguments can be either 2 or 4
        #  if 2, the first two inputs are the grid along the
        #  x,y axis
        #  if 4, the first two inputs are the grid along the
        #  x,y axis, while the last two inputs are the x-y
        # coordinates of the atoms if
        (len(args)>2):
            xg=around(args[0],5);
            yg=around(args[1],5);
            xC=around(args[2],5);
            yC=around(args[3],5);
            npC=size(xC);
        else:
            xg=around(args[0],5);
            yg=around(args[1],5);
            npC=0;

        #I create the grid if (npC!=0):
            #find the unique values for xC,yC and zC uxC=unique(xC);
            uyC=unique(yC);

            # I find the only the additional values which are in xg and not in uxC
            # the same for the other axis
```

```
        exg=intersect1d(setxor1d(xg,uxC),xg);
        eyg=intersect1d(setxor1d(yg,uyC),yg);

    if (npC!=0): x=unique(concatenate((uxC,xg),1));
        y=unique(concatenate((uyC,yg),1));
    else:
        x=xg;
        y=yg;


    #Number of points
    nx=size(x); ny=size(y);
    nxy=nx*ny; Np=nxy;
    string="Number of grid points %s " %Np if (rank == 0):
    writeout(string)


##########################################################################
##############
    #I create the Volume elements using the sorted grid xd=avervect(x);
    yd=avervect(y);
    X,Y=meshgrid(x,y);

    XD,YD=meshgrid(xd,yd);
    surfxy=XD*YD;

    if (rank == 0): writeout("Volumes computed")


##########################################################################
##############
    # I create the dist vectors
    dists=zeros((Np,4));

    # I take care of dists[:,1] i=arange(0,nx);
    ip1=i+1; ip1[nx-1]=nx-1;
    xdistp=x[ip1]-x[i];
    dists[:,1]=meshgrid(xdistp,y)[0].flatten(); del ip1,xdistp;

    # I take care of dists[:,0]
    im1=i-1;
    im1[0]=0;
    xdistm=x[i]-x[im1]; dists[:,0]=meshgrid(xdistm,y)[0].flatten()
    del i,im1,xdistm;

    # I take care of dists[:,3] j=arange(0,ny);
    jp1=j+1; jp1[ny-1]=ny-1;
    ydistp=y[jp1]-y[j];
    dists[:,3]=meshgrid(x,ydistp)[1].flatten() del jp1,ydistp;
```

```
        #  I take care of dists[:,2]
        jm1=j-1;
        jm1[0]=0;
        ydistm=y[j]-y[jm1]; dists[:,2]=meshgrid(x,ydistm)[1].flatten();
        del j,jm1,ydistm;


#########################################################################
##############
        #Now I work on the surface

        XD,YD=meshgrid(xd,yd)
        surfs=(XD*YD).flatten();

        if (rank == 0): writeout("Surface created")



#########################################################################
##############
        #Now I have to go back to the unsorted grid.

        #I create the sorted and unsorted coordinates #vectors as a function
        of the index


        #sorted positions
        x2Ds=meshgrid(x,y)[0].flatten();
        y2Ds=meshgrid(x,y)[1].flatten();

        #unsorted positions

        if (npC!=0): xtemp=unique(concatenate((uxC,xg),1));
            ytemp=unique(concatenate((uyC,yg),1));

            if (rank == 0): writeout("I work on the swap array"); NpC=size(xC);
            swap=array(arange(0,NpC),int); for i in
            range(0,NpC):
                ixC=nonzero(xtemp==xC[i])[0][0];
                iyC=nonzero(ytemp==yC[i])[0][0];
                ii=ixC+iyC*nx;
                swap[i]=ii;



#########################################################################
##############
        # I now fill the attributes of the istance of the grid class self.x2D=x2Ds;
        self.y2D=y2Ds
        self.surf=surfs;
        self.dist=dists;
        self.nx=nx;
```

```
        self.ny=ny;
        self.Np=Np;
        self.gridx=x;
        self.gridy=y; if
        (npC!=0):
            self.swap=swap;
        self.xmin=min(x);
        self.xmax=max(x);
        self.ymin=min(y);
        self.ymax=max(y);
        return;

class grid1D:
    def __init__(self,*args):

        # I initialize the rank if
        (mpi4py_loaded):
            rank = MPI.COMM_WORLD.Get_rank() else:
            rank=0;

        #  args is a tuple and len(args) return
        #  the number of arguments
        #  the number of arguments can be either 1 or 2
        #  if 1, the first input is the grid along the
        #  x axis
        #  if 2, the first input is the grid along the
        #  x axis, while the second input is the x
        #  coordinates of the atoms
        if (len(args)>1): xg=around(args[0],5);
            xC=around(args[1],5); # attenzione: modificato il
28/5/2011
            npC=size(xC);
        else:
            xg=around(args[0],5);
            npC=0;

        #I create the grid if (npC!=0):
            #find the unique values for xC
            uxC=unique(xC);

            # I find the only the additional values which are in xg and not in uxC
            exg=intersect1d(setxor1d(xg,uxC),xg);

        if (npC!=0): x=unique(concatenate((uxC,xg),1));
        else:
            x=xg;

        #Number of points
        nx=size(x); Np=nx;
        if (rank == 0): print(("Number of grid points ",Np))
```

```
##########################################################################
##############
        # I create the dist vectors
        dists=zeros((Np,4));

        #  I take care of dists[:,1] i=arange(0,nx);
        ip1=i+1; ip1[nx-1]=nx-1;
        xdistp=x[ip1]-x[i];
        dists[:,1]=xdistp; del
        ip1,xdistp;


        # I take care of dists[:,0] im1=i-1;
        im1[0]=0; xdistm=x[i]-x[im1];
        dists[:,0]=xdistm; del
        i,im1,xdistm;


##########################################################################
##############
        #Now I have to go back to the unsorted grid. #I create the sorted
        and unsorted coordinates #vectors as a function of the index

        if (npC!=0): xtemp=unique(concatenate((uxC,xg),1));

            if (rank == 0): print("I work on the swap array"); NpC=size(xC);
            swap=array(arange(0,NpC),int); for i in
            range(0,NpC):
                ixC=nonzero(xtemp==xC[i])[0][0];
                ii=ixC;
                swap[i]=ii;



##########################################################################
##############
        # I now fill the attributes of the istance of the grid class self.x=x;
        self.dist=dists;
        self.nx=nx;
        self.Np=Np;
        self.gridx=x; if
        (npC!=0):
            self.swap=swap;
        self.xmin=min(x);
        self.xmax=max(x);
        return;

class region:
    def __init__(self,*args):
        self.name="none";
```

```
            self.geometry="hex";
            self.eps=3.9; self.rho=0;
            if (args[0]=="hex"): if
                (len(args)>5):
                        self.xmin=args[1];
                        self.xmax=args[2];
                        self.ymin=args[3];
                        self.ymax=args[4];
                        self.zmin=args[5];
                        self.zmax=args[6];
                elif ((len(args)>3)&(len(args)<=5)):
                        self.xmin=args[1]; self.xmax=args[2];
                        self.ymin=args[3]; self.ymax=args[4];
                elif (len(args)<=3):
                        self.xmin=args[1];
                        self.xmax=args[2];
        def set_material(self,material): if
            (material.lower()=="sio2"):
                self.eps=3.9;
                self.mel=0.5;
                self.met=0.5;
                self.Egap=8.05;
                self.chi=0.95;
                self.mhole=0.42
            if (material.lower()=="si"): self.eps=11.8;
                self.mel=0.916; self.met=0.19;
                self.Egap=1.124519; self.chi=4.05;
                self.mhole=0.549;
class gate:
        def __init__(self,*args):
            self.geometry="hex"; self.Ef=0;
            self.wf=4.1;
            if (args[0]=="hex"): if
                (len(args)>5):
                        self.xmin=args[1];
                        self.xmax=args[2];
                        self.ymin=args[3];
                        self.ymax=args[4];
                        self.zmin=args[5];
                        self.zmax=args[6];
                elif ((len(args)>3)&(len(args)<=5)):
                        self.xmin=args[1]; self.xmax=args[2];
                        self.ymin=args[3]; self.ymax=args[4];
                elif (len(args)<=3):
                        self.xmin=args[1];
                        self.xmax=args[2];
            if (args[0]=="cyl"): self.xc=args[1];
                self.yc=args[2];
                self.radius=args[3];
```

```
                    self.geometry="cyl" if
                        (args[0]=="trapz"):
                         self.xmin=args[1];
                         self.xmax=args[2];
                self.y1=args[3];
                self.z1=args[4];
                self.y2=args[5];
                self.z2=args[6];
                self.y3=args[7];
                self.z3=args[8];
                self.y4=args[9];
                self.z4=args[10];
                self.geometry="trapz"

class interface3D:
    def __init__(self,*args):

        #  I set the rank if
        (mpi4py_loaded):
            rank    =    MPI.COMM_WORLD.Get_rank()
            self.rank=rank;
        else:
            self.rank=0;

        #  I compute the number of arguments (classes) Narg=size(args);
        #  I first find the index of the class grid igrid=-10;
        for i in range(0,Narg):
            name=args[i].__class__.__name__ if
            (name=="grid3D"):
                igrid=i;
        #  If no grid class is specified I exit
        if (igrid==-10):
            writeout("ERROR: grid not passed to structure") return;

        # I   create   the   arrays   to   be   used
        self.eps=zeros(args[igrid].Np);

        #  I create the vector, where the boundary conditions
        #  are specified:
        #  if 2000   : inner point
        #  if 1001   : Neumann 1
        #  if 1002   : Neumann 2
        #  if 1003   : Neumann 3
        #  if 1004   : Neumann 4
        #  if 1005   : Neumann 5
        #  if 1006   : Neumann 6
        #  if <= 1000: Fermi level of the gate
```

```
        #  I start defining all the points as inner points
        self.boundary_conditions=2000*ones(args[igrid].Np);


#########################################################################
########################
        #  Now I impose the Neumann Boundary conditions on
        #  the surfaces delimiting the 3D domain

#########################################################################
########################

        #  I take care of Neumann1
        indexNeu1=nonzero(args[igrid].x3D==min(args[igrid].gridx));
        self.boundary_conditions[indexNeu1]=1001;

        #  I take care of Neumann2
        indexNeu2=nonzero(args[igrid].x3D==max(args[igrid].gridx));
        self.boundary_conditions[indexNeu2]=1002;

        #  I take care of Neumann3
        indexNeu3=nonzero(args[igrid].y3D==min(args[igrid].gridy));
        self.boundary_conditions[indexNeu3]=1003;

        #  I take care of Neumann4
        indexNeu4=nonzero(args[igrid].y3D==max(args[igrid].gridy));
        self.boundary_conditions[indexNeu4]=1004


        #  I take care of Neumann5 and Neumann6
        indexNeu5=nonzero(args[igrid].z3D==min(args[igrid].gridz));
        self.boundary_conditions[indexNeu5]=1005;
        indexNeu6=nonzero(args[igrid].z3D==max(args[igrid].gridz));
        self.boundary_conditions[indexNeu6]=1006;


#########################################################################
########################
        #  I check to which class the args belongs to
        #  and I proceed accordingly

#########################################################################
########################

        for i in range(0,Narg):
            name=args[i].__class__.__name__
            # I check if the class is a gate if (name=="gate"):
                #I check if the geometry is an hexahedron if
                (args[i].geometry=="hex"):
                    # I find the indexes of the 3D grid which belongs
to the gate
```

```
                        # with hex geometry


index=nonzero((args[i].xmin<=args[igrid].x3D)&(args[i].xmax>=args[igri
d].x3D)&

(args[i].ymin<=args[igrid].y3D)&(args[i].ymax>=args[igrid].y3D)&

(args[i].zmin<=args[igrid].z3D)&(args[i].zmax>=args[igrid].z3D));
                        self.boundary_conditions[index]=args[i].Ef; args[i].index=index;
                    if (args[i].geometry=="trapz"):
                        # I find the indexes of the 2D grid which belongs
to the gate
                        # with trapezoidal geometry if
                        (args[i].y2==args[i].y1):
                            m1=(args[i].z2-args[i].z1)/(args[i].y2-
args[i].y1+1e-3)
                        else: m1=(args[i].z2-args[i].z1)/(args[i].y2-
args[i].y1)
                        if (args[i].y3==args[i].y2): m2=(args[i].z3-
                            args[i].z2)/(args[i].y3-
args[i].y2+1e-3)
                        else: m2=(args[i].z3-args[i].z2)/(args[i].y3-
args[i].y2)
                        if (args[i].y4==args[i].y3): m3=(args[i].z4-
                            args[i].z3)/(args[i].y4-
args[i].y3+1e-3)
                        else: m3=(args[i].z4-args[i].z3)/(args[i].y4-
args[i].y3)
                        if (args[i].y4==args[i].y1): m4=(args[i].z4-
                            args[i].z1)/(args[i].y4-
args[i].y1+1e-3)
                        else: m4=(args[i].z4-args[i].z1)/(args[i].y4-
args[i].y1)


index=nonzero((args[igrid].z3D>=(m1*(args[igrid].y3D-
args[i].y1)+args[i].z1))&

(args[igrid].z3D>=(m2*(args[igrid].y3D-args[i].y2)+args[i].z2))&

(args[igrid].z3D<=(m3*(args[igrid].y3D-args[i].y3)+args[i].z3))&

(args[igrid].z3D<=(m2*(args[igrid].y3D-args[i].y1)+args[i].z1))&

(args[i].xmin<=args[igrid].x3D)&(args[i].xmax>=args[igrid].x3D));
                        self.boundary_conditions[index]=args[i].Ef; args[i].index=index;
```

```
                elif (name=="region"):
                        if (args[i].geometry=="hex"):
                                # I find the indexes of the 3D grid which belongs
to the gate
                                # with hex geometry

index=nonzero((args[i].xmin<=args[igrid].x3D)&(args[i].xmax>=args[igri
d].x3D)&

(args[i].ymin<=args[igrid].y3D)&(args[i].ymax>=args[igrid].y3D)&

(args[i].zmin<=args[igrid].z3D)&(args[i].zmax>=args[igrid].z3D));
                                self.eps[index]=args[i].eps; elif
                (name=="grid3D"):
                        #dummy line name;
                else:
                        writeout("ERROR: Unrecognized input") return;


#########################################################################
########################
        # I fill the field of the interface class

#########################################################################
########################

        #self.boundary already filled #self.eps already
        filled self.Phiold=zeros(args[igrid].Np)
        self.Phi=zeros(args[igrid].Np);
        self.normpoisson=1e-3; self.tolldomn=1e-1;
        self.underel=0;
        self.free_charge=zeros(args[igrid].Np);
        self.fixed_charge=zeros(args[igrid].Np); self.normd=5e-2;
        self.modespace="no"
        self.MPI="no"
        self.MPI_kt="no" return;

class interface2D:
    def __init__(self,*args):

        # I set the rank if
        (mpi4py_loaded):
                rank = MPI.COMM_WORLD.Get_rank()
                self.rank=rank;
        else:
                self.rank=0;


        #  I compute the number of arguments (classes) Narg=size(args);
        #  I first find the index of the class grid igrid=-10;
        for i in range(0,Narg):
```

```
        name=args[i].__class__.__name__ if
        (name=="grid2D"):
            igrid=i;
    #  If no grid class is specified I exit
    if (igrid==-10):
        writeout("ERROR: grid not passed to structure") return;

    # I create the arrays to be used
    self.eps=zeros(args[igrid].Np);

    #  I create the vector, where the boundary conditions
    #  are specified:
    #  if 2000   : inner point
    #  if 1001   : Neumann 1
    #  if 1002   : Neumann 2
    #  if 1003   : Neumann 3
    #  if 1004   : Neumann 4
    #  if <= 1000: Fermi level of the gate

    #  I start defining all the points as inner points
    self.boundary_conditions=2000*ones(args[igrid].Np);


#########################################################################
########################
    #  Now I impose the Neumann Boundary conditions on
    #  the surfaces delimiting the 3D domain

#########################################################################
########################

    #  I take care of Neumann1
    indexNeu1=nonzero(args[igrid].x2D==min(args[igrid].gridx));
    self.boundary_conditions[indexNeu1]=1001;

    #  I take care of Neumann2
    indexNeu2=nonzero(args[igrid].x2D==max(args[igrid].gridx));
    self.boundary_conditions[indexNeu2]=1002;

    #  I take care of Neumann3
    indexNeu3=nonzero(args[igrid].y2D==min(args[igrid].gridy));
    self.boundary_conditions[indexNeu3]=1003;

    #  I take care of Neumann4
    indexNeu4=nonzero(args[igrid].y2D==max(args[igrid].gridy));

    self.boundary_conditions[indexNeu4]=1004
```

```
##########################################################################
########################
        #  I check to which class the args belongs to
        #  and I proceed accordingly

##########################################################################
########################

        for i in range(0,Narg):
            name=args[i].__class__.__name__
            # I check if the class is a gate if (name=="gate"):
                #I check if the geometry is an hexahedron if
                (args[i].geometry=="hex"):
                    # I find the indexes of the 2D grid which belongs
to the gate
                    # with hex geometry

index=nonzero((args[i].xmin<=args[igrid].x2D)&(args[i].xmax>=args[igri
d].x2D)&

(args[i].ymin<=args[igrid].y2D)&(args[i].ymax>=args[igrid].y2D));
                    self.boundary_conditions[index]=args[i].Ef; args[i].index=index;
                #I check if the geometry is an cylindrical if
                (args[i].geometry=="cyl"):
                    # I find the indexes of the 2D grid which belongs
to the gate
                    # with cyl geometry
                    index=nonzero(((args[i].xc-
args[igrid].x2D)**2+(args[i].yc-
args[igrid].y2D)**2)<(args[i].radius)**2);
                    self.boundary_conditions[index]=args[i].Ef;
                    args[i].index=index;
            elif (name=="region"):
                if (args[i].geometry=="hex"):
                    # I find the indexes of the 2D grid which belongs
to the gate
                    # with hex geometry

index=nonzero((args[i].xmin<=args[igrid].x2D)&(args[i].xmax>=args[igri
d].x2D)&

(args[i].ymin<=args[igrid].y2D)&(args[i].ymax>=args[igrid].y2D));
                    self.eps[index]=args[i].eps; elif
            (name=="grid2D"):
                #dummy line name;


            else:
                writeout("ERROR: Unrecognized input") return;
```

```
#########################################################################
########################
        # I fill the field of the interface class

#########################################################################
########################

        #self.boundary already filled #self.eps already
        filled self.Phiold=zeros(args[igrid].Np)
        self.Phi=zeros(args[igrid].Np);
        self.normpoisson=1e-3; self.tolldomn=1e-1;
        self.underel=0;
        self.free_charge=zeros(args[igrid].Np);
        self.fixed_charge=zeros(args[igrid].Np); self.normd=5e-2;
        self.modespace="no"
        self.MPI="no"
        self.MPI_kt="no" return;

class interface1D:
    def __init__(self,*args):

        #  I set the rank if
        (mpi4py_loaded):
            rank    =    MPI.COMM_WORLD.Get_rank()
            self.rank=rank;
        else:
            self.rank=0;

        #  I compute the number of arguments (classes) Narg=size(args);
        #  I first find the index of the class grid igrid=-10;
        for i in range(0,Narg):
            name=args[i].__class__.__name__ if
            (name=="grid1D"):
                igrid=i;
        #  If no grid class is specified I exit
        if (igrid==-10):
            print("ERROR: grid not passed to structure") return;

        # I create the arrays to be used
        self.eps=zeros(args[igrid].Np);


        self.mel=zeros(args[igrid].Np);
        self.met=zeros(args[igrid].Np);
        self.chi=zeros(args[igrid].Np);
        self.Egap=zeros(args[igrid].Np);
        self.fixed_charge=zeros(args[igrid].Np);
        self.mhole=zeros(args[igrid].Np);
```

```
        #  I create the vector, where the boundary conditions
        #  are specified:
        #  if 2000   : inner point
        #  if 1001   : Neumann 1
        #  if 1002   : Neumann 2
        #  if <= 1000: Fermi level of the gate

        #  I start defining all the points as inner points
        self.boundary_conditions=2000*ones(args[igrid].Np);


##########################################################################
########################
        #  Now I impose the Neumann Boundary conditions on
        #  the surfaces delimiting the 3D domain

##########################################################################
########################

        #  I take care of Neumann1
        indexNeu1=nonzero(args[igrid].x==min(args[igrid].gridx));
        self.boundary_conditions[indexNeu1]=1001;

        #  I take care of Neumann2
        indexNeu2=nonzero(args[igrid].x==max(args[igrid].gridx));
        self.boundary_conditions[indexNeu2]=1002;



##########################################################################
########################
        #  I check to which class the args belongs to
        #  and I proceed accordingly

##########################################################################
########################

        for i in range(0,Narg):
            name=args[i].__class__.__name__
            # I check if the class is a gate if (name=="gate"):
                #I check if the geometry is an hexahedron if
                (args[i].geometry=="hex"):
                    # I find the indexes of the 2D grid which belongs
to the gate
```

```
                        # with hex geometry

index=nonzero((args[i].xmin<=args[igrid].x)&(args[i].xmax>=args[igrid]
.x));
                        self.boundary_conditions[index]=args[i].Ef;
                        args[i].index=index;
                elif (name=="region"):
                    if (args[i].geometry=="hex"):
                        dist=avervect(args[igrid].x)*1e-9;
                        # I find the indexes of the 2D grid which belongs
to the gate
                        # with hex geometry

index=nonzero((args[i].xmin<=args[igrid].x)&(args[i].xmax>=args[igrid]
.x));
                        self.eps[index]=args[i].eps;
                        self.mel[index]=args[i].mel;
                        self.met[index]=args[i].met;
                        self.chi[index]=args[i].chi;
                        self.Egap[index]=args[i].Egap;
                        self.fixed_charge[index]=args[i].rho*dist[index];
                        self.mhole[index]=args[i].mhole;

                elif (name=="grid1D"): #dummy
                    line
                    name;
                else:
                    print("ERROR: Unrecognized input") return;


##########################################################################
########################
        # I fill the field of the interface class

##########################################################################
########################

        #self.boundary already filled #self.eps already
        filled self.Phiold=zeros(args[igrid].Np)
        self.Phi=zeros(args[igrid].Np);
        self.normpoisson=1e-3; self.tolldomn=1e-1;
        self.underel=0;
        self.free_charge=zeros(args[igrid].Np); self.normd=5e-2;
        self.modespace="no"
        self.MPI="no"
        self.MPI_kt="no" return;
```

```
def dope_reservoir(grid,interface,channel,molar_fraction,bbox):
    name=grid.__class__.__name__;
    if (name=="grid3D"):
        xmin=bbox[0];
        xmax=bbox[1];
        ymin=bbox[2];
        ymax=bbox[3];
        zmin=bbox[4];
        zmax=bbox[5];


index=nonzero((xmin<=grid.x3D[grid.swap])&(xmax>=grid.x3D[grid.swap])&

(ymin<=grid.y3D[grid.swap])&(ymax>=grid.y3D[grid.swap])&

(zmin<=grid.z3D[grid.swap])&(zmax>=grid.z3D[grid.swap]))
        interface.fixed_charge[grid.swap[index]]=molar_fraction;
    elif (name=="grid2D"):
        xmin=bbox[0];
        xmax=bbox[1];
        ymin=bbox[2];
        ymax=bbox[3];


index=nonzero((xmin<=grid.x2D[grid.swap])&(xmax>=grid.x2D[grid.swap])&

(ymin<=grid.y2D[grid.swap])&(ymax>=grid.y2D[grid.swap]))

interface.fixed_charge[grid.swap[index]]=molar_fraction/channel.delta* 1e9;
    elif (name=="grid1D"):
        xmin=bbox[0];
        xmax=bbox[1];


index=nonzero((xmin<=grid.x[grid.swap])&(xmax>=grid.x[grid.swap]));

interface.fixed_charge[grid.swap[index]]=molar_fraction/(channel.delta z*channel.deltay)*1e18;
# MODIFICATO IL 6/6/2011: aggiunto il deltay e deltaz

    return index;

class Device:
    def __init__(self): self.Nregions=1;
        self.regions=[];
        self.E=zeros(NEmax);
    def test(self): return self.E;


def test_var_args(farg, *args): writeout("formal arg:"),
    size(args) for arg in args:
        writeout("another arg:"), arg
```

```
def avervect(x):
        #  This function compute the length of
        #  the Voronoi segment of a one-dimensional array x nx=size(x);
        xd=zeros(nx);
        xini=x[0]; xd[0]=abs(x[0]-x[1])*0.5;
        for i in range(1,nx-1):
                xd[i]=abs((x[i+1]-x[i-1])*0.5); xd[nx-
        1]=abs(x[nx-1]-x[nx-2])*0.5 return xd;

def save_format_xyz(outputfile,x,y,z,atom):

        if sys.version > '3': import
                subprocess;
        else:
                import subprocess

        out=[x*10,y*10,z*10]
        fp=open(outputfile,"w");
        fp.write(str(size(x)));
        fp.write("\n");
        fp.write("\n");
        for i in range(0,size(x)):
                string="%s %s %s %s" %(atom,out[0][i],out[1][i],out[2][i]); fp.write(string);
                fp.write(" ");
                fp.write("\n");
        fp.close()
        return;

"""def convert_pdb(filename,thop):
        fp=open(filename,"r");
        hh=[];
        atoms=0;
        i=0;
        x=[];
        y=[];
        z=[];
        h=[];
        h.append([1,0,0]); for line in
        fp:
                hh.append(line); atoms=atoms+(hh[i].split()).count('HETATM');

                if
(((hh[i].split()).count('HETATM')==1)|((hh[i].split()).count('ATOM')== 1)):
                        x.append((hh[i].split())[5]);
                        y.append((hh[i].split())[6]);
                        z.append((hh[i].split())[7]);

h.append([int((hh[i].split())[1]),int((hh[i].split())[1]),0]); if
                ((hh[i].split()).count('CONECT')==1):
                        a=(hh[i].split());
```

```
                NPV=size(a)-1
                for j in range(0,NPV): a1=int(a[1]);
                    if (a1<int(a[j+1])): h.append([a1,int(a[j+1]),thop])
            if ((hh[i].split()).count('CRYST1')==1): a=(hh[i].split());
                if (double(a[1])>=100): deltax=0.0;
                else:
                    deltax=double(a[1])/10.0; if
                (double(a[2])>=100):
                    deltay=0.0;
                else:
                    deltay=double(a[2])/10.0; if
                (double(a[3])>=100):
                    deltaz=0.0;
                else:
                    deltaz=double(a[3])/10.0;


            i=i+1;
        fp.close()
        H=array(h,dtype(complex));
        x=array(x,dtype(float))/10.0;
        y=array(y,dtype(float))/10.0;
        z=array(z,dtype(float))/10.0;
        return H,x,y,z,deltax,deltay,deltaz;"""

def create_H_from_xyz(x,y,z,orbitals,onsite,thop,d_bond,Nbond):
        #  WE ASSUME THAT:
#
        #  1) TRANSPORT IS IN THE Z DIRECTION
        #  2) THE STRUCTURE IS COMPOSED BY THE SAME TYPE OF ATOMS
        # 3) ALONG THE Z-DIRECTION THE STRUCTURE IS PERIODIC WITH PERIOD EQUAL TO 4 SLICES
#

        #  I find the minimum and maximum coordinates at the border
        #  so to take care of the passivation of the atoms at the borders xmin=min(x);
        xmax=max(x);
        ymin=min(y);
        ymax=max(y);
        zmin=min(z);
        zmax=max(z);

        # I compute the number of slices (ASSUMPTION 2)
        Nc=int(size(unique(z)));
        #  I have already computed n at the beginning
        #       n=int(size(nonzero(z==zmin)));
        # I compute the number of atoms in the first 4 slices temp=unique(z);
        Natom_slices=size(nonzero(z<=temp[3]));
        del temp;
```

```
    # I check the maximum number of atoms on each slice; u=unique(z);
    Nuz=size(u); n=-1;
    for i in range(0,Nuz):
        nnew=size(nonzero(z==u[i])); if
        (nnew>=n):
            n=nnew;
    del i;

    # Now I start doing though stuff
    # I fill x,y and z with dummy atoms
    # If it is a dummy atom, the coordinate is equal to dummy_coord

    dummy_coord=10000;
    xa=[];
    ya=[];
    za=[];
    k=0;
    for i in range(0,Nuz):
#         print ya
        nnew=size(nonzero(z==u[i]));
        for j in range(0,nnew):
            xa.append(x[k]);
            ya.append(y[k]);
            za.append(z[k]);
            k=k+1;
        if (nnew<n):
            for j in range(nnew,n):
                xa.append(dummy_coord);
                ya.append(dummy_coord);
                za.append(dummy_coord);
#                 k=k+1;

    del x,y,z,u,i
    x=array(xa,dtype(float));
    y=array(ya,dtype(float));
    z=array(za,dtype(float));

    del xa,ya,za

    Np=size(x);
    Ncol_max=10;
    NN=zeros((Np,Ncol_max),dtype(int)); border=[]
    # I first find the Nearest Neighbour for i in
    range(0,Np):
        ind=nonzero((sqrt((x-x[i])**2+(y-y[i])**2+(z-z[i])**2)<=d_bond)&(sqrt((x-
x[i])**2+(y-y[i])**2+(z-z[i])**2)>1e-10))[0];
        if (size(ind)>Ncol_max):
            print()
            writeout("ERROR IN create_H_from_xyz subroutine in
NanoTCAD_ViDES.py file")
            writeout("Use a larger value for Ncol_max")
```

```
                print()
                exit(0);
#               print i
            NN[i,0]=i+1;
            NN[i,1:size(ind)+1]=ind+1;
            NPV=size(nonzero(NN[i,:]))-1; if
            (NPV<Nbond):
                border.append(i);


    # Now I work on the Hamiltonian atoms=0;
    i=0;
    h=[];

    # I fill the h list with the number of orbitals ll=[orbitals,0];
    fill=zeros(orbitals**2);
    h.append(ll+list(fill)) del ll,i




    # I take care of the diagonal elements for i in
    range(0,Np):
        if ((x[i]<dummy_coord)): if
            (orbitals>1):
                    # (ASSUMPTION 1) if i in
                        border: xfn=zeros(4);
                    yfn=zeros(4); zfn=zeros(4);
                        if (z[i]==zmin): NPV=size(nonzero(NN[i+4*n,:]))-1;
                            xfn=x[NN[i+n*4,1:NPV+1]-1];
                            yfn=y[NN[i+n*4,1:NPV+1]-1];
                            zfn=z[NN[i+n*4,1:NPV+1]-1];
                            xp=x[i+n*4];
                            yp=y[i+n*4];
                            zp=z[i+n*4]; elif
                        (z[i]==zmax):
                            NPV=size(nonzero(NN[i-4*n,:]))-1; xfn=x[NN[i-
                            n*4,1:NPV+1]-1]; yfn=y[NN[i-n*4,1:NPV+1]-1];
                            zfn=z[NN[i-n*4,1:NPV+1]-1]; xp=x[i-n*4];
                            yp=y[i-n*4]; zp=z[i-
                            n*4];
                        else: NPV=size(nonzero(NN[i,:]))-1;
                            xfn=x[NN[i,1:NPV+1]-1];
                            yfn=y[NN[i,1:NPV+1]-1];
                            zfn=z[NN[i,1:NPV+1]-1]; xp=x[i];

                            yp=y[i];
                            zp=z[i];

                        deltae=20.0;
```

```
tempM=Sipassivation(xp,yp,zp,NPV,xfn,yfn,zfn,deltae);
        #                       print tempM
        #                       print x[i],y[i],z[i]
        #                       print xfn
        #                       print yfn
        #                       print zfn
        #                       exit(0);
                                B=zeros((10,10));
                                B[:4,:4]=tempM.reshape(4,4);

h.append([i+1,i+1]+list((diag(onsite)+B).flatten()));
        #
h.append([i+1,i+1]+list((diag(onsite)).flatten())); del B,tempM,xfn,yfn,zfn;
                        else:

h.append([i+1,i+1]+list((diag(onsite)).flatten())); else:
                        h.append([i+1,i+1]+list(fill));
                else:
                        #  If the atom is dummy then I mark it with the 77777 value
                        #  Right now it works only for one orbital
                        h.append([i+1,i+1]+list(77777*ones(orbitals**2)));


        #  I take care of the off-diagonal elements
        for i in range(0,Np): NPV=size(nonzero(NN[i,:]))-1;


                for j in range(0,NPV):
                        a1=int(NN[i,0]);
                        if (a1<int(NN[i,j+1])): if
                                (orbitals>1):
                                        # I compute the cosine
                                        module=sqrt(((double(x[a1-1])-
double(x[int(NN[i,j+1])-1]))**2)+(double(y[a1-1])-
double(y[int(NN[i,j+1])-1]))**2+(double(z[a1-1])-
double(z[int(NN[i,j+1])-1]))**2);
                                        cosx=(-double(x[a1-1])+double(x[int(NN[i,j+1])-
1]))/module;
                                        cosy=(-double(y[a1-1])+double(y[int(NN[i,j+1])-
1]))/module;
                                        cosz=(-double(z[a1-1])+double(z[int(NN[i,j+1])-
1]))/module;
#                                       print a1,int(NN[i,j+1]),cosx,cosy,cosz,module
#                                       input=hstack((array([cosx,cosy,cosy]),thop));
#                                       print input
#                                       matrix_thop=Simatrix(input);
                                        matrix_thop=Simatrix(cosx,cosy,cosz,thop);
#                                       print matrix_thop
#                                       print "----------------"
                                        h.append([a1,int(NN[i,j+1])]+list(matrix_thop)); else:
                                        h.append([a1,int(NN[i,j+1]),thop])
```

```
        H=array(h,dtype=complex); return
        H,n,Nc;

def get_xyz_from_file(filename):
        fp=open(filename,"r"); xa=[]

        ya=[]
        za=[]
        for line in fp:
                if (size(line.split())>3):
                        xa.append((line.split())[1]);
                        ya.append((line.split())[2]);
                        za.append((line.split())[3]);
        x=array(xa,dtype(float));
        y=array(ya,dtype(float));
        z=array(za,dtype(float)); del xa,ya,za
        return x,y,z;


def convert_pdb(filename,orbitals,thop):
        #  ASSUMPTION: ALL THE ATOMS ARE OF THE SAME MATERIAL

        #  I first read the atoms coordinates
        hh=[];
        deltax=0;
        deltay=0;
        deltaz=0;
        x=[];
        y=[];
        z=[];
        i=0;
        fp=open(filename,"r"); for line in
        fp:
                hh.append(line); if
(((hh[i].split()).count('HETATM')==1)|((hh[i].split()).count('ATOM')== 1)):
# ATOM_TYPE=(hh[i].split())[2]; x.append((hh[i].split())[5]);
                        y.append((hh[i].split())[6]);
                        z.append((hh[i].split())[7]);
                i=i+1;
        fp.close() del hh;

        #  Now I work on the Hamiltonian hh=[];
        atoms=0;
        i=0;
        h=[];

        #  I fill the h list with the number of orbitals ll=[orbitals,0];
        fill=zeros(orbitals**2);
        h.append(ll+list(fill)) del ll
```

```
        #  I fill the rest of the h list
        fp=open(filename,"r");
        for line in fp: hh.append(line);
              atoms=atoms+(hh[i].split()).count('HETATM'); if
(((hh[i].split()).count('HETATM')==1)|((hh[i].split()).count('ATOM')== 1)):
                    if (orbitals>1):

h.append([int((hh[i].split())[1]),int((hh[i].split())[1])]+list((diag( onsite)).flatten()));

                    else:

h.append([int((hh[i].split())[1]),int((hh[i].split())[1])]+list(fill))
;
              if ((hh[i].split()).count('CONECT')==1): a=(hh[i].split());
                    NPV=size(a)-1
                    for j in range(0,NPV): a1=int(a[1]);


                          if (a1<int(a[j+1])): if
                                (orbitals>1):
                                      # I compute the cosine
                                      module=sqrt(((double(x[a1-1])-
double(x[int(a[j+1])-1]))**2)+(double(y[a1-1])-double(y[int(a[j+1])-1]))**2+(double(z[a1-1])-
double(z[int(a[j+1])-1]))**2);
                                      cosx=(double(x[a1-1])-double(x[int(a[j+1])-
1]))/module;
                                      cosy=(double(y[a1-1])-double(y[int(a[j+1])-
1]))/module;
                                      cosz=(double(z[a1-1])-double(z[int(a[j+1])-
1]))/module;
                                      cosx=1;cosy=1;cosz=1;
                                      input=hstack((array([cosx,cosy,cosy]),thop));
                                      matrix_thop=Simatrix(input);
                                      h.append([a1,int(a[j+1])]+list(matrix_thop));
                                else:
                                      h.append([a1,int(a[j+1]),thop])

              if ((hh[i].split()).count('CRYST1')==1): a=(hh[i].split());
                    if (double(a[1])>=100): deltax=0.0;
                    else:
                          deltax=double(a[1])/10.0; if
                    (double(a[2])>=100):
                          deltay=0.0;
                    else:
                          deltay=double(a[2])/10.0; if
                    (double(a[3])>=100):
                          deltaz=0.0;
                    else:
                          deltaz=double(a[3])/10.0;
```

```
        i=i+1;
    fp.close()

    H=array(h,dtype(complex));
    x=array(x,dtype(float))/10.0;
    y=array(y,dtype(float))/10.0;
    z=array(z,dtype(float))/10.0; return
    H,x,y,z,deltax,deltay,deltaz;

def Hamiltonian_per(H,x,y,z,deltax,deltay,deltaz,aCC,thop,k): Np=size(x);
    Hnew=H.copy();
    conn_per=[]
    for ii in range(0,Np): xc=x[ii];
        yc=y[ii]; zc=z[ii];

        # Here I compare with 1.05*aCC in order to take into account numerical tollerances
        indp=nonzero(sqrt((x-xc+deltax)**2+(y-yc+deltay)**2+(z-
zc+deltaz)**2)<aCC*1.05)[0]+1;
        indm=nonzero(sqrt((x-xc-deltax)**2+(y-yc-deltay)**2+(z-zc-
deltaz)**2)<aCC*1.05)[0]+1;
        if (size(indp)>0):
            for j in range(0,size(indp)):
                conn_per.append([ii+1,indp[j]]);
        if (size(indm)>0):
            for j in range(0,size(indm)):
                conn_per.append([ii+1,indm[j]]);

    del ii Nconn=len(conn_per); for ii in
    range(Nconn):

ind=nonzero((H[:,0]==conn_per[ii][0])&(H[:,1]==conn_per[ii][1]))[0] if (size(ind)>0):
            if (deltax>0): segno=sign(x[int(abs(H[ind,0]))-1]-
x[int(abs(H[ind,1]))-1]); Hnew[ind,2]=H[ind,2]+thop*exp(-segno*k*deltax*1j);
            elif (deltay>0): segno=sign(y[int(abs(H[ind,0]))-1]-
y[int(abs(H[ind,1]))-1]); Hnew[ind,2]=H[ind,2]+thop*exp(-segno*k*deltay*1j);
            else: segno=sign(z[int(abs(H[ind,0]))-1]-
z[int(abs(H[ind,1]))-1]); Hnew[ind,2]=H[ind,2]+thop*exp(-segno*k*deltaz*1j);
        else:
            if (conn_per[ii][0]<conn_per[ii][1]): if (deltax>0):
                    segno=sign(x[conn_per[ii][0]-1]-x[conn_per[ii][1]-
1]);

temp=array([conn_per[ii][0],conn_per[ii][1],thop*exp(-segno*k*deltax*1j)]);
                elif (deltay>0): segno=sign(y[conn_per[ii][0]-1]-y[conn_per[ii][1]-
1]);

temp=array([conn_per[ii][0],conn_per[ii][1],thop*exp(-segno*k*deltay*1j)]);
                else: segno=sign(z[conn_per[ii][0]-1]-z[conn_per[ii][1]-
1]);
```

```
temp=array([conn_per[ii][0],conn_per[ii][1],thop*exp(-segno*k*deltaz*1j)]);

                    Hnew=vstack([Hnew,temp]);
    del ii return Hnew


class nanoribbon_fast_ohmic: acc=0.144;
    def __init__(self,n,L): self.Nc=int(4*(floor((floor(L/nanoribbon_fast_ohmic.acc)-
1)/3)));
        self.n=n;
        self.Phi=zeros(n*self.Nc);
        self.Eupper=1000.0;
        self.Elower=-1000.0;
        self.dE=1e-3; self.thop=-2.7;
        self.eta=1e-8; self.mu1=0;
        self.mu2=0; self.Temp=300;
        self.E=zeros(NEmax);
        self.T=zeros(NEmax);
        self.charge=zeros(self.n*self.Nc);
        self.rank=0; self.atoms_coordinates();
        self.defects_list=[] self.onsite_E=-1.5;
    def atoms_coordinates(self):
        GNR_atoms_coordinates(self);
        self.x=array(self.x); self.y=array(self.y);
        self.z=array(self.z); return;
    def gap(self):
        return GNRgap(self); def
    charge_T(self):

        M=self.Nc;
        N=self.n;
        t=self.thop; Energy =
        0.0 Ene = 0.0
        p = 0.0 d = 0.0
        orbitals = [1, 0] hamiltonian = []
        zeroes = [0, 0, 0, 0]
        ene = [Energy, 0, 0, Ene] coupling1 = [t, 0,
        0, p] coupling2 = [t*1.12, 0, 0, p] orbitals =
        orbitals + zeroes
        hamiltonian.append(orbitals)

for j in range(M): for i in range(N):
        n = i + 1 + j*N p = [n,n]
        p = p + ene hamiltonian.append(p)

for j in range(1, M-1, +4): for i in range(1, N):
        n = i + 1 + j*N m = i + (j+1)*N p =
        [n,m]
```

```
            p = p + coupling1 hamiltonian.append(p)
    #         hamiltonian.append([m, n, t, p, d])

for j in range(3, M-1, +4): for i in range(0, N-1):
            n = i + 1 + j*N
            m = i + 2 + (j+1)*N p = [n,m]
            p = p + coupling1 hamiltonian.append(p)
     #        hamiltonian.append([m, n, t, p, d])


#  nell'if ripristinare il fattore t*1.12 for j in range(0, M-1, +4):
       for i in range(N): n = i + 1 + j*N
            m = i + 1 + (j+1)*N
            if i == 0:
                  p = [n,m]
                  p = p + coupling2 hamiltonian.append(p)
       # hamiltonian.append([m, n, t*1.12, p, d]) else :

                  p = [n,m]
                  p = p + coupling1 hamiltonian.append(p)
        #           hamiltonian.append([m, n, t, p, d])

for j in range(1, M-1, +4): for i in range(N):
            n = i + 1 + j*N
            m = i + 1 + (j+1)*N p = [n,m]
            p = p + coupling1 hamiltonian.append(p)

  #                          hamiltonian.append([m, n, t, p, d])

                           # nell'if ripristinare il fattore t*1.12
                    for j in range(2, M-1, +4):
                       for i in range(N):
                        n = i + 1      + j*N
                       m = i + 1       + (j+1)*N
                        if i == (N-1):
                             p = [n,m]
                           p =  p + coupling2
                           hamiltonian.append(p)
                      #                    hamiltonian.append([m, n, t*1.12, p,
d])
                      else :
                           p = [n,m]
                           p =  p + coupling1
                           hamiltonian.append(p)
#                      hamiltonian.append([m, n, t, p, d])

            for j in range(3, M-1, +4): for i in
                  range(N):
                      n = i + 1 + j*N
                      m = i + 1 + (j+1)*N p = [n,m]
```

```
                        p = p + coupling1
                        hamiltonian.append(p)
#               hamiltonian.append([m, n, t, p, d])

            H = Hamiltonian(N,M)
            # I work on the defects
            ind=array(self.defects_list,dtype=int);
            H.H=array(hamiltonian,dtype=complex)
            H.H[ind,2]=self.onsite_E;
            H.Eupper = self.Eupper; H.Elower =
            self.Elower; H.rank=self.rank;
            H.dE=self.dE; H.Phi=self.Phi;
            H.Ei=-self.Phi; H.eta=self.eta;
            H.mu1=self.mu1; H.mu2=self.mu2;
            H.Egap=self.gap();

            H.charge_T()

            self.E=array(H.E);
            self.T=array(H.T);
            self.charge=array(H.charge); del
            hamiltonian,H
            return;

        def current(self): vt=kboltz*self.Temp/q;
            E=array(self.E); T=array(self.T);
            arg=2*q*q/(2*pi*hbar)*T*(Fermi((E-self.mu1)/vt)-Fermi((E-
self.mu2)/vt))*self.dE
            return sum(arg);

#  This is the class for the solution of the 1D drift-diffusion class multisubband1D:
        def __init__(self, nx, ny, Neig): self.ny=ny;
            self.nx=nx;
            self.x=zeros(nx);
            self.y=zeros(ny);
            self.Phi=zeros(nx*self.ny);
            self.Ei=zeros(nx*self.ny);
            self.Egap=zeros(nx*self.ny);
            self.Temp=300;
            self.charge=zeros(nx*self.ny);
            self.rank=0;
            self.Neig=Neig;
            self.Psi=zeros((nx*ny,Neig));
            self.eig=zeros((ny,Neig));
            self.mass=zeros((nx,ny)); self.mu=100e-
            4*ones(self.ny); self.genric=zeros(self.ny);
            self.n1d=zeros(self.ny);
            self.ecs=zeros(self.ny);
            self.charge_left_contact=0;
            self.charge_right_contact=0; self.tolljay=1e-
            3;
```

```
#  This is the class for the solution of the QM 1D
class QM1D:
    def __init__(self, nx, Neig,gridx,p=None,charge_T=None): if charge_T is not
        None:
            self.charge_T=types.MethodType(charge_T,self); self.nx=nx;
        self.x=zeros(nx);
        self.ny=1;
        ny=1;
        self.Phi=zeros(nx*self.ny);
        self.Ei=zeros(nx*self.ny);
        self.Temp=300;
        self.charge=zeros(nx*self.ny);
        self.rank=0;
        self.Neig=Neig;
        self.Psi=zeros((nx*ny,Neig));
        self.eig=zeros((ny,Neig)); if p is not
        None:

            self.Egap=p.Egap;
            self.massl=p.mel
            self.masst=p.met;
            self.massh=p.mhole
            self.chi=p.chi
            self.mass=p.mel;
        else:
            self.Egap=zeros(nx*self.ny)
            self.massl=zeros(nx*self.ny)
            self.masst=zeros(nx*self.ny)
            self.massh=zeros(nx*self.ny)
            self.chi=zeros(nx*self.ny)
            self.mass=zeros(nx*self.ny)
        self.Ef=0;
        self.x=gridx;
        self.ecs=zeros(self.ny); def
    charge_T(self):
        del self.charge self.charge=zeros(self.nx*self.ny);
        self.Ei=-self.Phi;
        # I compute the confined electrons
        dist=avervect(self.x)
# self.Ei=4.05-self.Phi-self.chi-self.Egap*0.5 self.mass=self.massl;
        solve_schroedinger_1D(self); vt=self.Temp*kboltz/q;
        for i in range(0,self.Neig): self.charge=self.charge-
            2*dist*1e-
9*(self.Psi[:,i])**2*self.masst*m0*kboltz*self.Temp/pi/hbar**2*log(1+e xp(-(self.eig[0,i]-
self.Ef)/vt));
        self.mass=self.masst;
        solve_schroedinger_1D(self);
        vt=self.Temp*kboltz/q;
        for i in range(0,self.Neig): self.charge=self.charge-
            4*dist*1e-
```

```
9*(self.Psi[:,i])**2*self.massl*m0*kboltz*self.Temp/pi/hbar**2*log(1+e xp(-(self.eig[0,i]-
self.Ef)/vt));
            # I now add the holes
            for i in range(0,size(self.charge)):
                self.charge[i]=self.charge[i]+dist[i]*1e-
9*(2/sqrt(pi))*2*(vt/(2*pi)*(self.massh[i]*m0/hbar)*(q/hbar))**1.5*fph alf((self.Ei[i]-
self.Egap[i]*0.5-self.Ef)/vt)

            return;
        def current(self): return 0;
```